

NONDESTRUCTIVE MEASUREMENT OF POSTHARVEST CHANGES IN LAMB'S LETTUCE

Bert JACOBS

Supervisors:
Prof. B.M. Nicolai
Prof. W. Saeys

Members of the Examination
Committee:
Dr. P. Bleyaert
Prof. M. De Proft
Prof. J. Lammertyn
Dr. B. E. Verlinden

Chairman:
Prof. J. Delcour

Dissertation presented in
partial fulfilment of the
requirements for the degree
of Doctor of Bioscience
Engineering (PhD)

February 2019

Doctoraatsproefschrift nr. 1441 aan de faculteit Bio-
ingenieurswetenschappen van de KU Leuven

© 2019 KU Leuven, Science, Engineering & Technology
Uitgegeven in eigen beheer, Bert Jacobs, Aarschot

Alle rechten voorbehouden. Niets uit deze uitgave mag worden vermenigvuldigd en/of openbaar gemaakt worden door middel van druk, fotokopie, microfilm, elektronisch of op welke andere wijze ook zonder voorafgaandelijke schriftelijke toestemming van de uitgever.

All rights reserved. No part of the publication may be reproduced in any form by print, photoprint, microfilm, electronic or any other means without written permission from the publisher.

Dankwoord

Hier zijn we dan, 2287 dagen na de start van mijn doctoraat bij MeBioS. Terwijl ik dit aan het schrijven ben is het einde in zicht en tijdens deze periode van 2.287×10^3 dagen heb ik veel ervaren en geleerd. Hiervoor wil ik een aantal mensen bedanken.

Om te beginnen wil ik mijn promotor, Bart Nicolai, en copromotor, Wouter Saeys, bedanken. Zonder jullie zou het niet mogelijk geweest zijn voor mij om dit werk af te leveren. Ik wil jullie voornamelijk bedanken voor het nalezen van mijn publicaties en natuurlijk ook deze scriptie.

De juryleden van mijn examencomité; Jeroen Lammertyn, Maurice De Proft en Peter Bleyaert; samen met de voorzitter Jan Delcour mogen natuurlijk niet ontbreken. Hartelijk bedankt voor jullie tijd, de interesse in mijn werk en jullie nuttige opmerkingen die dit werk naar een hoger niveau hebben getild.

Daarnaast kan ik natuurlijk niet rond Bert Verlinden, jurylid en mijn dagelijkse begeleider. Jij gaf me altijd constructieve feedback over alles waar je iets van wist en dankzij jou weet ik ook meer over de Hagelandse Academie voor Beeldende Kunst, Chinese internetwinkels en robots.

Bij deze wil ik ook graag de proeftuin Inagro bedanken voor het produceren van mijn planten die ik allemaal, zonder een traan weg te pinken, heb vermoord.

I may not forget to mention my (ex-)colleagues. Thank you for the great atmosphere, the nice and disturbing chats, lunches at Via Via, after-work drinks at the Baarr,... Without a doubt I consider a lot of you now as my friends. But I would like to mention a few people by name. Matthias, my desk buddie, I would like to thank you for helping me with whatever you did all these years. It is something like 'co-slatistician' or fellow 'sIA-hole'. Jelena,

thank you for that one time you were there helping me with extremely rotten lettuce (Can we still call it lettuce? Lettuce just forget about it). I would also like to thank you for all the other help as mental coach and just being the social creature that you are. The same can be said for a lot of other people e.g. Bram, Michael, Kostas, Siem, Zi, Mattias, Niels, Bart, Clara, Iris, Wouter, Sofie, Belfie, ... I could thank each and every one of you for some specific thing, but that would take up to much space. In general, I would like to thank all of you for the nice atmosphere at S.E.G. and helping me out when I needed a hand.

Een dikke merci is ook op zijn plaats voor mijn andere vrienden. Of ze nu uit de regio Beringen (PJ, Stijn, Dimi, Jonas, Jan, Wout en Jasper), Neerpelt (Jeroen, Nicky en Bart) of één of andere rosse buurt (Dries en Jeffrey) komen. Jullie stonden altijd klaar om mij van de nodige afleiding te voorzien wanneer ik dat het meeste nodig had. Daarnaast verdient Jeroen Carrein een extra bedankje voor de mooie tekening op de kaft.

Mijn huidige collega's mag ik ook niet vergeten. Voornamelijk omdat ze zo begripvol zijn omgegaan met mijn vermoeide toestand en afwezigheden. Bij deze excuseer ik mij ook voor mijn occasioneel slecht humeur veroorzaakt door chronisch slaapttekort.

Daarnaast moet ik natuurlijk mijn familie bedanken. Ik heb het de laatste tijd nogal druk gehad en mijn goed voornemen is om wat vaker langs te komen. Ik wil jullie dan ook bedanken dat jullie daar heel begripvol mee zijn omgegaan.

Tenslotte wil ik mijn verloofde, Elien, bedanken. Dank je wel voor de steun en liefde, het coördineren van de bouw van ons huis, het opnemen van taken in het huis waar ik geen tijd of energie voor had, mijn grootste fan te zijn en mij onvoorwaardelijk te steunen in dit 'slavontuur'. Zonder jou was ik niet begonnen aan deze studie en had ik deze zeker niet afgemaakt.

Bedankt!

Bert Jacobs

Abstract

A healthy lifestyle is becoming more and more important for the modern day consumer and fresh, minimally processed, ready-to-eat vegetables play an essential role. Lamb's lettuce (*Valerianella locusta*) is a popular greenhouse vegetable mainly thanks to these characteristics. It is used as an ingredient in salad mixtures and as a leafy salad making it an ideal healthy food for the modern day consumer. However, lamb's lettuce plants presented to the market are not always freshly harvested. Producers can store them up to four weeks in their cooling facility, because fresh produce and stored samples are indistinguishable by the human eye. However, the latter have an impaired shelf life potential leading to significant economic losses in distribution and lower consumption quality. Hence, the main objective was to develop a fast and nondestructive methodology to estimate how long a batch of lamb's lettuce has been stored before it is presented to the market.

In the first part of this dissertation, lettuce from commercial producers was stored at 1 and 4 °C for 21 d and the effects on metabolite content and respiration rate were studied. After 21 d of storage, the general sugar content of lamb's lettuce had decreased. The RQ value indicated that carbohydrates remained the main carbon source during storage. However, the increase of free amino acids due to proteolysis indicated that the plants coped with nutrient stress and that amino acids were made available for respiration. The respiration rate decreased during storage, which implied a shortage in soluble carbohydrates. In conclusion, after 21 d of storage, carbohydrates were still the main energy source but the lamb's lettuce was preparing to use a mixture of different carbon sources for respiration. As the main purpose of respiration during postharvest storage is to provide energy

for maintenance purposes, the energy production decreased and this likely would also affect shelf life potential.

In the second part of the research, visible / near infrared (Vis/NIR) spectroscopy and chlorophyll fluorescence emission ratios were evaluated as a fast and non-destructive method to detect and quantify a prior storage period. Lamb's lettuce from commercial producers was stored at 1 and 4 °C and the Vis/NIR spectra and fluorescence emission ratios were linked to the time in storage by partial least squares regression (PLSR). Preprocessing and variable selection techniques (interval PLS, Variable Importance in Projection scores, Genetic Algorithms PLS and Monte Carlo Uninformative Variable Elimination PLS) were used to improve the performance of the PLSR models. The PLSR model based on Vis/NIR spectra made successful predictions on a possible storage period. This was not possible for PLSR models based on chlorophyll fluorescence emission ratios without a correction for the storage temperature. The unsuccessful predictions based on chlorophyll fluorescence emission ratios could be due to a smaller calibration dataset which contained a lot of variation. The final prediction model based on Vis/NIR spectra used only 10% of the original wavelength variables and had a root mean squared error of cross validation of 3.6 d. This model was tested using 2 external test sets and had a maximum root mean square error of prediction of 3.7 d. Hence, Vis/NIR spectroscopy can be a valuable, rapid and non-destructive method for identifying and quantifying a prior storage period of lamb's lettuce.

Samenvatting

Verse, minimaal verwerkte, direct eetbare groenten spelen een belangrijke rol in een gezonde levensstijl. Veldsla (*Valerianella locusta*) is een populaire glasgroente vanwege deze eigenschappen. Het wordt gebruikt als ingrediënt in vooraf klaargemaakte salades en het is ideaal gezond voedsel voor de hedendaagse consument. Veldsla die op de markt gebracht wordt, is echter niet altijd vers geoogst. Telers kunnen de planten tot wel vier weken bewaren in hun eigen koelfaciliteiten, omdat verse en bewaarde veldsla visueel niet te onderscheiden zijn. Bewaarde veldsla heeft echter een korter potentieel uitstalleven wat aanleiding geeft tot economische verliezen in de distributieketen en een lagere kwaliteit voor de consument. Vandaar dat de ontwikkeling van een snelle niet-destructieve methodologie voor het identificeren en kwantificeren van een voorafgaande bewaarperiode bij veldsla het hoofddoel was van dit proefschrift.

In het eerste deel van dit proefschrift werd veldsla van commerciële telers gedurende 21 dagen bewaard bij 1 en 4 °C. De effecten van deze bewaarperiode op het gehalte van verschillende metabolieten en de respiratiesnelheid werd bestudeerd. Na een bewaarperiode van 21 dagen was het algemeen suikergehalte gedaald. De RQ waarde gaf aan dat koolhydraten de voornaamste koolstofbron waren. Gedurende deze bewaarperiode was echter ook een toename van vrije aminozuren vanwege proteolyse. Dit was een indicatie dat de planten moesten omgaan met nutriëntenstress en dat vrije aminozuren beschikbaar waren voor respiratie. Gedurende de bewaarperiode daalde de respiratiesnelheid. Dit impliceert een tekort aan oplosbare koolhydraten. Vandaar dat geconcludeerd werd dat na een bewaarperiode van 21 dagen veldsla nog koolhydraten gebruikte

als voornaamste energiebron, maar dat daarnaast veldsla voorbereidingen trof om andere koolstofbronnen te gebruiken voor respiratie. Het voornaamste doel van respiratie gedurende een bewaarperiode is om energie te voorzien voor onderhoudsdoeleinden in de plant. De energieproductie verminderde en dit zou waarschijnlijk het potentieel uitstalleven beïnvloeden.

In het tweede deel van dit onderzoek werden zichtbaar / nabij-infrarood (Vis/NIR) spectroscopie en chlorofylfluorescentie emissieratio's geëvalueerd als een snelle, niet-destructieve meetmethode om een voorafgaande bewaarperiode voor veldsla te detecteren en te kwantificeren. Veldsla van commerciële telers werd bewaard bij 1 en 4 °C. Vervolgens werden de Vis/NIR-spectra en fluorescentie-emissieratio's gelinkt aan de bewaarduur met behulp van 'partial least squares regression' (PLSR). Voorbehandelingen en selectietechnieken op de variabelen (interval PLS, Variable Importance in Projection scores, Genetic Algorithms PLS en Monte Carlo Uninformative Variable Elimination PLS) werden toegepast om de performantie van de PLSR modellen te verbeteren. PLSR modellen gebaseerd op Vis/NIR-spectra maakten succesvolle voorspellingen over een voorafgaande bewaarperiode. Voorspellingen gebaseerd op chlorofylfluorescentie emissieratio's waren niet succesvol zonder een correctie voor de bewaartemperatuur. Het feit dat de voorspellingen op basis van chlorofylfluorescentie-emissieratio's niet succesvol waren, kan te wijten zijn aan de kleinere kalibratiedataset die veel variatie omvatte. Het uiteindelijke PLS-voorspellingsmodel gebaseerd op Vis/NIR-spectra gebruikte slechts 10 % van de originele golflengtes en had een gemiddelde fout in crossvalidatie van 3.6 dagen. Dit model werd getest door gebruik te maken van 2 externe testdatasets en kon de bewaartijden voorspellen met een gemiddelde fout van 3.7 dagen. Dit biedt perspectieven om Vis/NIR-spectroscopie in de praktijk toe te passen als snelle en niet-destructieve methode voor het identificeren en kwantificeren van een voorafgaande bewaarperiode bij veldsla.

List of abbreviations

ADP	Adenosine diphosphate
ANOVA	Analysis of variance
ANTH	Anthocyanin index
ATP	Adenosine triphosphate
B	Blue excitation light
CoA	Coenzyme A
CV	Cross validation
Cyt c	Cytochrome c
EPO	External parameter orthogonalization
FAD	Flavin adenine dinucleotide
FADH ²	Reduced form of FAD
Fd	Ferredoxin
FER	Fluorescence excitation ratio
FERARI	Fluorescence excitation ratio anthocyanin relative index
FLAV	Flavonol index
FNR	Ferredoxin-NADP reductase
FRF	Far-red fluorescence
G	Green excitation light
G6P	Glucose-6-phosphate
GABA	Gamma-aminobutyric acid
GA-PLS	Genetic algorithms PLS
GC-MS	Gas chromatography - mass spectrometry
GLSW	Generalized least squares weighting
InGaAs	Indium Gallium Arsenide
iPLS	Interval PLS

IR	Infrared
LED	Light emitting diodes
LOOCV	Leave-one-out cross validation
LV	Latent variable
MC-UVE-PLS	Monte carlo uninformative variable elimination PLS
MSC	Multiplicative scatter correction
BSTFA	N,O-Bis (trimethylsilyl)trifluoroacetamide
NAD ⁺	Nicotinamide adenine dinucleotide
NADH	Reduced form of NAD ⁺
NADP ⁺	Nicotinamide adenine dinucleotide phosphate
NADPH	Reduced form of NADP ⁺
NBI	Nitrogen balance index
NIR	Near infrared light
OSC	Orthogonal signal correction
P680	Reaction centers of PSI
P700	Reaction centers of PSII
PAM	Pulse amplitude modulation
PC	Plastocyanin
PC	Principal component
PCA	Principal component analysis
PCR	Principal component regression
P _i	Inorganic phosphate
PLSR	Partial least squares regression
PPP	Pentose phosphate pathway
PQ	Plastoquinone
PQH ₂	Plastohydroquinone
PSI	Photosystem I
PSII	Photosystem II
PTFE	Polytetrafluorethene
Q	Quality parameter
QC	Quality control
R	Red excitation light

RF	Red fluorescence
RI	Reliability Index
RMSE	Root mean square error
RMSECV	Root mean square error of cross validation
RMSEP	Root mean square error of prediction
RMSEV	Root mean square error of validation
RQ	Respiratory quotient
S/N	Signal to noise ratio
SFR	Simple chlorophyll fluorescence ratio
Si	Silicon
SNV	Standard normal variate
TCA	Tricarboxylic acid
UQ	Ubiquinon
UQH ₂	Ubiquinol
UV	Ultraviolet A excitation light
UVE-PLS	Uninformative variable elimination PLS
VIP	Variable importance in projection
Vis	Visible light
YF	Yellow fluorescence

Table of Contents

Dankwoord.....	i
Abstract.....	iii
Samenvatting.....	v
List of abbreviations.....	vii
Table of Contents	xi
1. General introduction	1
1.1. Introduction	1
1.2. Post-harvest changes in lamb's lettuce	3
1.3. Measurement of the quality of fresh produce	4
1.4. Objectives and outline of the dissertation	6
2. State of the art	9
2.1. Lamb's lettuce as a fresh, ready-to-eat consumable.....	9
2.2. Taxonomy, presence, morphology and leaf anatomy.....	10
2.3. Energy metabolism	12
2.3.1. Photosynthesis	12
2.3.2. Respiration	14
2.3.3. Alternative pathways	19
2.3.4. Respiratory Quotient	20
2.3.5. Postharvest changes in energy metabolism	20
2.4. Fast and non-destructive measurement techniques.....	22
2.4.1. Interaction of light with plant tissue	22
2.4.2. Visible / near infrared spectroscopy	27

2.4.3. Chlorophyll fluorescence	30
2.4.4. A need for multivariate statistics	37
2.4.5. On-line measurements of fresh produce.....	37
2.5. Chemometrics	39
2.5.1. Data compression and regression	39
2.5.2. Identifying outliers	41
2.5.3. Validation methods.....	42
2.5.4. Evaluating model performance	44
2.5.5. Pre-processing methods	44
2.5.6. Variable selection	46
2.6. Conclusions.....	50
3. Respiration and physiological events of lamb's lettuce during storage...	53
3.1. Introduction	53
3.2. Materials and methods.....	54
3.2.1. Plant material and storage conditions	54
3.2.2. Respiration	55
3.2.3. Metabolite analysis.....	56
3.2.4. Statistical analysis	58
3.3. Results	60
3.3.1. Respiration	60
3.3.2. Metabolites	61
3.4. Discussion.....	66
3.4.1. Grower effect.....	66
3.4.2. Sugars and sugar alcohols.....	67
3.4.3. Amino acids.....	68
3.4.4. Pyruvate, GABA and TCA cycle metabolites	70
3.5. Conclusions.....	71
4. Estimation of storage time of lamb's lettuce based on Vis / NIR spectroscopy.....	73

4.1. Introduction	73
4.2. Materials and methods.....	75
4.2.1. Plant material and storage conditions	75
4.2.2. Quality attributes	76
4.2.3. Vis/NIR transreflectance spectroscopy	77
4.2.4. Prediction model.....	77
4.2.5. Predicting shelf life potential	83
4.3. Results and discussion	84
4.3.1. Adaxial and abaxial spectra	84
4.3.2. Evaluation of initial model	84
4.3.3. Wavelength selection	88
4.3.4. Comparison of the selected wavelength variables.....	90
4.3.5. Combining wavelength selections.....	91
4.3.6. Practical implementation	94
4.3.7. Physiological interpretation of selected wavelengths.....	95
4.3.8. Predicting shelf life potential	97
4.4. Conclusions.....	99
5. Estimation of storage time of lamb's lettuce based on chlorophyll fluorescence	101
5.1. Introduction	101
5.2. Materials and methods.....	102
5.2.1. Plant material and storage conditions	102
5.2.2. Chlorophyll fluorescence emission measurements.....	103
5.2.3. Prediction model with separate temperatures.....	104
5.3. Results	109
5.3.1. Chlorophyll fluorescence emission signals	109
5.3.2. Chlorophyll fluorescence emission ratios.....	112
5.4. Discussion.....	118
5.5. Conclusions.....	121

6. General conclusions and future perspectives	123
6.1. General conclusions	123
6.2. Future perspectives	126
7. Bibliography	129
8. List of publications	139
8.1. Articles in internationally reviewed journals	139
8.2. Conference proceedings	139
8.3. Science popularisation	139

1. General introduction

1.1. Introduction

Consumers are becoming more and more aware of the importance of a healthy lifestyle in which vegetables play an essential role (Cox et al., 1998; FAO/WHO, 2003; Ragaert et al., 2004). With time pressure as an important reason for consumers to be more convenience orientated regarding the choice of food, and prepared meals and food processing methods receiving skeptical responses, the consumption pattern is shifting towards minimally processed ready-to-eat products (Ahvenainen, 1996; Candel, 2001; Creed, 2001; Rico et al., 2007; Rodgers, 2007; Verlegh and Candel, 1999). These foods are characterized by their fresh appearance and their ease of use (Dinnella et al., 2014; Kumpulainen et al., 2016). Lamb's lettuce (*Valerianella locusta*) is a popular greenhouse vegetable, mainly thanks to these characteristics. It is used as an ingredient in salad mixtures and as a leafy salad making it an ideal healthy food for the modern day consumer (Enninghorst and Lippert, 2003; Ragaert et al., 2004). In a survey in 2004 which aimed at gaining insight in consumer decision-making towards purchasing minimally processed vegetables and packaged fruits, lamb's lettuce as part of a 'gourmand salad' was the third most purchased minimally processed vegetable. As a vegetable on its own, it was the seventh most purchased minimally processed product overall and second most purchased minimally processed single-vegetable product (Ragaert et al., 2004). In 2015 alone, LAVA, the umbrella organization that promotes co-operation between the five most important fruit and vegetable auctions in Belgium, noted a 20% increase in yearly revenue from lamb's lettuce. This resulted in 4.5 million

euros of revenue (Ceulemans, 2017). This increase can be attributed to higher demands and improved selling price. The production of lamb's lettuce is fairly stable through the years, with LAVA reporting around 1500 tons of lamb's lettuce being sold annually (Ceulemans, 2017).

Lamb's lettuce grows in a low rosette with spatula shaped leaves which can grow up to 15 cm long (Fig. 1.1). It naturally occurs in mild climates and is traditionally grown as a winter green. However, it is commercially produced in Belgium all year round via greenhouses. (Abrams and Ferris, 1960; Ceulemans, 2015; Ward, 1911). The peak in production is during the first 5 weeks of the year. LAVA reports during this period a production of 30 000 kg of lamb's lettuce per week (Ceulemans, 2015).



Fig. 1.1 Image of lamb's lettuce with a clear view of the rosette shape and spatulate leaves (bostonfoodandwhine.com, 2009)

1.2. Post-harvest changes in lamb's lettuce

Lamb's lettuce is still metabolically active after harvest. The metabolism is a complex process which is highly regulated to adapt to changes in the environment. These can be subdivided into anabolic and catabolic processes, where the first are related to the production of new cell components and the latter are related to the breakdown of energy rich nutrients (Taiz and Zeiger, 2010). Harvested lamb's lettuce is kept in the dark at a low temperature (1 - 4 °C). In such an environment photosynthesis is no longer possible as a source of energy. Also, lamb's lettuce does not have a large pool of soluble sugars to be used as an energy source (Enninghorst and Lippert, 2003). The only available carbohydrates are those synthesized through photosynthesis before harvest. It has been shown that leaves of *Arabidopsis thaliana* can experience sugar starvation (Morkunas et al., 2012). Sugar starvation has been reported to induce metabolic changes. The carbohydrate metabolism is replaced and alternative substrates are used to sustain respiration and metabolic processes. In the final phases of sugar starvation, even cellular organelles are degraded and this eventually leads to cell death (Mbong et al., 2017b).

After harvest, leafy vegetables are usually exposed to uncontrolled humidity conditions. Low relative humidity is often the main cause of lettuce deterioration. It causes degradation of cell walls and affects other quality attributes, e.g., turgidity, texture, enzymatic browning (Ansorena et al., 2012). Other changes during storage include a gradual decrease of the antioxidant content of which ascorbic acid, phenylpropanoids and carotenoids are the most important in leafy vegetables (Ferrante et al., 2009). When stored at low temperatures (< 4 °C), lamb's lettuce has a very slow chlorophyll reduction (Ferrante and Maggiore, 2007). However, the decline of chlorophyll and carotenoid content starts quickly after harvest at ambient temperatures (Ferrante and Maggiore, 2007; Yamauchi, 2015). The loss of chlorophyll during storage has been found in many vegetables and

the accompanied yellowing or browning spots reduce the shelf life and commercial value (Ferrante et al., 2004; Rico et al., 2007).

1.3. Measurement of the quality of fresh produce

To determine the quality of fresh produce fast and non-destructive measurement set-ups are needed. The advantage of such techniques is that they require minimal sample preparation, produce no waste, and typically are fast so that they can be incorporated in sorting lines (Nicolai et al., 2014). Two of those techniques are visible / near infrared (Vis/NIR) spectroscopy and measurements of chlorophyll fluorescence emission ratios.

The visible and NIR parts of the electromagnetic spectrum encompass wavelengths between 380 and 780 nm, and 780 and 2500 nm, respectively (Fig. 1.2). In Vis/NIR spectroscopy, the sample to be measured is irradiated with light (electromagnetic radiation). The radiation can be transmitted, absorbed or reflected by the sample. The chemical and physical properties of the sample influence the contribution of each of these effects (Nicolai et al., 2007). In NIR, most absorption bands are complex with broad overlapping peaks due to overtones and combinations of fundamental absorptions in the far and mid infrared part of the electromagnetic spectrum (Reich, 2005). Hence, there is a need for chemometric data processing to relate spectral information to certain properties of the sample (Nicolai et al., 2007).

The principle of chlorophyll fluorescence emission signals is straightforward. When light is absorbed by chlorophyll it can drive photosynthesis, but it can also be dissipated as heat or re-emitted as light with a longer wavelength. The latter is known as chlorophyll fluorescence (Henriques, 2009; Maxwell and Johnson, 2000). Other compounds besides chlorophyll can absorb light which reduces the intensity of chlorophyll fluorescence. When leaves are exposed to different wavelengths of light, the intensities of chlorophyll

fluorescence can be compared. The intensities of these signals are sensitive to the distance between the sample and the detector which is why the signals are combined in ratios (Cerovic et al., 2009). Depending on the composition of the sample, different fluorescence ratios are measured which can be related to certain properties of the sample using chemometrics (Cerovic et al., 2009; Tremblay et al., 2011).

Both Vis/NIR spectroscopy and chlorophyll fluorescence emission ratios result in output data with a lot of variables which are not straightforward to interpret. Multivariate statistics, also called chemometrics, is employed to process these variables. Statistical models can be created to extract useful information but they can also be used to make predictions on future unknown samples by finding correlations between complex output variables and a response variable of interest (Ghozlen et al., 2010; Nicolai et al., 2007).

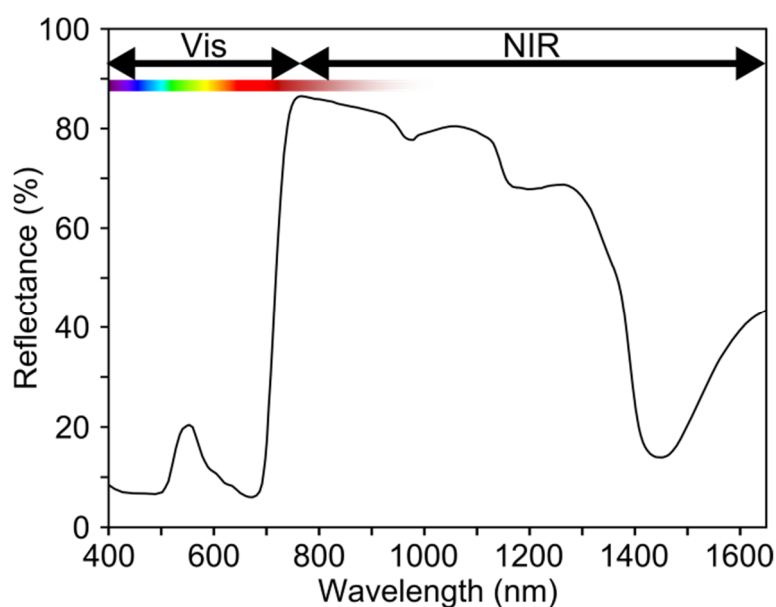


Fig. 1.2 Example of a Vis / NIR reflectance spectrum of a leaf of lamb's lettuce.

1.4. Objectives and outline of the dissertation

Lamb's lettuce plants presented to the market are not always freshly harvested. In winter time, growers can store them up to four weeks in their cooling facility. Fresh produce and stored samples are indistinguishable by the human eye. However, the latter have an impaired shelf life potential leading to significant economic losses in distribution and lower consumption quality (Fao, 1989; Ferrante et al., 2009; Rico et al., 2007). The perceived level of freshness and appearance are two of the most important attributes for fresh ready-to-eat salads according to consumers. This emphasizes the need for a better control system for the freshness of lamb's lettuce (Bublitz et al., 2010; Dinnella et al., 2014; Lennernäs et al., 1997). Hence, the **main objective** of this dissertation is to *develop a fast and nondestructive methodology to estimate how long a batch of lamb's lettuce has been stored before it is presented to the market*. The hypothesis is that invisible changes in the plants during post-harvest storage have a physiological base which is detectable by Vis/NIR spectroscopy or chlorophyll fluorescence emission ratios. Hence, the following **research questions** were formulated:

- What metabolic changes are present in lamb's lettuce during a post-harvest storage period?
- Can Vis/NIR spectroscopy or chlorophyll fluorescence emission ratios be used to monitor such changes and allow to estimate the prior storage period or even predict shelf life potential?

The outline of this dissertation is schematically illustrated in Fig. 1.3. In chapter 2, the state of the art is reviewed, starting with a description of lamb's lettuce leaf anatomy, morphology and physiology with a focus on the leaf structure, the main metabolic pathways concerning the energy metabolism and the interaction of light with plant tissue. Also, fast non-destructive measurement techniques are discussed including Vis/NIR reflectance spectroscopy and measurements of chlorophyll fluorescence emission ratios. As these multivariate techniques require chemometrics to extract the information of interest from the acquired signals, the most

important techniques for data preprocessing, variable selection, compression and regression are reviewed as well.

The postharvest changes in the lamb's lettuce's energy metabolism are investigated in chapter 3. A gas chromatography - mass spectrometry based protocol is used to separate, identify and quantify intracellular metabolites in lamb's lettuce plants stored after harvest at 1 and 4 °C. Respiration measurements are performed on similar samples to have an idea of any changes in the O₂ consumption and CO₂ production rate. Also, physiological changes during the storage period can be a possible source of information which can be detected by the fast and non-destructive measurement techniques.

Chapters 4 and 5 investigate the possibility to use Vis/NIR spectroscopy and chlorophyll fluorescence emission ratios, respectively, as fast and non-destructive measurement techniques to detect a prior storage period and predict shelf life potential. Internal non visual changes during a postharvest storage period may be detected using these techniques. The potential of both techniques have been evaluated based on a dataset with samples from different growers and cultivars stored for a few weeks at different temperatures. Using chemometrics, prediction models are constructed and the prediction potential of these models is evaluated and discussed.

In Chapter 6, general conclusions are drawn from this PhD research and suggestions for future research are presented.

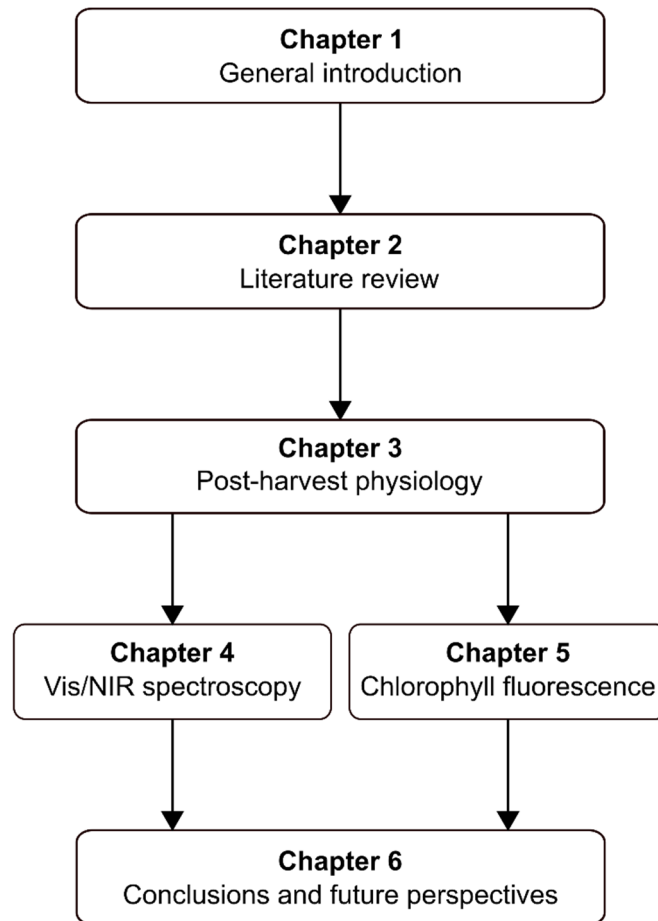


Fig. 1.3 Overview of the structure of the dissertation

2. State of the art

2.1. Lamb's lettuce as a fresh, ready-to-eat consumable

Society nowadays is more and more aware of healthy foods and the link between vegetables and their benefits towards healthy living are fully recognized (Cox et al., 1998; Ragaert et al., 2004). The consumption of 400 g of vegetables a day in addition to cooked or raw starch foods is recommended by the World Health Organization (FAO/WHO, 2003). National recommendations can differ, but in general these guidelines are hard to meet (Kumpulainen et al., 2016). Multiple studies have shown that taste, price and freshness are the main reasons for consumers to buy certain foods, but having a healthy diet is not always easily achieved in practice (Bublitz et al., 2010; Dalton et al., 1986; Glanz et al., 1998; Lennernäs et al., 1997). Consumers want to eat healthy, but are unable to differentiate between nutritionally poor and nutritionally rich foods. This is due to health claims of functional foods which are used as substitutes for healthy foods such as fruits and vegetables (Cornish, 2012). Other constraints to vegetable and fruit consumption are related to time pressure, which is one of the main reasons for consumers to be more convenience oriented when it comes to food choices (Candel, 2001; Verlegh and Candel, 1999).

In general, consumers tend to be skeptical towards different food processing methods and prepared meals (Creed, 2001). The change in consumption pattern has already lead to a shift in the food industry to minimally processed ready-to-use products (Ahvenainen, 1996; Rodgers, 2007). Minimally processed vegetables are fresh vegetables that are processed for improved

functionality without an alteration of the fresh-like properties. This processing method depends on the type of produce and can be washing, cutting, mixing and packaging. The final product is still perceived fresh, convenient in use and has no preservatives (Ragaert et al., 2004). The fact that these foods look fresh and are easy-to-use are important aspects for an increase in the consumption of healthy food (Dinnella et al., 2014; Kumpulainen et al., 2016; Neumark-Sztainer et al., 1999; Ragaert et al., 2004). Leafy salads are healthy due to their vitamin and fiber content. Of these leafy salads, lamb's lettuce is a popular greenhouse vegetable thanks to its ease of use and fresh, ready-to-eat characteristics. It is used as an ingredient in ready-to-eat salad mixtures and as a leafy salad making it a perfect healthy food for the modern consumer (Enninghorst and Lippert, 2003; Ragaert et al., 2004).

2.2. Taxonomy, presence, morphology and leaf anatomy

Lamb's lettuce (*Valerianella Locusta* L.) is part of the Caprifoliaceae family, which is part of the order Dipsacales included within the asterid group of dicotyledons (The Angiosperm Phylogeny Group, 2009). It grows in mild climates and is traditionally grown as a winter green (Abrams and Ferris, 1960; Ward, 1911). Lamb's lettuce forms a low rosette. The leaves are spatula shaped and can be up to 15 cm long (Fig. 1.1).

Lamb's lettuce leaves are made up of an epidermis with stomata and vascular tissue surrounded with mesophyll (Fig. 2.1). The epidermis consists of flat, tabular epidermal cells and guard cells which make up the stomata. It is covered with a transparent layer called the cuticle which covers the epidermal cells and mainly consists of cutin and wax. The main function of the cuticle is to reduce the loss of water. Guard cells are specialized cells that are used to control gas exchange. They come in pairs and have a gap between them that forms the stomatal pore. This small opening enables gas exchange between the internal gas phase of the leaf and the surrounding

air. The size of the opening is regulated by changes in the shape of the guard cells which depends on the turgor pressure inside the guard cells (Cutler et al., 2008; Mauseth, 2008; Raven et al., 1999; Taiz and Zeiger, 2010). The epidermis forms the boundary between the atmosphere and the inside of the leaf.

The tissue interior to the epidermis is called the mesophyll. The mesophyll along the adaxial side of the leaf is called the palisade parenchyma. This contains the main photosynthetic tissue and contains more chlorophyll than the other tissues. The mesophyll in the abaxial side of the leaf is the spongy parenchyma. It contains large intercellular spaces that improve the transport of gasses like CO_2 , O_2 and water vapor. Inside the mesophyll there are vascular bundles consisting of xylem and phloem. (Cutler et al., 2008; Mauseth, 2008; Raven et al., 1999; Taiz and Zeiger, 2010).

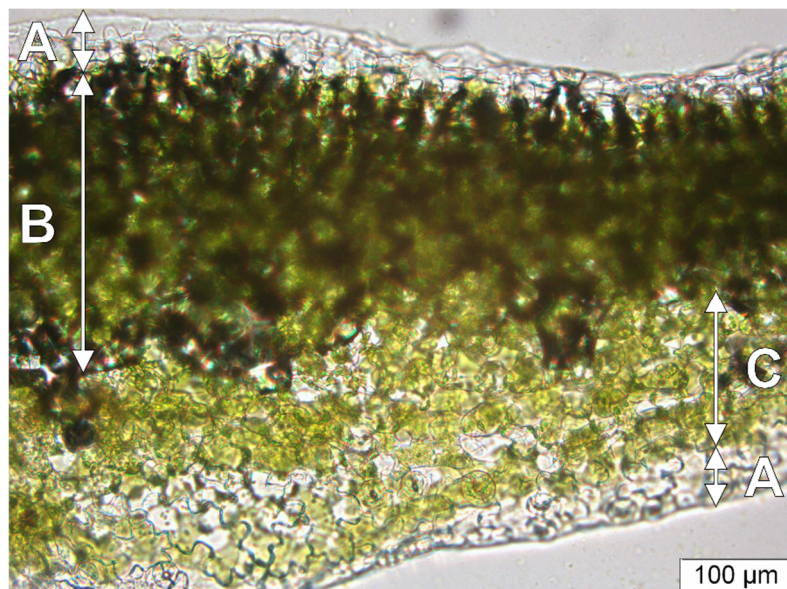


Fig. 2.1 Microscopic cross section of a lamb's lettuce leaf where the epidermis with cuticle (A) is visible on both leaf sides. Also, more chlorophyll containing and densely packed cells on the adaxial side called palisade parenchyma (B), and loosely packed cells with intercellular spaces on the abaxial side called spongy parenchyma (C) are clearly visible. No vascular tissue is present in this cross section (own work).

2.3. Energy metabolism

Plants have several energy related metabolic pathways. When solar energy is used to synthesize complex carbon compounds out of carbon dioxide (CO_2) and water (H_2O), this is referred to as photosynthesis. The energy of these carbon compounds can be released in a controlled manner by respiration. During respiration, carbon precursors for biosynthesis can be generated (Mauseth, 2008; Taiz and Zeiger, 2010).

2.3.1. Photosynthesis

Most photosynthetic tissue is divided in palisade and spongy parenchyma. These cells contain chloroplasts which have specialized internal membranes called thylakoids. In the chloroplast two photochemical complexes called photosystem I (PSI) and photosystem II (PSII) convert the energy from light captured by antenna systems made up of chlorophylls into chemical energy (Fig. 2.2). The reactions for which light is necessary are called the light reactions. In these reactions, PSI and PSII operate in series and use light from 400 to 700 nm. The reaction centers of PSI and PSII are specialized chlorophyll molecules called P700 and P680, respectively. Photons excite these reaction centers resulting in an excited electron. Photosynthesis begins when an electron of the reaction center P680 achieves this higher energy level. PSII oxidizes water to O_2 and a proton (H^+) in the lumen of the chloroplasts. At the same time, PSII reduces plastoquinone (PQ) to plastoquinone (PQH₂). PQH₂ in turn gets oxidized back to PQ by cytochrome b₆/f. This oxidation is coupled with a proton transfer from the stroma into the lumen which leads to a proton gradient over the thylakoid membrane. The electrons get delivered to PSI through plastocyanin (PC) and this leads to the reduction of nicotinamide adenine dinucleotide phosphate (NADP^+) to NADPH in the stroma by Ferredoxin (Fd) and ferredoxin-NADP reductase (FNR). Additionally, the gradient generated over the thylakoid membrane is used to synthesize adenosine triphosphate (ATP) from adenosine diphosphate (ADP) and inorganic phosphate (P_i) by ATP

synthase (Garrett and Grisham, 2005; Mauseth, 2008; Taiz and Zeiger, 2010).

The high energy compounds ATP and NADH drive the reduction of atmospheric CO₂ to carbohydrates and other cell components in the carbon fixing reactions located in the stroma of the chloroplast. This cyclic reaction pathway is called the Calvin-Benson cycle (dark reaction) and proceeds in three phases: carboxylation of CO₂, reduction of 3-phosphoglycerate and regeneration of ribulose 1,5-biphosphate (Fig. 2.3). The first phase of the cycle is the incorporation of 3 CO₂ molecules in three ribulose 1,5-biphosphate molecules which results in six molecules of 3-phosphoglycerate. In the next phase, 3-phosphoglycerate is reduced in two reactions to triose phosphates. The last phase of the cycle regenerates ribulose 1,5-biphosphate through several reactions where three ATP's are used to drive one reaction for each incorporated CO₂ molecule. The output of one triose phosphate balances the carbon input. These triose phosphates are metabolized to products such as sucrose and other organic compounds (Garrett and Grisham, 2005; Mauseth, 2008; Taiz and Zeiger, 2010)

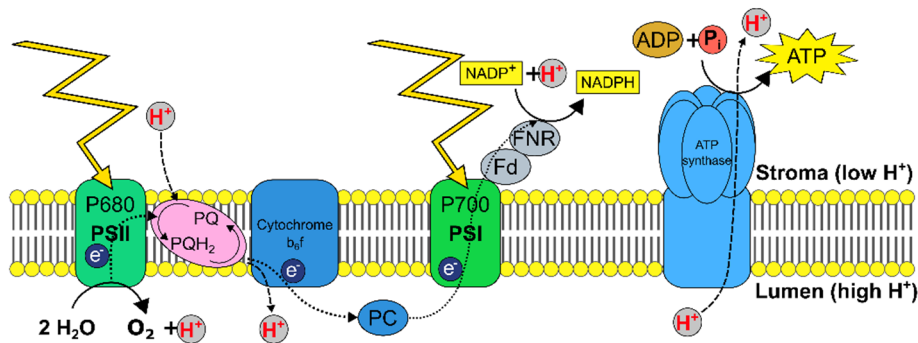


Fig. 2.2 The transfer of electrons and protons in the thylakoid membrane during the light reactions is carried out by four protein complexes: Photosystem I (PSI) with reaction center P700, Photosystem II (PSII) with reaction center P680, cytochrome *b₆f* and ATP synthase. Water is oxidized by PSII and protons are released in the lumen. Electrons (e^-) from PSII are used to reduce plastoquinone (PQ) to plastoquininol (PQH₂). PQH₂ is oxidized by cytochrome *b₆f* and a proton is transferred from the stroma to the lumen. Plastocyanin (PC) delivers the electrons in turn to PSI. NADP⁺ is reduced to NADPH in the stroma by PSI via Ferredoxin (Fd) and ferredoxin-NADP reductase (FNR). The protons in the lumen diffuse down the electrochemical potential gradient and are used to synthesize ATP in the stroma from ADP and inorganic phosphate (P_i) (Based on Taiz and Zeiger, 2010).

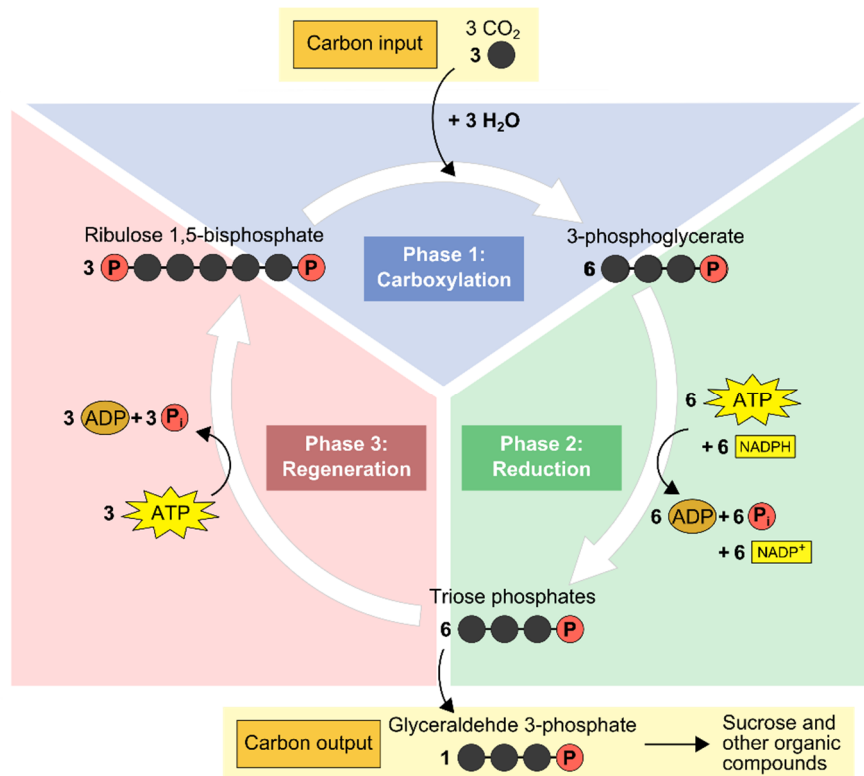


Fig. 2.3 An overview of the Calvin-Benson cycle with three clear phases: carboxylation, reduction and regeneration. The black and red circles represent carbon and phosphate atoms respectively (Based on Taiz and Zeiger, 2010)

2.3.2. Respiration

Respiration is the process where reduced organic compounds are oxidized in a controlled manner. It can be considered as the reversal of the photosynthetic process. Sucrose with 12 carbon atoms is oxidized to 12 molecules of CO_2 and 12 molecules of O_2 are reduced to water. The energy of this entire process is released in a series of reactions and is stored in ATP. The reactions of respiration can be grouped into four metabolic pathways: glycolysis, the pentose phosphate pathway (PPP), tricarboxylic acid (TCA) cycle, and oxidative phosphorylation. All these pathways are connected and respiratory substrates can enter at different points in the pathways (Garrett and Grisham, 2005; Mauseth, 2008; Taiz and Zeiger, 2010).

2.3.2.1. Glycolysis

Glycolysis is the pathway that converts glucose into pyruvate. The series of reactions catalyzing this process are located in the cytosol (Fig. 2.4). There are two phases in glycolysis: an energy consuming phase and an energy conserving phase. In the initial energy consuming phase a hexose (glucose) is phosphorylated twice using 2 molecules of ATP and in turn is split into 2 triose phosphates, i.e. glyceraldehyde 3-phosphate and dihydroxyacetone-phosphate. The energy conserving phase oxidizes each triose phosphate to yield one molecule of pyruvate. In these reactions, 2 molecules of ATP and 1 NADH are generated for each triose phosphate. Gluconeogenesis is the glycolysis process in the opposite direction where three glycolytic ATP dependent reactions are circumvented. It is used to produce sugars from organic acids (Garrett and Grisham, 2005; Mauseth, 2008; Taiz and Zeiger, 2010).

2.3.2.2. Pentose phosphate pathway

The pentose phosphate pathway (PPP) is an alternative way for the cell to oxidize sugars. The reactions are located in the cytosol and plastids, but under normal circumstances the pathway in the plastids is the dominant one (Fig. 2.4). The PPP has 2 distinct phases. The initial oxidative phase generates 2 NADPH molecules and oxidizes glucose 6-phosphate, a hexose phosphate, to ribulose 5-phosphate, a pentose phosphate. The second non-oxidative phase consists of freely reversible reactions and converts ribulose 5-phosphate to intermediates of the glycolysis, i.e., fructose 6-phosphate, a hexose phosphate, and glyceraldehyde 3-phosphate, a triose phosphate. These molecules can be converted to pyruvate in the glycolysis pathway, but alternatively they can be used to regenerate glucose 6-phosphate. The second phase can generate pentose sugars which can be used as a precursor for the synthesis of nucleotides. The PPP oxidizes hexose phosphates, but the PPP's function is anabolic rather than catabolic (Garrett and Grisham, 2005; Mauseth, 2008; Taiz and Zeiger, 2010).

2.3.2.3. Tricarboxylic acid cycle

The TCA cycle takes place in the matrix of the mitochondria and completely oxidizes pyruvate to 3 molecules of CO₂. It generates chemical energy and reducing power, but can also provide precursors of certain amino acids. First, pyruvate is transformed to acetyl-coenzyme A (CoA) (Fig. 2.4). This produces CO₂ and NADH. In the next reaction, acetyl-CoA is incorporated in the TCA cycle by combining acetyl-CoA with oxaloacetate to form citrate. In the following steps, the two remaining carbon atoms of pyruvate are released as CO₂ and these reactions generate two molecules of NADH. The remaining steps of the TCA cycle are used to regenerate oxaloacetate for a continued operation of the cycle. These reactions produce one molecule of ATP and reduce one molecule of flavin adenine dinucleotide (FAD) and one molecule of NAD⁺ to FADH₂ and to NADH, respectively. Thus, in the TCA cycle, pyruvate is completely oxidized to 3 molecules of CO₂ and the energy which is released generates four molecules of NADH, one molecule of FADH₂ and one molecule of ATP. Alternatively, it is possible for malate to be converted to pyruvate. This makes it possible for TCA cycle intermediates to be oxidized (Garrett and Grisham, 2005; Mauseth, 2008; Taiz and Zeiger, 2010).

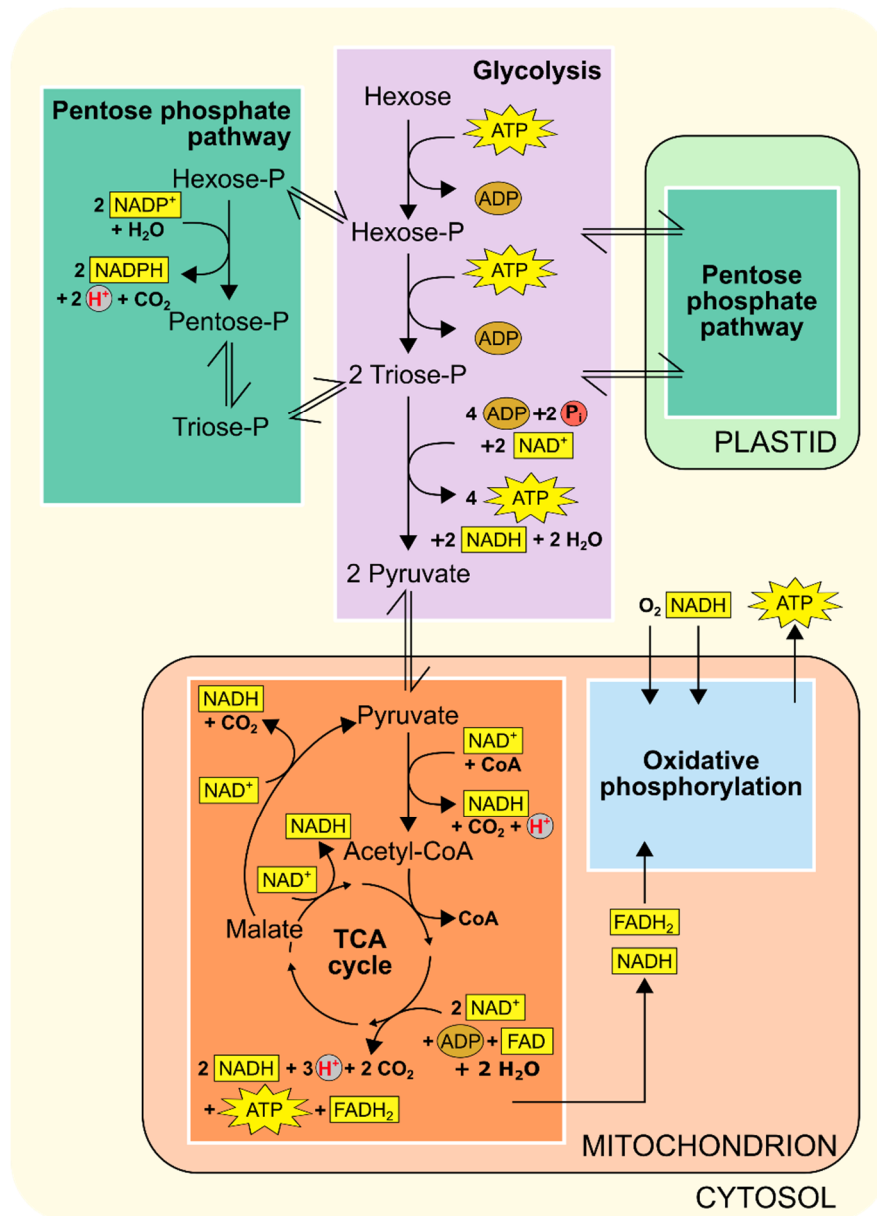


Fig. 2.4 Overview of respiration including glycolysis in the cytosol; pentose phosphate pathway in the cytosol and plastids; TCA cycle and oxidative phosphorylation in the mitochondria (Based on Taiz and Zeiger, 2010).

2.3.2.4. Oxidative phosphorylation

Oxidative phosphorylation occurs in the inner mitochondrial membrane and uses the chemical energy conserved in the glycolysis, PPP and TCA cycle (NADH and FADH₂) to generate ATP (Fig. 2.4). The reduced compounds (NADH and FADH₂) have to be oxidized or the respiration process comes to a halt. The electron transport chain catalyzes a flow of electrons from NADH (or FADH₂) to oxygen and in the process generates a proton gradient across the inner mitochondrial membrane (Fig. 2.5). There are four multiprotein complexes located in the inner mitochondrial membrane. Complex I oxidizes NADH and transfers the electrons to ubiquinon (UQ) reducing it to ubiquinol (UQH₂). Four protons are pumped from the matrix to the intermembrane space for each transferred electron pair. Complex II catalyzes the oxidation of succinate in the TCA cycle and the reducing equivalents are transferred via FADH₂ to UQ. UQH₂ gets oxidized to UQ by Complex III and four protons are pumped over the membrane for each electron pair. The electrons are passed on to cytochrome c (Cyt c), which transfers the electrons from Complex III to Complex IV. This complex reduces O₂ to two molecules of H₂O. Two protons are pumped over the membrane per electron pair. The transport of protons generates a proton gradient across the inner mitochondrial membrane. ATP synthase uses this potential energy to generate ATP from ADP by allowing protons to flow back across the membrane down the gradient (Garrett and Grisham, 2005; Mauseth, 2008; Taiz and Zeiger, 2010).

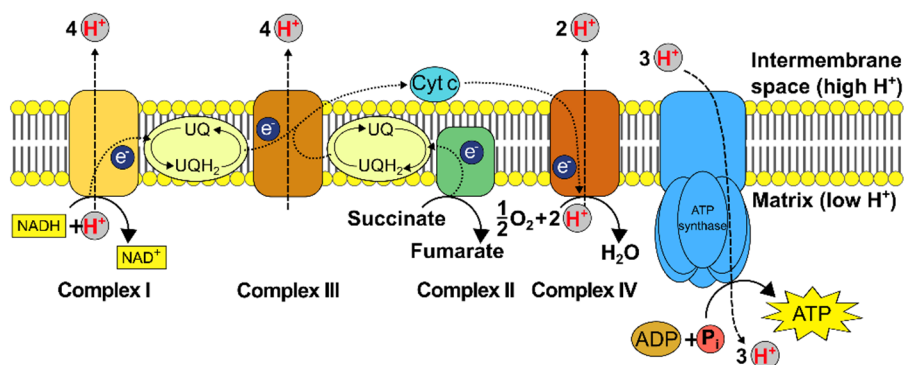


Fig. 2.5 The electron transport chain in the inner membrane of the mitochondria have five protein complexes: Complex I to IV, and ATP synthase. NADH is oxidized by complex I and electrons (e^-) are transferred to ubiquinone (UQ) reducing it to ubiquinol (UQH_2) while protons are transferred over the membrane. Complex II catalyzes the oxidation of succinate to fumarate and these electrons are transferred to UQ. Complex III oxidizes UQH_2 and pumps protons over the membrane. The electrons are transferred to cytochrome C (Cyt C) which transfers the electrons to Complex IV. Complex IV transfers protons over the membrane and produces H_2O from O_2 and a proton. The protons in the intermembrane space diffuse down the electrochemical potential gradient and are used to synthesize ATP in the matrix from ADP and inorganic phosphate (Pi) (Based on Garrett and Grisham, 2005; Taiz and Zeiger, 2010).

2.3.3. Alternative pathways

When no sugars are available, other metabolites like fatty acids and amino acids can be used as a carbon source (Aubert et al., 1996; Dieuaide-Noubhani et al., 1997; Hildebrandt et al., 2015; Inoue and Moriyasu, 2006; Mbong et al., 2017a, 2017b). This can lead to an increased protein breakdown which results in more amino acids. Autophagosomes can enclose proteins which can be broken down in amino acids or peptides by proteases (Aubert et al., 1996; Brouquisse et al., 1991; Dieuaide-Noubhani et al., 1997; Hildebrandt et al., 2015; Inoue and Moriyasu, 2006; Moriyasu and Ohsumi, 1996). The knowledge of the complete degradation pathways for all amino acids in plants is still rather limited. The first step involves the removal of nitrogen as ammonium and transferring it to storage compounds. Next, the carbon skeletons can be converted to precursors or intermediates of the TCA cycle (Hildebrandt et al., 2015).

Fatty acids can be oxidized to acetyl-CoA through β -oxidation. Acetyl-CoA can be fed into the TCA cycle and used as an energy source. Alternatively, the carbons can be fed through the glyoxylate cycle, which is an anabolic

variant of the TCA cycle, where the CO₂ producing steps are bypassed. This is achieved by converting isocitrate to succinate and glyoxylate. Glyoxylate is in turn combined with a second molecule of Acetyl-CoA to produce malate. Malate converts to oxaloacetate and the cycle can start again. Succinate is converted via malate to oxaloacetate in the TCA cycle. Oxaloacetate can be converted into carbohydrates by gluconeogenesis (Taiz and Zeiger, 2010).

2.3.4. Respiratory Quotient

The respiratory quotient (RQ) is the ratio of the amount of moles of CO₂ produced to those of O₂ consumed (Eq. 2.1). Depending on the substrates used for respiration, a different value is achieved for the RQ.

$$RQ \equiv \frac{r_{CO_2}}{r_{O_2}} \quad \text{Eq. 2.1}$$

Sugars have a theoretical RQ value of 1, because the oxidation of one mole of a hexose produces six moles of CO₂ and consumes six moles of O₂. The respiration of organic acids results in an RQ greater than 1. Due to the high oxygen content in these molecules less is needed to convert these molecules to CO₂. The respiration of fatty acids results in a lower RQ, because lipids contain less oxygen per carbon. Hence, oxygen has to be consumed not only to oxidize every carbon, but also every hydrogen. On the other hand, normal RQ values in literature for respiration are between 0.7 and 1.3. Fermentation leads to much higher RQ values, because no O₂ is consumed. The RQ is an easy to determine parameter and is often used to gain information about the respiratory metabolism (Fonseca et al., 2002; Ho et al., 2013; Mauseth, 2008; Taiz and Zeiger, 2010).

2.3.5. Postharvest changes in energy metabolism

Lamb's lettuce does not have a large pool of soluble carbohydrates which can be used as respiratory substrates (Enninghorst and Lippert, 2003). This

has also been shown for other leafy vegetables like butterhead lettuce (Varoquaux et al., 1996) and Chinese cabbage (Klieber et al., 2002). The carbohydrates synthesized through photosynthesis before harvest provide a limited energy source for respiration. Considering the fact that leafy vegetables are stored in dark environments where photosynthesis is not available, it is possible for them to experience sugar starvation (Morkunas et al., 2012). Limited information is available on sugar starvation in leafy vegetables during a postharvest storage period, but sugar starvation has been studied in sycamore cells (Journet et al., 1986), maize root tips (Brouquisse et al., 1991; Dieuaide-Noubhani et al., 1997), rice cells (Chen et al., 1994), Arabidopsis cells (Thimm et al., 2004), tobacco cells (Inoue and Moriyasu, 2006) and lamb's lettuce cells (Mbong et al., 2017a, 2017b).

Sugar starvation has been found to induce metabolic changes (Morkunas et al., 2012). An adaptation of the carbohydrate metabolism takes place with a gradual shift to alternative substrates to sustain respiration and metabolic processes. This may lead to autophagy (Brouquisse et al., 1991; Chen et al., 1994; Journet et al., 1986; Rose et al., 2006; Saglio and Pradet, 1980). In maize root tips, sugar starvation has been subdivided in three phases (Brouquisse et al., 1992). The first phase is acclimation. The carbohydrate levels and respiration rate decrease and nitrogen is released by protein degradation. The next phase is called the survival phase and is characterized by an intensive breakdown of lipids and proteins, and an increase of free amino acids. The final phase is cell disorganization. The enzymatic activity and metabolite levels decrease significantly. This final phase is irreversible and leads to irreversible damage and cell death. During the acclimation and survival phases the total protein content decreases, while free amino acid content and proteolytic activity increase temporarily (Borek and Ratajczak, 2002; Moriyasu and Ohsumi, 1996; Tassi et al., 1966). The metabolic changes are necessary to maintain respiration and basic metabolic processes in non-senescent cells. Even cellular organelles become degraded. Thus, energy acquisition is more essential for survival

even at the expense of organelles except for the nucleus and systems responsible for energy supply, i.e., mitochondria (Morkunas et al., 2012). Changes in metabolite content of lamb's lettuce during postharvest storage have only been investigated for cells in suspension (Mbong et al., 2017a, 2017b). Research on whole plants was limited to measurements of chlorophyll, carotenoids, total phenol, anthocyanins, ascorbic acid, glucose, fructose or sucrose content (Enninghorst and Lippert, 2003; Ferrante et al., 2009; Ferrante and Maggiore, 2007). Hence, no information is at hand of changes in metabolite content of lamb's lettuce during postharvest storage on a whole plant level.

2.4. Fast and non-destructive measurement techniques

Different techniques are available to measure quality of fresh produce. Non-destructive measurements are desirable, because they do not generate waste and can be applied to each individual plant instead of on a limited sample. Also, it is essential that the measurements can be performed on site, they need to be fast and provide accurate information about the quality of the produce before they are sold. Measurement techniques that meet all these conditions are different types of visible / near infrared spectroscopy and chlorophyll fluorescence measurements. All these techniques exploit the interaction of light with plant tissue to determine the quality of fresh produce.

2.4.1. Interaction of light with plant tissue

2.4.1.1. The electromagnetic spectrum

Electromagnetic radiation has properties which are wave and particle-like. An electromagnetic wave exists out of an electric and magnetic field vector in phase and perpendicular to each other and perpendicular to the direction

of the propagating wave (Tipler and Mosca, 2008). The electromagnetic spectrum exists out of various types of electromagnetic waves which differ only in wavelength (λ) and frequency (ν) (Fig. 2.6). Wavelength and frequency are inversely related to each other according to the equation:

$$\nu = c / \lambda \quad \text{Eq. 2.2}$$

Where c is the speed of light. The different wavelengths of electromagnetic waves have an influence on their properties. Short wavelengths are related to higher frequencies and contain more energy. Hence, electromagnetic waves with shorter wavelengths can penetrate many materials which are non-penetrable for longer wavelengths.

Electromagnetic waves have properties resembling those of particles where energy is quantized. These quantized packages of energy are called photons. The energy of a photon (E) is linked to the frequency according to the equation:

$$E = h\nu \quad \text{Eq. 2.3}$$

Where h is Planck's constant.

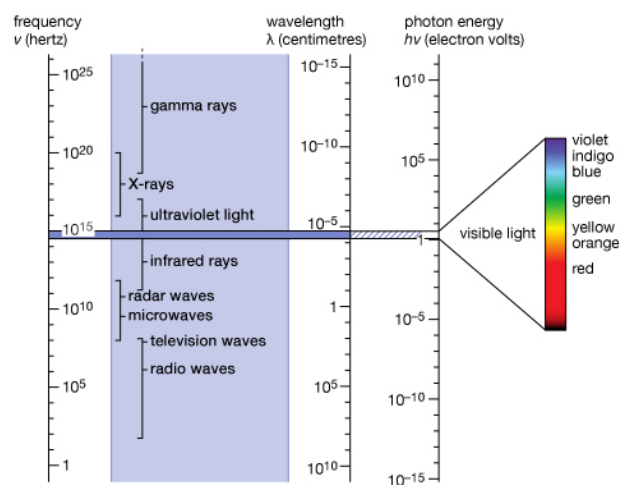


Fig. 2.6 The electromagnetic spectrum with the names of different frequency and wavelength ranges. These ranges are not well defined and can overlap. The visible range (shaded) is shown enlarged at the right (Encyclopaedia Britannica, 2018).

2.4.1.2. Interactions with light

Radiation can be reflected, refracted, transmitted or absorbed when it hits a sample (Tipler and Mosca, 2008). Direct reflection on the surface of a sample can be specular or diffuse. If the surface is smooth, the reflection is called specular reflection. If the rays of light are parallel before they reflect of a surface they stay parallel when they are reflected. If the surface is rough, the reflection is called diffuse reflection because the rays reflect in random directions. Refraction happens when a beam of light strikes a boundary surface which separates two media. The angle of the incoming rays is different from the outgoing ones and this effect is called refraction (Tipler and Mosca, 2008). Scattering in a sample results from multiple refractions at phase changes inside the material (Nicolai et al., 2007).

When radiation is absorbed, a transition of an atom or molecule to an excited state takes place. When a spontaneous transition to a less energetic state takes place, the atom or molecule undergoes transitions to one or more intermediate states before it returns to the ground state. Only the latter emits radiation. Hence, the energy in the emitted electromagnetic wave is lower and the wavelength longer. This process is often called fluorescence. The lifetime of an atom or molecule in the excited state is very low, the process of fluorescence seems to appear instantaneously. However, some excited states have longer lifetimes and can occur in a metastable state which emits light longer after the original excitation. This process is called phosphorescence (Tipler and Mosca, 2008; Visser and Rolinski, 2017).

2.4.1.3. Leaf pigments

A pigment is known as a substance that absorbs certain wavelengths specifically and has therefore a specific color. Most pigments absorb certain wavelengths and transmit or reflect wavelengths that they do not absorb. The spectrum of visible light ranges from violet with the shortest wavelength through indigo, blue, green, yellow, orange and finally red with the longest wavelength. Leaves have pigments that can absorb light in specific regions

of the spectrum and are optimized for photosynthesis in a chemical and structural way (Mauseth, 2008; Raven et al., 1999).

Chlorophylls

Green leaves are green due to the pigments chlorophyll a and chlorophyll b which are involved in photosynthesis. Chlorophyll a absorbs violet/blue and red wavelengths (Fig. 2.7). It interacts directly in the light requiring reactions of photosynthesis. Chlorophyll b is an accessory pigment and acts indirectly in photosynthesis by transferring light it absorbs to chlorophyll a. It is structurally slightly different from chlorophyll a as are the absorbed wavelengths, i.e., blue and orange/red (Fig. 2.7). The use of accessory pigments is broadening the range of light usable for photosynthesis. (Lee, 2007; Mauseth, 2008; Raven et al., 1999; Taiz and Zeiger, 2010).

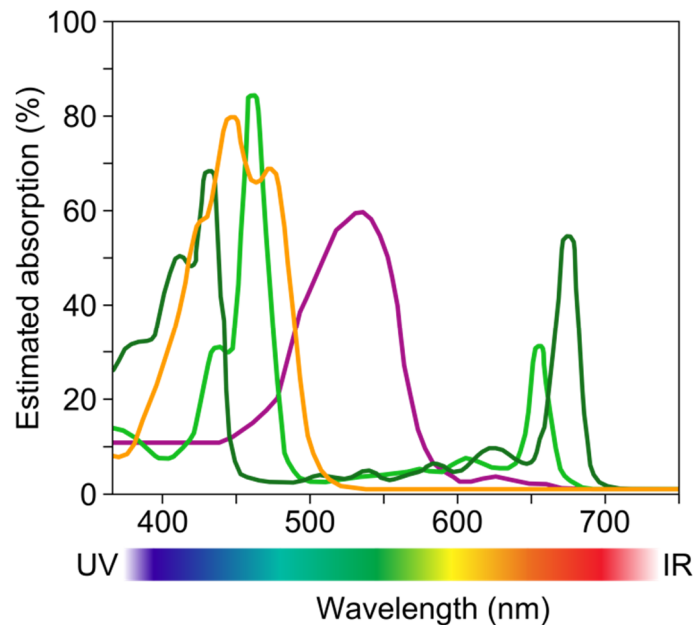


Fig. 2.7 Absorption spectra of chlorophyll a (dark green), chlorophyll b (light green), carotenoids (orange) and anthocyanins (purple). The wavelengths shown range from the edge of ultraviolet (UV) through the visible spectrum to the edge of infrared (IR) (Based on Lee, 2007 and Raven et al., 1999)

Carotenoids

Another family of accessory pigments is that of carotenoids. This family is split in two classes: xanthophylls and carotenes. Xanthophylls contain oxygen while carotenes are purely hydrocarbons. Both of these classes have a red, orange or yellow color due to absorption of wavelengths in the violet to green/blue part of the spectrum (Fig. 2.7). Carotenoids have another function besides being an accessory pigment. They also serve as an antioxidant preventing photo-oxidative damage to the chlorophyll molecules. In green leaves, chlorophyll masks the color of carotenoids. However, when chlorophyll breaks down, the carotenoids become visible, as is noticeable in yellow and orange colored autumn leaves (Mauseth, 2008; Raven et al., 1999; Taiz and Zeiger, 2010).

Flavonoids

Flavonoids are water-soluble pigments. They are one of the largest families of plant phenolic compounds and are divided in several classes amongst which anthocyanins, flavones and flavonols are the most common. Anthocyanins have a blue, purple or red color (Fig. 2.7). They protect leaves against excessive sunlight which can cause damage to leaf tissues. Flavones and flavonols are yellow or ivory-colored pigments. Sometimes they are colorless, but they can change the color of a plant part by forming complexes with anthocyanins and metal ions in a process called copigmentation (Raven et al., 1999; Taiz and Zeiger, 2010).

Postharvest changes in pigment content of leafy vegetables

After harvest, certain leaf pigments undergo degradation that leads to a change in leaf color. The decline of the total chlorophyll and carotenoid content starts quickly after harvest at ambient temperatures, but can be slowed down by storage at lower temperatures (Ferrante and Maggiore, 2007; Yamauchi, 2015). This has been observed in several horticultural products including rocket salad, Swiss chard and celery (Ferrante et al., 2004; Ferrante and Maggiore, 2007; Viña and Chaves, 2003). Chlorophyll

synthesis in angiosperms is light dependent. Hence, the production of chlorophyll is impossible if plants are stored in the dark (Heyes and Neil Hunter, 2009). In rocket salad, the degradation of chlorophyll and carotenoids has been shown to be stimulated by the presence of light which stimulates the production of reactive oxygen species (Ferrante et al., 2004). However, research on lamb's lettuce has shown that low-intensity light cycles have a positive effect on the concentrations of chlorophyll and carotenoids (Braidot et al., 2014). This is suggested to be due to the partial activation of photosynthesis which leads to the production of bioactive molecules and only low amounts of reactive oxygen species.

2.4.2. Visible / near infrared spectroscopy

Wavelengths of the electromagnetic spectrum between 780 and 2500 nm cover the near infrared (NIR) part, while wavelengths between 380 and 780 nm cover the visual (Vis) part of the electromagnetic spectrum. In Vis / NIR spectroscopy, the sample which is measured is irradiated with electromagnetic radiation. This radiation hits the sample and can be transmitted, absorbed or reflected. The contribution of each of these effects depends on the chemical and physical properties of the sample (Nicolai et al., 2007).

Absorption of a photon by C-H, O-H and N-H bonds of sugars, water and other organic compounds are the most dominant (Nicolai et al., 2014). The fundamental vibrations occur in the infrared region. Hence, the most prominent absorption bands occurring in the NIR region of the spectrum are related to overtones and combinations of fundamental absorptions in the far and mid infrared (IR) part of the electromagnetic spectrum. Overtones occur when an atom or molecule is excited to another state than the first excited state. Combinations are observed when multiple vibrations are excited at the same time. This results in broad, overlapping and weaker absorption bands than in the far and mid IR region (Reich, 2005). In complex mixtures such as biological tissues the NIR spectra have no sharp peaks and they all look similar (Fig. 1.2). The spectra are dominated by overtone bands of the OH-

bonds of water at 760, 970 and 1450 nm and carbohydrate absorbance bands exist around 750, 900, 1175 and 1400 nm (Nicolai et al., 2007; Xiaobo et al., 2010). Also, there are a lot of variables which are strongly correlated. These peculiarities of NIR spectra are the reason why chemometric data processing is essential to relate spectral information to sample properties (Nicolai et al., 2007).

An NIR spectrophotometer is composed of a light source, which is usually a tungsten halogen light bulb, a sample presentation accessory, detector and extra optical components. The latter can be lenses, collimators, beam splitters, integrating spheres and optical fibers (Nicolai et al., 2007; Reich, 2005). The classification of spectrophotometers is made based on the method to quantify the light intensity at different wavelengths and some examples are listed in Table 2.1 (Nicolai et al., 2007).

Table 2.1 A list of monochromators used in Vis / NIR spectroscopy

Name	Explanation
Filter	The monochromator is a wheel with absorption or interference filters. The spectral resolution is limited.
Scanning monochromator	A rotatable grating or a prism separate individual frequencies of radiation when these enter or leave the sample. The rotation is used to make the radiation of the individual wavelengths reach the detector.
Fourier transform	An interferometer is used to generate modulated light; the time domain signal of the light reflected or transmitted by the sample can be converted into a spectrum via a Fourier transform.
Photodiode array	A fixed grating disperses radiation onto an array of photodiode detectors. These can vary in material e.g. silicon (350–1100 nm), InGaAs (Indium Gallium Arsenide, 950 – 1700 nm).
Laser based	No monochromator is present, but instead different lasers are used or the tuning of the laser is changed.
Acoustic optic tunable filter	A diffraction based optical-band-pass filter is used that is tunable to pass different wavelengths by changing the frequency of an acoustic wave propagating through an anisotropic crystal medium.
Liquid crystal tunable filter	A birefringent filter is used to create constructive and destructive interference based on the retardation, in phase between the ordinary and extraordinary light rays passing through a liquid crystal. In this way, they act as an interference filter to pass a narrow waveband of light.

Different measurement set-ups are available for obtaining near infrared spectra, i.e., reflectance, transmittance, transreflectance and interactance (Fig. 2.8). In a reflectance set-up the light source and detector are placed under a specific angle to avoid specular reflection. In a transmittance configuration the detector is positioned on the opposite side of the detector. Transreflectance is a combination of these two. A highly reflective background is placed behind the sample which reflects all the radiation which would have passed through the sample. This radiation reflects off the background and interacts again with the sample. The detector is placed under an angle similar to the reflectance set-up. An interactance set-up has a light source and detector parallel to each other. It is necessary that the specular reflection cannot reach the detector. This can be achieved by using a cable which contains parallel optic fibers connected to the source or the detector on one side and the sample on the other side (Nicolai et al., 2007; Reich, 2005).

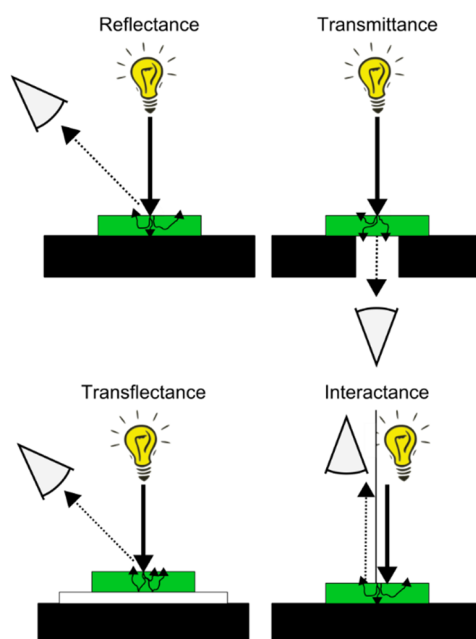


Fig. 2.8 Setup for the acquisition of NIR spectra, with a light source (light bulb), sample (green), monochromator/detector (grey), support (black) and reflective background (white). The radiation is depicted as a thick solid arrow for incoming light, small solid arrow for internal scattering and a dotted arrow is used for the measured outgoing light. The interactance setup has a physical separation between the incoming and outgoing light.

The potential of NIR spectroscopy to analyze and characterize vegetables and fruits has been shown before (Nicolai et al., 2007). Applications include the nondestructive determination of soluble solids content and dry matter of kiwifruit (McGlone et al., 2002); firmness and soluble solids content of pear (Nicolai et al., 2008); soluble solids content of stone fruit (Golic and Walsh, 2006); internal quality and optimal harvest date of apple (Lu et al., 2000; Peirs et al., 2001); bitterness, sweetness and crunchiness of chicory (François et al., 2008); moisture, ascorbic acid and soluble solids content of cabbage (Kramchote et al., 2014), among others.

Specifically on leafy greens, NIR spectroscopy has been used to distinguish between differences in production methods of *Lactuca sativa* L. (Brito et al., 2015); determine the nitrogen content in *Lactuca sativa* L. (Mao et al., 2015); determine the chlorophyll content in *Lactuca sativa* L. leaves (Yongli Zhu et al., 2011); predict the nitrate concentration of *Lactuca sativa* L. (Itoh et al., 2015); predict chlorophyll, carotenoid and anthocyanin content of green and red lettuces (Steidle Neto et al., 2017); determine pH, water content and total phenol content of fresh cut lamb's lettuce (Beghi et al., 2014; Giovenzana et al., 2014), among others. Hence, NIR spectroscopy has a lot of potential to determine the postharvest quality and freshness of lamb's lettuce.

2.4.3. Chlorophyll fluorescence

When light is absorbed by chlorophyll molecules in a leaf, one of three things can happen. In most cases, the light is used to drive photosynthesis, but it can also be dissipated as heat or re-emitted as light. The latter is chlorophyll fluorescence. By measuring chlorophyll fluorescence, information about photochemistry can be gained (Henriques, 2009; Maxwell and Johnson, 2000).

The origin of chlorophyll fluorescence can be found in PSII (Fig. 2.2). The electrons of PSII need to pass through the different steps of the electron transport chain. As long as the first electron carrier (Q_A from PQ) has not passed the electron to the next one (Q_B from PQ), it is impossible for the first

acceptor to accept another electron from PSII. In this state, the reaction center is said to be in a closed state. This leads to a reduction in the efficiency of photosynthesis and an increase in chlorophyll fluorescence and heat dissipation. Of the absorbed light not used for photochemistry, most is converted into heat. (Henriques, 2009; Maxwell and Johnson, 2000; Taiz and Zeiger, 2010).

2.4.3.1. Variable chlorophyll fluorescence

When a leaf has been in the dark long enough, all the components of the photosynthetic electron transport chain are in the oxidized state. PSII is open and ready for photosynthesis. However, the mechanism for heat dissipation is not operational, because it needs a proton gradient over the thylakoid membrane. Hence, it needs the photosynthetic electron transport chain to work for a certain time to build its gradient. In this case, fluorescence is the only alternative to deactivate the excitation energy from PSII (Henriques, 2009).

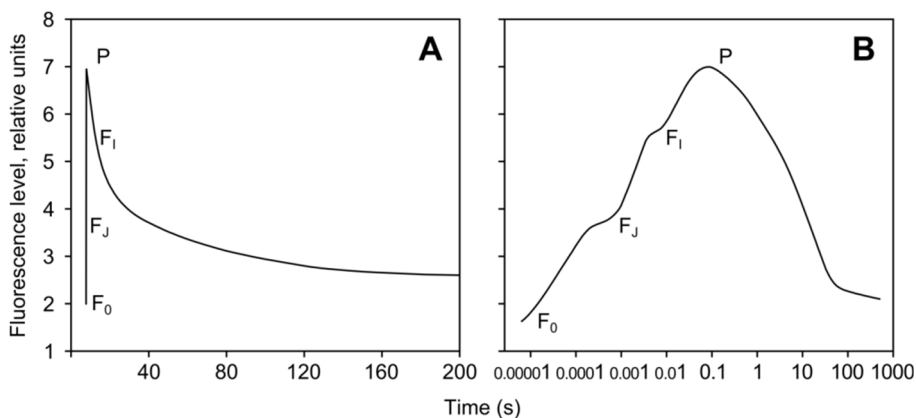


Fig. 2.9 Typical response of a dark adapted leaf to a saturating flash of light plotted in a linear (A) and logarithmic (B) timescale (Based on Henriques, 2009).

A typical response of a dark adapted leaf to a saturating flash of light is shown in Fig. 2.9. In a linear timescale, the increase in fluorescence due to the closing reaction centers is shown by a vertical straight line from its origin (O) to its peak (P) (Fig. 2.9A). The decrease in fluorescence afterwards is mostly due to the reopening of the reaction centers when electrons move from the PQ to electron acceptors downhill in the photosynthetic electron transport chain. When the x axis is plotted on a logarithmic scale the vertical straight line is waved with two inflections at J and I (Fig. 2.9B). This OJIP curve shows the filling of PSII electron acceptors (Henriques, 2009). The rise from O to J is due to the closure of PSII reaction centers due to the oxidation of Q_A . Next, Q_A is reoxidized by Q_B which opens PSII and the curve becomes a bit less steep. The following steep rise from J to I reflects a new closure of PSII when Q_A is reduced. The reoxidation of Q_A causes the curve to level off again at point I. The last rise to P corresponds to a full closure of PSII (Strasser and Srivastava, 1995).

The change in chlorophyll fluorescence with dark adapted leaves yields no information on the performance of PSII under real life continuous light conditions. Pulse amplitude modulation (PAM) fluorometers are used to measure chlorophyll fluorescence kinetics of leaves under field conditions (Brooks and Niyogi, 2011). PAM fluorometers use three types of light sources: weak modulated measuring light, actinic light with a moderate intensity and saturating light. The weak modulated measuring light is used to excite fluorescence and actinic light is used to drive photosynthesis. The detector is only sensitive to radiation which is modulated due to selective amplification of its low signal. Reflected or refracted actinic light is filtered out which makes it possible to measure fluorescence yield in sunlight (Brooks and Niyogi, 2011; Henriques, 2009). An example of a typical PAM trace is given in Fig. 2.10. Note that the maximum fluorescence yield in the light (F_m') is lower than the one in the dark (F_m). This is due to the fact that part of the absorbed radiation can now be dissipated as heat.

Chlorophyll fluorescence measurements are frequently used in photosynthesis research (Lu et al., 2002; Weng et al., 2005). After harvest, a

decrease in chlorophyll content is noticeable and can lead to a decrease in chlorophyll fluorescence (Agüero et al., 2007, 2011; Henriques, 2009; Krause and Weis, 1991). It has been shown that chlorophyll fluorescence measurements on iceberg lettuce heads at the time of harvest can be used to predict their postharvest quality (Schofield et al., 2005). However, it has to be noted that this experiment used a small amount of samples with a limited variation. Also, lamb's lettuce and cucumber quality during storage could be evaluated using chlorophyll fluorescence measurements (Ferrante and Maggiore, 2007; Lin and Jolliffe, 2000). Hence, chlorophyll fluorescence measurements might be interesting to evaluate the postharvest quality and freshness of lamb's lettuce.

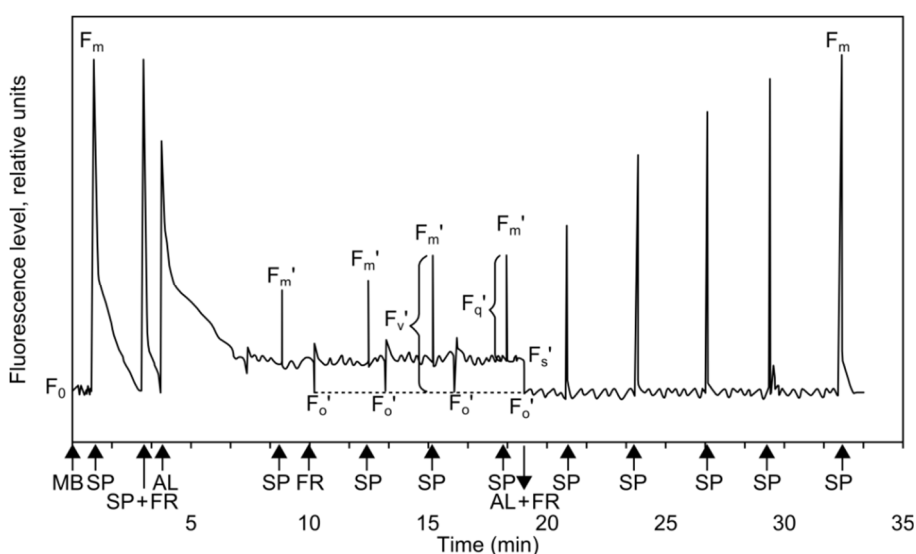


Fig. 2.10 Example of a PAM trace with the fluorescence yield of dark adapted (F_0) and light adapted (F_0') leaves; the maximum fluorescence yield in the dark (F_m) and in the light (F_m'); F_v' is the difference between F_m' and F_0' ; F_s' is the steady state fluorescence yield in actinic light; F_q' is the fluorescence quenching under actinic light due to photochemistry at PSII. The dark adapted sample is initially submitted to a weak measuring beam (MB) to determine F_0 . Next, a saturating pulse (SP) is applied to obtain F_m . After reaching F_m the chlorophyll fluorescence returns to F_0 . This process can be speeded up by applying far-red (FR) light which is preferentially absorbed by PSI and leads to a faster oxidation of the PSII-associated electron transport chain. Actinic light (AL) is turned on and a number of spikes are given to suppress photochemical quenching. This reveals the F_m' . After the AL has been switched off, a progressive recovery of the F_m takes place to detect possible damaged reaction centers due to the light period. (Based on Henriques, 2009).

2.4.3.2. Chlorophyll fluorescence emission ratios

Chlorophyll fluorescence intensities can be compared when exposed to different wavelengths of excitation light. This way, absorption of these wavelengths by other compounds can be seen as a change in the intensity of chlorophyll fluorescence. In tobacco leaves, flavonoids can screen off UV radiation (Fig. 2.11). When the UV light is absorbed by flavonoids in the adaxial epidermis, less light is absorbed by chlorophyll in the parenchyma cells. Hence, less fluorescence can be emitted. This leads to a smaller intensity of chlorophyll fluorescence when the leaves are exposed to UV light compared to when they are exposed to red light. The same principle has also been used in grape berries where green light was screened off by anthocyanins (Bengtsson et al., 2006; Ghozlen et al., 2010).

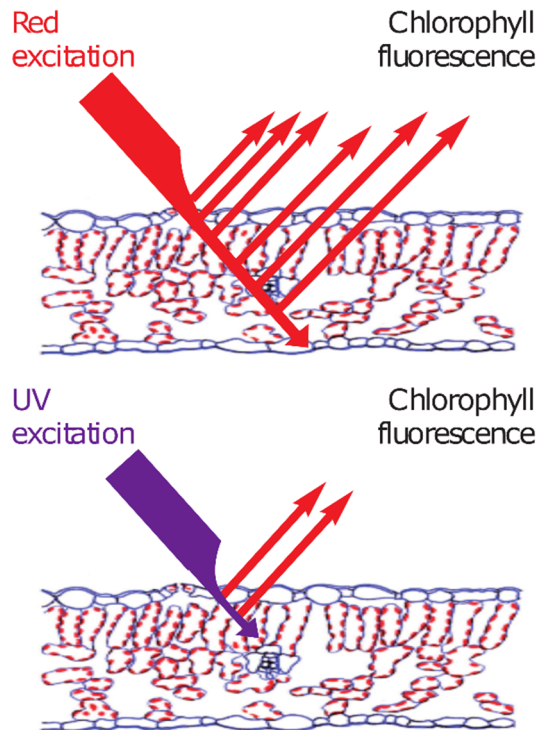


Fig. 2.11 Example of the variable absorption of light with a different wavelength in tobacco leaves. UV light is absorbed by flavonoid accumulation in the adaxial epidermis, while this is not the case for red light. This leads to a larger signal in chlorophyll fluorescence when the leaves are exposed to red light compared to UV light (Tremblay et al., 2011).

Table 2.2 Nomenclature of fluorescence emission signals. The central wavelength of the excitation and emission band is indicated between brackets.

Emission (nm)	Excitation			
	Ultraviolet A (373 nm)	Blue (470 nm)	Green (516 nm)	Red-orange (635 nm)
Yellow fluorescence (590 nm)	YF _{UV}	YF _B ^a	YF _G ^a	YF _R ^a
Red fluorescence (685 nm)	RF _{UV}	RF _B	RF _G	RF _R
Far-red fluorescence (735 nm)	FRF _{UV}	FRF _B	FRF _G	FRF _R

^a These signals are reflected light rather than fluorescence

Multiple excitation fluorescence sensors using light emitting diodes (LED's) are commercially available. Each LED emits a narrow wavelength band of light onto the sample, one wavelength band at a time (Cerovic et al., 2009; Tremblay et al., 2011). These bands are typically situated in the ultraviolet A (UV, 375 nm), blue (B, 470 nm), green (G, 516 nm) and red-orange (R, 625 nm) regions of the electromagnetic spectrum (Fig. 2.12). The pulsation of these LED's is synchronized with three photodiode detectors which detect the yellow (YF, 590 nm), red (RF, 685 nm) and far-red (FRF, 735 nm) fluorescence emitted by the sample. Hence, for each excitation wavelength band there are three fluorescence emission signals. An overview of the nomenclature is shown in Table 2.2. (Cerovic et al., 2009; Ghozlen et al., 2010; Tremblay et al., 2011).

Fluorescence signals are sensitive to the distance between the sample and the detector, and the light scattering in the tissue. Hence, it is encouraged to combine fluorescence signals in ratios (Cerovic et al., 2009). Ratios have been used to determine chlorophyll, anthocyanin and flavonol content (Agati et al., 2007, 2005; Buschmann, 2007; Cerovic et al., 2002). Also, a nitrogen balance index has been developed which provides information on the carbon-nitrogen ratio (Cartelat et al., 2005; Demotes-Mainard et al., 2008; Meyer et al., 2006). Some combinations of different fluorescence signals are summarized in Table 2.3.

Fluorescence emission ratios have been used for determining wine grape phenolic maturity, flavonols and anthocyanin content (Cerovic et al., 2008; Ghozlen et al., 2010; Kolb et al., 2003); estimating anthocyanin and

flavonoid content in apples (Hagen et al., 2006; Merzlyak et al., 2008); and determining anthocyanin content in olives (Agati et al., 2005); among others. More specific on leaf samples, fluorescence emission ratios have been successful in determining photo protection in leaves (Bilger et al., 2001; Cerovic et al., 2002); identifying phenolic and flavonoid content in lettuce plants (Zivcak et al., 2017); estimating anthocyanin content in leaves of different species (Bidel et al., 2015; Müller et al., 2013; Pfündel et al., 2007); estimating flavonoid content in leaves of different species (Agati et al., 2011; Latouche et al., 2013; Sytar et al., 2015, 2014); in monitoring the nitrogen status in grapevine and tobacco leaves (Cerovic et al., 2015; Tremblay et al., 2011). Hence, plant pigment fluorescence emission ratios could also be informative on the postharvest quality and freshness of lamb's lettuce.

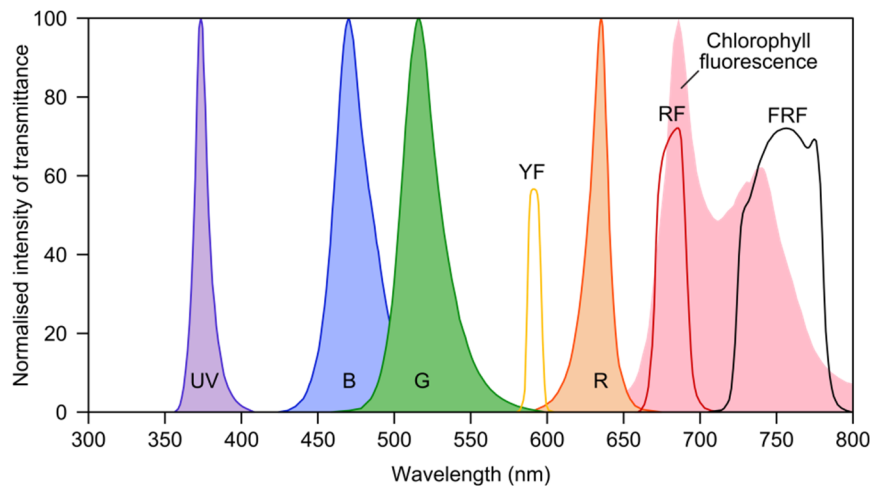


Fig. 2.12 The excitation light frequencies (UV, B, G, R) and fluorescence detection frequencies (YF, RF, FRF) of the Multiplex 3 (Based on Tremblay et al., 2011).

2.4.4. A need for multivariate statistics

The output of certain measurement set-up, e.g. Vis/NIR spectroscopy and chlorophyll fluorescence emission ratios, produces a lot more data which can be strongly correlated. Hence, these datasets can be less straight forward to interpret than the variables of measurement techniques with only a few variables with lower correlation, as is the case for the chlorophyll fluorescence measurements. Hence, it is necessary to apply multivariate statistics (also called chemometrics) to search for correlations between the measured independent variables and the response variable of interest (Ghozlen et al., 2010; Nicolai et al., 2007).

2.4.5. On-line measurements of fresh produce

Fast and non-destructive measurements are essential for on-line measurement of fresh produce. Compared to Vis/NIR spectroscopy and chlorophyll fluorescence emission ratios, classical chlorophyll fluorescence measurements in daylight take up more time for each measurement or the measured leaves need a dark adaptation period before the actual measurement, which can take up to 30 minutes (Henriques, 2009; Maxwell and Johnson, 2000). Besides, only information on the status of PSII is gathered which can be considered as limited for a measurement technique which requires 30 min per measurement. Vis/NIR spectroscopy and chlorophyll fluorescence emission ratios can be performed in ambient light in a shorter time (< 1 s) without any dark adaptation period and seem more suited for on-line measurements (Cerovic et al., 2009; Nicolai et al., 2007).

Table 2.3 Commonly used fluorescence ratios

Acronym	Formula	Description	Reference
SFR _G	$\frac{FRF_G}{RF_G}$	Simple chlorophyll Fluorescence Ratio (Green excitation LED); linked to chlorophyll content in the sample.	Buschmann, 2007
SFR _R	$\frac{FRF_R}{RF_R}$	Simple chlorophyll Fluorescence Ratio (Red excitation LED); linked to chlorophyll content in the sample.	Buschmann, 2007
FER _{RG}	$\frac{FRF_R}{FRF_G}$	Fluorescence Excitation Ratio (Red and Green LED's); linked to the screening of leaves by anthocyanins.	Pfündel et al., 2007
FLAV	$\log\left(\frac{FRF_R}{FRF_{UV}}\right)$	Flavonol index; directly proportional to the flavonol content in the sample.	Cerovic et al., 2002
ANTH _{RG}	$\log\left(\frac{FRF_R}{FRF_G}\right)$	Anthocyanin index (Red and Green excitation LED's); proportional to the anthocyanin content of the sample.	Agati et al., 2007, 2005
ANTH _{RB}	$\log\left(\frac{FRF_R}{FRF_B}\right)$	Anthocyanin index (Red and Blue excitation LED's); proportional to the anthocyanin content of the sample.	Agati et al., 2007, 2005
FERARI	$\log\left(\frac{5000}{FRF_R}\right)$	Fluorescence Excitation Ratio Anthocyanin Relative Index; has a positive correlation with anthocyanin content of red grape berries.	Ghozlen et al., 2010
NBI _R	$\frac{SFR_R}{\left(\frac{FRF_R}{FRF_{UV}}\right)} = \frac{FRF_{UV}}{RF_R}$	Nitrogen Balance Index based on SFR _R ; complex ratio that depends on epidermal phenol and chlorophyll content. It responds to the nitrogen nutrition of the plant.	Cartelat et al., 2005; Demotes-Mainard et al., 2008; Meyer et al., 2006
NBI _G	$\frac{SFR_G}{\left(\frac{FRF_R}{FRF_{UV}}\right)} = \frac{FRF_{UV}}{RF_G}$	Nitrogen Balance Index based on SFR _G ; complex ratio that depends on epidermal phenol and chlorophyll content. It responds to the nitrogen nutrition of the plant.	Cartelat et al., 2005; Demotes-Mainard et al., 2008; Meyer et al., 2006

2.5. Chemometrics

Chlorophyll fluorescence emission ratios and Vis/NIR spectroscopy yield a complex fingerprint of the measured sample which requires advanced statistical data processing to extract chemical information from these multivariate signals. This branch of analytical chemistry involving advanced statistics is known as chemometrics. Models can be created to extract useful information, but can also be used to make predictions on future unknown samples. The construction of these models is carried out in different steps and is based on different algorithms. All of these influence the final model performance.

2.5.1. Data compression and regression

When measurement set-ups produce a high number of correlated variables, there is a need for statistical techniques that replace these by a smaller set of uncorrelated variables. The process of reducing the size of the dataset is referred to as data compression.

2.5.1.1. Principal component analysis

Principal component analysis (PCA) is a projection method that transforms a given set of variables into new orthogonal variables called principal components (PC). These PC's are linear combinations of the original variables and are calculated in an iterative process. The first PC explains the most variance in the data. The second PC explains as much as possible of the remaining variance orthogonal to the first one and so on (MacGregor and Kourti, 1995; Naes et al., 2002). Hence, the PC's are in such an order that each one covers more of the variance than the following one (Fig. 2.13). Any remaining variance is called the residual. Usually, only a few PC's are required to cover the larger part of the variance in the data, resulting in an easier interpretation of the PCA model compared to the original data (MacGregor and Kourti, 1995; Naes et al., 2002). The purpose of PCA is to

find the directions in the data space where the variance between the data points is the largest.

Scores and loadings are important for interpreting data correctly in PCA. Scores are the coordinates of the samples in the new coordinate system of PC's, while loadings are the contribution of each of the original variables to the new PC's (Fig. 2.13). Loadings and scores plots are plots with the PC's on the axis where the loading vectors or scores are plotted. In a bi-plot, both loadings and scores are shown in the same plot.

The covariance between variables and the differences between samples are easily visualized using PCA, because similar variables and samples are grouped together in a loadings and scores plot, respectively. This makes PCA useful for exploration of the data at the initial stages of data analysis.

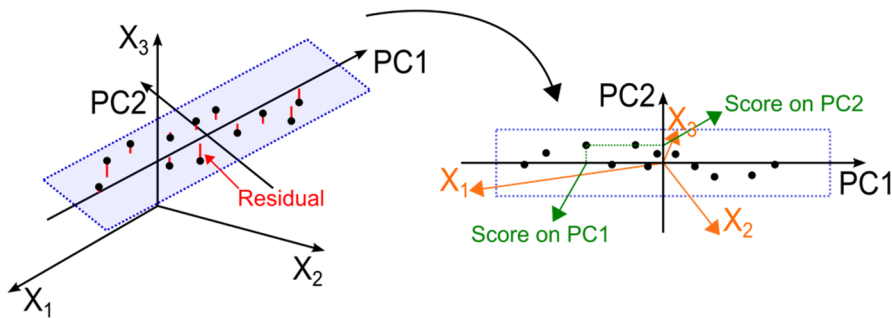


Fig. 2.13 An example of PCA on a three variable dataset (X_1 , X_2 , X_3). On the left, the data is shown in three dimensions where the variables are plotted on each axis. In a PCA the first PC is drawn in the direction where it explains the most variance. Next the second PC is drawn orthogonal onto the first one in the direction which it explains the most of the remaining variance. The red lines between the data points and the blue plain of PC1 and PC2 are the residuals, the variance not explained by either of the 2 PC's. On the right the blue plain is plotted in two dimensions with PC1 and PC2 as the axis. It describes the same dataset in less variables. It is called a scores plot. The data points have scores for each PC which are highlighted in green for one point, any remaining information in the residuals is lost. Also on the right, the loading vectors of the original variables are plotted in orange. This is called a loadings plot. The length and direction of each vector illustrates the importance of each variable for the PC's. When scores and loadings are plotted together, it is called a bi-plot (Based on Saeys, 2014).

2.5.1.2. Principal component regression

Principal component regression (PCR) is a multivariate regression technique aimed at establishing a relationship between independent X variables and an observed response variable Y (Wold et al., 2001). PCR has 2 steps. First the independent X variables are decomposed using PCA. Next, a multiple linear regression is performed on the first PC's instead of using the original variables. The advantages are that less variables are used. Hence, less coefficients have to be estimated which results in a more reliable estimation of the regression coefficients. Also, PC's are orthogonal and thus uncorrelated which is good for multiple linear regression which does not perform well with highly correlated data (Naes et al., 2002). The downside of using PC's is that they are focused on explaining the variance of X variables which are not necessarily the most informative with respect to the response variable Y (Wold et al., 2001).

2.5.1.3. Partial least squares regression

Partial least squares regression (PLSR) is a multivariate regression technique which overcomes the disadvantages of PCR (Wold et al., 2001). The new orthogonal variables in PLSR, called latent variables (LV's), are constructed in such a way that they maximally capture the covariance between the independent X variables and the response variable Y. Hence, LV's are ordered according to their relevance with respect to the response variable Y. The number of LV's required to capture a certain fraction of the variation in Y is typically lower than the number of PC's in a PCR model with similar performance (Nicolai et al., 2007).

2.5.2. Identifying outliers

Outliers are samples which are substantially different from the other samples in a population. They can have different origins, i.e., typing error, errors in the sensor, bad calibration, bad sample presentation, etc. A sample can be an outlier according to its values for the X variables and/or the Y variables. It

may also have a different relation between the X and Y variables than the other samples in the population. If an outliers is not dealt with through correction or removal, it can disturb the subsequent analyses (Bro et al., 2014; Nicolai et al., 2007).

An important first step in outlier detection is to inspect the raw data (Bro et al., 2014). However, for multivariate data it may be difficult to identify samples which have a different relation between the variables. Therefore, multivariate statistics have been proposed to detect points which are outside of the normal group of sample points of the population (Nicolai et al., 2007). The Q residual is a measure for the lack-of-fit of the lower dimensional representation of the data by the model. It is a residual between the sample and the projection of the sample on the hyperplane defined by the model. The Hotelling T^2 statistic is a measure for the distance of a sample's projection on the model hyperplane to the center of that hyperplane (Bro et al., 2014; Wise et al., 2006). Samples can be outliers due to being faulty samples or due to being underrepresented. If the latter is true, removing the sample is not the solution, but similar samples should be added to the population (Bro et al., 2014). In practice, only outliers which have a negative effect on the regression model should be removed from the dataset (Martens and Naes, 1989).

2.5.3. Validation methods

The goal of making a prediction model is to construct a model which will perform well on future samples. This is not the same as describing the calibration data very well, because there is a chance of overfitting these training data. Hence, it is necessary to evaluate the model performance on data which was not used for training the model (Andersen and Bro, 2010). This can be obtained by splitting the dataset in a calibration set and a validation set. Typically, the ratio of the number of calibration to validation samples is 2 to 1. The calibration data is used for the construction of the model, while the validation data is used for determining the prediction error. The selection of the data from the calibration set can be at random, manual

or groupwise. However, there is always the chance that the calibration and validation dataset are not representative for the complete population (Wise et al., 2006), such that the obtained results depend on the data split.

Cross validation (CV) is a method for testing a model's performance where different splits of the data in calibration and validation are used and for each combination a calibration and prediction are performed (Naes et al., 2002). A leave-one-out cross validation (LOOCV) removes one sample from the calibration dataset at a time and a model is constructed from the remaining samples. The value of the response variable for this one sample is estimated by this model. Next, the following sample is taken out of the calibration dataset and the previous sample is placed back. This procedure is repeated until all the samples have been left out once and the variance of all the prediction residuals is estimated (Naes et al., 2002). However, for larger data sets this procedure is computationally intensive and has a great tendency to underestimate the true prediction error. Hence, it is recommended to leave multiple samples out in each round (Baumann, 2003). Several methods of splitting up the data in CV are known, e.g. venetian blinds, contiguous blocks, random segments, groupwise (Naes et al., 2002; Wise et al., 2006).

Apart from such internal validation strategies involving the splitting of a dataset, one can also evaluate the model performance on an independent test set, e.g., measured in a different year, at a different location, in a different season, on a different cultivar, etc. (Nicolai et al., 2007). This is known as external validation. Such an independent test set provides a more realistic way of testing the prediction performance of the model. Therefore, it is recommended to use an external validation when possible.

2.5.4. Evaluating model performance

It is necessary to evaluate the prediction error of a calibration model and a common way to describe it is with the root mean square error (RMSE):

$$RMSE = \sqrt{\frac{1}{n} \sum_{i=1}^n (y_i - \hat{y}_i)^2} \quad \text{Eq. 2.4}$$

where n is the number of samples in the CV or validation dataset, \hat{y}_i and y_i are the predicted and measured values for the i^{th} sample respectively. This value gives the average uncertainty for future predictions on new samples expressed in the same units as the original response variable (Naes et al., 2002). Depending on the residuals on which it is calculated, it is defined as the root mean square error of cross validation (RMSECV), validation (RMSEV) or prediction (RMSEP). The value is also used to determine the model complexity by choosing the number of LV's which minimizes the RMSECV or RMSEV (Nicolai et al., 2007).

The coefficient of determination (R^2) is another useful statistic. It has a value between 0 and 1 and represents the fraction of the variance of the response variable Y that is explained by the model based on the X variance (Wright, 1921).

2.5.5. Pre-processing methods

Modification of the data before analysis is called pre-processing. It is used to remove irrelevant variance and linearize the variables to improve the performance of the regression techniques (Nicolai et al., 2007; Wise et al., 2006). Linearization is important, because most modelling methods imply a linear relation (e.g., PCR, PLS) and this is easier to model than non-linear ones. Irrelevant sources of variation in the data will force the model to consume more degrees of freedom (more PC's or LV's). Thus, it is advisable to remove as much of this interfering variation as possible. A variety of pre-processing methods have been developed (Rinnan et al., 2009) and the ones used in this PhD research are briefly explained below.

2.5.5.1. Mean centering and standardization

Mean centering subtracts the average from each variable. It makes all the variables interpretable in terms of variation around the mean. Standardization divides each variable of a sample by the standard deviation of this variable calculated over all samples. In this way, all variables are given an equal importance when the typical variance is standardized to one, but other standardizations are possible (Naes et al., 2002). Standardization is very useful when variables expressed in different units are included as X variables (Nicolai et al., 2007). When mean centering and standardization are combined, it is often referred to as autoscaling (Wise et al., 2006)

2.5.5.2. Scatter correction

The most commonly used scatter correction methods are multiplicative scatter correction (MSC), standard normal variate (SNV) and normalization (Rinnan et al., 2009). These techniques are designed to reduce the variability caused by light scattering between samples and are frequently used with NIR spectroscopic data. MSC is probably one of the most used pre-processing techniques. It is applied when additive (baseline shift) and multiplicative (tilt) effects have to be removed from the spectrum. MSC tries to remove the scatter effect by linearizing each spectrum to a reference spectrum. Typically, the average of all the spectra is chosen as a reference spectrum, but it can also be a generic reference spectrum (Nicolai et al., 2007; Rinnan et al., 2009). SNV is another popular method for scatter correction of NIR data which gives very similar results to MSC (Dhanoa et al., 1994). SNV normalizes each spectrum to a zero mean and unit variance. Compared to standardization, SNV normalizes all the variables over the entire spectrum for each sample instead of each variable being standardized to the standard deviation of that column. (Nicolai et al., 2007; Rinnan et al., 2009).

2.5.5.3. Multivariate filtering

Sometimes, pre-processing techniques are not selective enough to remove signals which interfere with a good calibration. Multivariate filtering methods before the calibration can improve this calibration process. These filtering methods identify how variables change together and filter out patterns in these variables which are not beneficial to the model. A common way these filters work is by downweighting X variables which change when the Y variables are similar or by removing variation in the X variables which is uncorrelated to the Y variation, because samples with similar Y variables should theoretically have a similar covariance structure (Wise et al., 2006). The most popular techniques working according to this principle are Orthogonal Signal Correction (OSC), which downweights variance in the X-block that is orthogonal to the Y-block (Wold et al., 1998); External Parameter Orthogonalization (EPO), which orthogonalizes a number of patterns identified as clutter based on differences between similar samples (Roger et al., 2003) and Generalized Least Squares Weighting (GLSW) (Martens et al., 2003; Zorzetti et al., 2011), which downweights variables based on differences between similar samples with an amount based on a weighting parameter α .

2.5.6. Variable selection

Variable selection encompasses the removal of irrelevant, noisy or unreliable variables. This improves model performance resulting in better predictions, reduced model complexity and improved robustness (Andersen and Bro, 2010; Mehmood et al., 2012; Xiaobo et al., 2010). This might seem unnecessary, because up and downweighting of variables in relation to the response variable is an inherent property of PLS. However, The PLS-algorithms accuracy is reduced when more variables are used (Mehmood et al., 2012). Likewise, irrelevant variables can negatively affect the model robustness (Höskuldsson, 2001).

The ideal way to perform variable selection could be seen as trying all different combinations of variables and choosing the best set. However, this is not feasible, due to the fact that there are too many possible combinations which would make this too cumbersome and would take up too much time. Also, there is a high risk of overfitting unless the number of samples is much higher than the number of possible combinations of variables (Andersen and Bro, 2010). Hence, variable selection techniques have been developed which try to find a good set of variables instead of the optimal set of variables (Andersen and Bro, 2010).

Variable selection techniques can improve model performance, but on the other hand useful variables can be eliminated which should always be avoided. Likewise, using fewer variables makes each variable more influential for the final model. This makes a correct selection of variables even more important (Nørgaard et al., 2000). A wide variety of variable selection techniques are described in literature (Mehmood et al., 2012; Xiaobo et al., 2010). Hence, the techniques explained below are limited to the ones which have been used in this PhD research. This selection was made based on the software at hand.

2.5.6.1. Variable Importance in Projection scores

The Variable Importance in Projection (VIP) score of a certain variable is a summary of the importance of that variable for the projections to find the LV's. The VIP score for the j^{th} variable is defined as:

$$VIP_j = \sqrt{\frac{p \cdot \sum_{a=1}^A (w_{aj} / \|w_a\|)^2 \cdot SS_a}{\sum_{a=1}^A SS_a}} \quad \text{Eq. 2.5}$$

where p is the total number of variables, A the number of used LV's, $(w_{aj} / \|w_a\|)^2$ represents the importance of the j^{th} variable for the a^{th} LV and SS_a is the sum of squares explained by the a^{th} LV. Variables with a value

lower than 1 are considered unimportant while variables with a higher VIP score are considered more important. (Chong and Jun, 2005; Mehmood et al., 2012).

2.5.6.2. Interval PLS

When data are highly correlated, a window of variables is better in use instead of variable selection on each variable individually. Spectral data is highly correlated which is why interval PLS (iPLS) is a variable selection technique commonly used in spectroscopy. (Andersen and Bro, 2010; Nicolai et al., 2007; Wise et al., 2006). The first step in interval PLS (iPLS) is determining the interval size which can be a window of adjacent variables or limited to one variable. Forward iPLS fits a PLSR model to each interval and the interval with the smallest prediction error is selected. Next, combinations of this interval with each of the remaining intervals are made and a PLSR model is fitted to each combination. The combination with the smallest prediction error is selected. The process of adding an interval to the previously selected intervals is repeated until there is no improvement in the prediction error when an extra interval is added. Backward iPLS starts initially with all the intervals included in the selection and in turn each interval is excluded. A PLSR model is fitted to each combination of remaining intervals and the combination with the smallest prediction error is selected. This process is repeated and each time one interval is excluded until there is no further improvement in the prediction error when an extra interval is excluded (Nørgaard et al., 2000; Wise et al., 2006; Xiaobo et al., 2010). A consideration which should be made when using iPLS is that it may be that the best single-interval model is not included in the best dual-interval model. The latter selection of intervals cannot be found using iPLS, due to the stepwise approach (Wise et al., 2006).

2.5.6.3. Monte Carlo Uninformative Variable Elimination

Monte Carlo Uninformative Variable Elimination (MC-UVE) PLS is a Monte Carlo based variant of UVE-PLS. In UVE-PLS a set of random variables with the same size as the original set of X variables is added to the independent X variables (Centner et al., 1996). Next, a PLSR model is constructed with a LOOCV. For each of the variables a reliability index (RI) is calculated based on the stability and importance of the regression coefficients of the PLSR model as estimated by each cycle of the LOOCV. The RI for the j^{th} variable is defined as:

$$RI_j = \frac{\bar{\beta}_j}{\sigma_j} \quad \text{Eq. 2.6}$$

where $\bar{\beta}_j$ and σ_j are the mean and standard deviation of the regression coefficients which have been calculated for variable j on the different calibration subsets in the LOOCV. The random artificial X variables contain no useful information for the PLSR model to work with. Hence, the original X variables with an RI smaller than or equal to the largest RI obtained for the random artificial X variables are considered uninformative and are excluded (Centner et al., 1996; Mehmood et al., 2012; Xiaobo et al., 2010).

MC-UVE-PLS does not use random artificial variables. Instead, a Monte Carlo sampling of the samples is used instead of an LOOCV. The $\bar{\beta}_j$, σ_j and RI are calculated from the PLSR models based on the different Monte Carlo subsets (Cai et al., 2008; Mehmood et al., 2012). The RI ranks the variables from good (high RI) to bad (low RI) and new PLSR models are made with different amounts of variables where variables with a lower RI are discarded first. The final selection of variables to retain is based on the model performance of the different PLSR models. In most cases, this is the RMSECV or RMSEV.

2.5.6.4. Genetic algorithms PLS

Genetic algorithms PLS (GA-PLS) is a variable selection technique which is inspired by Darwin's theory of natural selection combined with PLSR (Andersen and Bro, 2010; Lucasius et al., 1994). First, the data is divided in intervals of equal size. Different combinations of these intervals, called individuals, are created by coding their 'chromosomes' as a sequence of zeros and ones indicating for each interval of variables whether it is used or not (genes) (Wise et al., 2006). The PLSR model performance of each individual is evaluated in cross validation (CV) to determine which are the 'fittest' individuals. The worst performing half of the individuals are removed and the best performing half is used to 'breed' new individuals. This is done by pairing up individuals and exchange sections of the 'chromosomes' with a single or double cross over (Fig. 2.14). These new individuals are combined with the best half of the previous generation and all of these individuals are again evaluated based on their PLSR model performance in CV. This process is repeated until a predefined fraction of the population of individuals shares the same genes or until a certain number of generations has been completed (Lucasius et al., 1994; Mehmood et al., 2012; Wise et al., 2006).

2.6. Conclusions

In this chapter, an overview has been given of the main physiological pathways in plant leaves (photosynthesis, respiration, alternative pathways) and how they can change during postharvest storage period. Limited information was found on the physiological changes in lamb's lettuce during a postharvest storage period. It is known that they can be stored at low temperatures (<4 °C) up to four weeks without any visual indication of this storage period (Chapter 1). The changes in metabolite content and respiration rate during postharvest storage may allow to evaluate if there are

still sugars available for the energy metabolism or whether other energy sources, e.g., amino or fatty acids, are used. Therefore, this will be investigated in chapter three.

Long storage periods prior to commercialization are undesirable, because they reduce the remaining storage life available to consumers after purchase. Therefore, there is a demand for a fast and non-destructive method to detect undesirable storage periods. Non-destructive measurements are desirable, because they do not generate waste and can deliver fast accurate information about the quality of lettuce before it is sold. This chapter gave an overview of some known techniques, i.e. Vis/NIR spectroscopy, chlorophyll fluorescence emission ratios and chlorophyll fluorescence. The latter measurements are less useful in practice due to the fact that these measurements need to be performed in the dark or after a

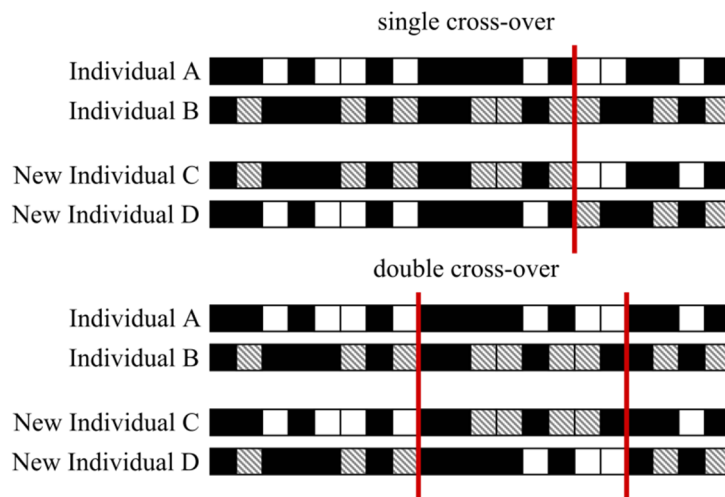


Fig. 2.14 Schematic of single and double cross-over breeding. Two individuals A and B produce new individuals C and D based on their own information. This information is represented as dark and light squares and represent included and excluded variables respectively. The information from individual B is colored darker than the information from individual A to visualize the cross-over proces. In a single cross-over there is only one cross-over point, shown here as a vertical red line. For individual C the first part of its information originates from individual B, but after the cross-over point, the remaining information is from individual A. the opposite is noticable for individual D. In double cross-over breeding there are two cross-over points. In this case for individual C, before the first and after the last cross-over point, the data originates from individual A and between these cross-over points the data originates from individual B (Wise et al., 2006).

dark adaptation period which can last up to 30 minutes. Also, only information on the status of PSII can be obtained from such measurements which can be considered as limited for a 'fast' measurement technique lasting as much as 30 min. Vis/NIR spectroscopy and chlorophyll fluorescence emission ratios can be performed in ambient light in a shorter time (< 1 s) without any dark adaptation period and seem more suited for on-line measurements. Hence, the potential of Vis/NIR spectroscopy and chlorophyll fluorescence emission ratios to estimate the prior storage period of lamb's lettuce will be investigated in chapter four and five, respectively.

3. Respiration and physiological events of lamb's lettuce during storage

3.1. Introduction

During storage, leafy vegetables are kept within an optimal range of temperature and relative humidity to maintain their quality (Kader, 2013, 2002). A lower temperature preserves quality by reducing the speed of metabolic processes. The optimal temperatures for leafy vegetables are between 1 and 4 °C (Kader, 2002). The soluble photosynthetic sugars, mainly glucose, fructose and sucrose, are the main energy reserves during postharvest storage. Lamb's lettuce has hardly any starch present as a carbon source (Enninghorst and Lippert, 2003). Glucose, fructose and sucrose can be respired or employed in biosynthetic reactions. The carbohydrates synthesized through photosynthesis before harvest result in a limited energy source for respiration. Leafy vegetables stored in dark environments are incapable of performing photosynthesis. Hence, it is possible for them to experience sugar starvation (Morkunas et al., 2012). To cope with nutrient stress, plants change their metabolism to employ different energy sources through protein and lipid breakdown (Brouquisse et al., 1991; Chen et al., 1994). These metabolic changes are essential to maintain respiration and basic metabolic processes (Morkunas et al., 2012). The

objective of this work was to study the metabolic changes occurring in lamb's lettuce during postharvest storage to get a better view on the effects it has on the shelf life potential. The hypothesis is that postharvest storage leads to a decrease in soluble carbohydrate content and a shift of the metabolism to alternative energy sources.

3.2. Materials and methods

3.2.1. Plant material and storage conditions

Lamb's lettuce (*Valerianella locusta* L.) samples were harvested on March 24, 2015, by six different commercial growers and immediately stored in refrigerated rooms (2 - 3 °C). One grower provided samples of cv 'Festival', another one provided samples of cv 'Audace' and four growers provided samples of cv 'Trophy'. An overview of the growing and harvesting conditions for each batch of lamb's lettuce are shown in Table 3.1. During the day of harvest the samples were transported to the nearby experimental station Inagro (Rumbeke-Beitem, Belgium) where the storage experiment took place. The samples were stored at 1 °C and 4 °C to evaluate the influence of storage temperature on the metabolism (Fig. 3.1). Preliminary experiments (data not shown) showed that post-harvest handling and packaging had a significant influence on the storage potential of the samples. Therefore, all samples were only analyzed once.

Table 3.1 Overview of the growing and harvesting conditions for each batch of lamb's lettuce used in the experiment.

Grower	Cultivar*	Sowing density (seeds/m ²)	Growing period (days)	Harvest date	Harvest mechanism	Rinsing time	Storage temperature local facility (°C)
1	Trophy	412	100	24/03	manual	10:00	2.0
2	Festival	850	65	24/03	automated	19:00	2.0
3	Trophy	Unknown	unknown	24/03	manual	Unknown	2.0
4	Trophy	360	103	24/03	manual	Unknown	2.8
5	Trophy	700	75	24/03	automated	19:00	3.0
6	Audace	780	87	24/03	automated	8:30	2.0

* All cultivars were from the seed company HM. Clause

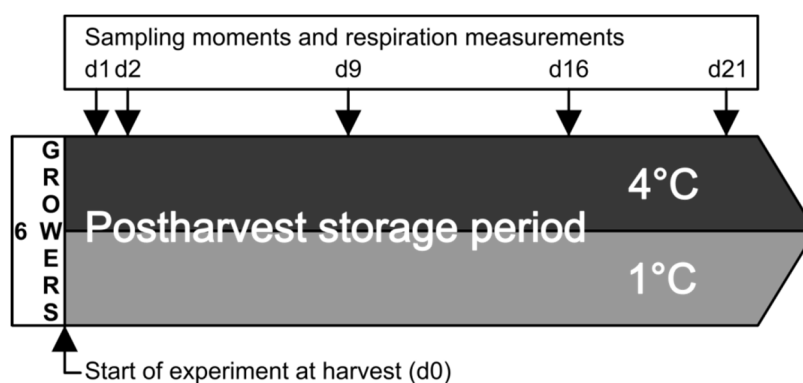


Fig. 3.1 Outline of the experimental setup. The number of days indicates the duration from the start of the experiment.

3.2.2. Respiration

After 1, 2, 9, 16 and 21 d in storage, 40 g of lamb's lettuce plant material was used for respiration measurements (Fig. 3.1). The density of lamb's lettuce was determined in previous research using Archimedes' principle (data not shown). This value ($\rho = 237 \text{ g/L}$) was used to determine the volume taken by the plant material. Each measurement day, new plants were used for respiration measurements. The plant material ($\pm 0.2 \text{ L}$) was placed in a 1.7 L respiration jar with a solid block of 0.6 L at the bottom to reduce the volume of the headspace, resulting in a remaining space around 0.9 L. Of each grower both the samples stored at 1 °C and 4 °C were used. The CO_2 and O_2 partial pressure of the headspace of the respiration jars which contained sample material were determined using a Compact Gas Chromatograph (Interscience, Louvain-la-Neuve, Belgium) and a Checkmate II (PBI Dansensor, Denmark), respectively. After the initial measurement, the airtight respiration jars were stored overnight in a cool room at 1 °C and 4 °C. After 17 h, a second measurement of the headspace was performed. The largest average increase of CO_2 in the headspace after 17 h was 0,75%. The O_2 consumption rates and CO_2 production rates were calculated by taking the difference of the gas measurements between the initial and final measurement and dividing it by the sample mass and time between two measurements (Bekele et al., 2015). The respiration quotient (RQ) was

calculated from these measurements as the ratio of the CO₂ produced to the O₂ consumed (Fonseca et al., 2002; Ho et al., 2013). The oxidation of 1 mole of hexose produces 6 mole of CO₂ and consumes 6 mole of O₂.

3.2.3. Metabolite analysis

3.2.3.1. Sample preparation

Lamb's lettuce leaves were sampled at 1, 2, 9, 16 and 21 d (Fig. 3.1). A sample for each grower at each storage temperature was taken. The leaves were ground into a fine powder after freezing in liquid nitrogen and were then stored at -80 °C. Hundred milligrams of ground powder was extracted at 70 °C for 15 min with 700 µL methanol containing 30 µL of 291 mg L⁻¹ internal standard (phenyl-β-D-glucopyranoside in methanol). Next, 700 µL distilled water was added and vortexed vigorously. Chloroform (350 µL) was added to the mixture to separate the non-polar fraction. Subsequently, the mixture was centrifuged for 15 min at 20800 g at 4 °C. The polar fraction was pipetted into a new safe-lock tube and dried with N₂ at 50 °C. The dried residue was oxidized by dissolving the residue in 40 µL of 20 g L⁻¹ methoxyamine hydrochloride in pyridine. The mixture was vortexed vigorously and incubated for 90 min at 30 °C. Next, 60 µL N, O-Bis (trimethylsilyl) trifluoroacetamide (BSTFA) was added to derivatize the mixture. BSTFA reacts with both alcohols and acids and the reaction results in trimethylsilyl ethers and trimethylsilyl esters, respectively, which are more volatile. Finally, the derivatization was carried out at 37 °C for 30 min (Mbong et al., 2017b; Oms-Oliu et al., 2011; Roessner et al., 2000).

3.2.3.2. Apparatus

A GC-MS system consisting of a 7890A gas chromatograph (Agilent Technologies, Palo Alto, CA, USA) and 5975C VLMSD mass spectrometer with triple-axis detector (Agilent Technologies) was used to separate the metabolites. A 30 m HP-5MS column (with a 5 % phenyl methysilox

stationary phase) with 250 μm internal diameter and 0.25 μm film thickness (Agilent Technologies) was used for the analysis. A split ratio of 5:1 and 20:1 was used for the analysis of acids and sugars, respectively. A 2-layer sandwich injection was used as injection type containing a 0.2 μL external standard (Tetradecane) and a 0.2 μL air gap. The carrier gas was helium at a flow rate of 1 mL min^{-1} . The temperature of the sample inlet and ion source was set to 230 $^{\circ}\text{C}$, while the temperature of the interface was set to 250 $^{\circ}\text{C}$. In the oven, the temperature cycles for the acid and sugar runs were different to get the optimized run times of 34.5 and 17.3 min. The acid run started with a 2 min heating period at 50 $^{\circ}\text{C}$ followed by a continuous increase of 10 $^{\circ}\text{C min}^{-1}$ to a final temperature of 325 $^{\circ}\text{C}$. The sugar run started with a 2 min heating period at 90 $^{\circ}\text{C}$ followed by a continuous increase of 50 $^{\circ}\text{C min}^{-1}$ to 160 $^{\circ}\text{C}$, 10 $^{\circ}\text{C min}^{-1}$ to 180 $^{\circ}\text{C}$, 50 $^{\circ}\text{C min}^{-1}$ to 215 $^{\circ}\text{C}$, 10 $^{\circ}\text{C min}^{-1}$ to 230 $^{\circ}\text{C}$, 50 $^{\circ}\text{C min}^{-1}$ to 255 $^{\circ}\text{C}$, 10 $^{\circ}\text{C min}^{-1}$ to 290 $^{\circ}\text{C}$ and 50 $^{\circ}\text{C min}^{-1}$ to a final temperature of 325 $^{\circ}\text{C}$. In both runs, the final temperature was maintained for 5 min. Before the injection of the subsequent sample, the system was equilibrated for 1 min at an initial temperature of 50 $^{\circ}\text{C}$ or 90 $^{\circ}\text{C}$ for acids and sugars, respectively. The GC-MS program was retention time-locked to tetracosane (Agilent Technologies).

3.2.3.3. Quality Control

Four quality control (QC) samples, which were a mixture of all the measured samples, were measured for both the sugar and acid run on each day spread out evenly between the samples. This resulted in a QC sample every 3 to 4 samples which were used to detect possible drifting of the GC-MS.

3.2.3.4. GC-MS analysis

The chromatograms and mass spectra generated by the GC-MS were evaluated and deconvoluted using Agilent MSD Chemstation (Agilent Technologies Inc., Wilmington, USA), AMDIS (Automated Mass Spectral

Deconvolution and Identification System, National Institute of Standards and Technology, Gaithersburg, Maryland; USA) and NIST MS Search (National institute of standards and technology Mass Spectral Search Program for the NIST/EPA/NIH Mass Spectral Library, National Institute of Standards and Technology, Gaithersburg, Maryland, USA). The retention times and mass spectra of the metabolites were compared with Agilent Fiehn GC-MS Metabolomics RTL library (Agilent Technologies) for identification. A second confirmation was done using an in-house built library. The levels of the metabolites were normalized using internal standard (phenyl- β -D-glucopyranoside in methanol), external standard (Tetradecane), peak area and sample weight. Calibration curves were obtained using pure standards and the content of each metabolite was calculated. All standards were purchased from Sigma Aldrich, Belgium.

Lists of metabolites measured with the sugar and acid runs are shown in Table 3.2 and 3.3 respectively. These metabolites were used in standard mixtures and they were extracted from lamb's lettuce samples. They are listed with the m/z used for quantification and the retention time. For each analyte, two extra qualifier ions were used to prevent misidentification. Metabolites in the text are not mentioned with the derivatized name of the molecule, but with the underivatized one. The content is expressed on a dry weight basis.

3.2.4. Statistical analysis

An ANOVA ($\alpha=0.05$) was carried out in JMP Pro (JMP® Pro, Version 12, SAS Institute Inc., Cary, North Carolina, United States). Time in storage and storage temperature were considered as continuous variables while the growers were a categorical variable. Also, an interaction term for time in storage and storage temperature was included together with a quadratic time effect.

Table 3.2 Analyte derivatives which were identified in standard mixtures and in lamb's lettuce samples using the **sugar run**.

Analyte	Retention time (min)	m/z used for quantification
Fructose 3TMS	7.988	307.2
Glucose 3TMS	8.119	319.1
Glucose-6-phosphate 3TMS	10.127	387.1
Mannitol 3TMS	8.272	319
Myo-inositol 3TMS	9.016	305.1
Ribose 3TMS	6.864	307.1
Sucrose 4TMS	11.823	451.2

Table 3.3 Analyte derivatives which were identified in standard mixtures and in lamb's lettuce samples using the **acid run**.

Analyte	Retention time (min)	m/z used for quantification
Aspartate 2TMS	14.646	232.1
Beta-alanine 3TMS	13.441	290.1
Citrate 4TMS	18.103	273.1
Fumarate 2TMS	12.321	245
GABA 3TMS	14.75	304.1
Glutamate 2TMS	15.811	246.1
Glutamine 3TMS	17.529	156
Glycine 2TMS	11.841	174.1
Isoleucine 1TMS	11.663	158
L-alanine 1TMS	8.864	116.1
Leucine 1TMS	11.654	158
Malate 4TMS	14.259	233.1
Norleucine	10.261	86
Pyroglutamate 1TMS	14.643	156
Pyruvate 1TMS	8.04	174
Serine 3TMS	12.61	204.1
Succinate 2TMS	11.886	247
Valine 1TMS	10.547	144

3.3. Results

3.3.1. Respiration

During the storage period of 21 d, the CO₂ production rate and O₂ consumption rate gradually declined (Fig. 3.2). There was no significant difference between lamb's lettuce stored at 1 °C and 4 °C. Only the time in storage was significant for the respiration rates. The respiratory quotient (RQ) remained constant over time and there was no influence of storage temperature on respiration rates or RQ.

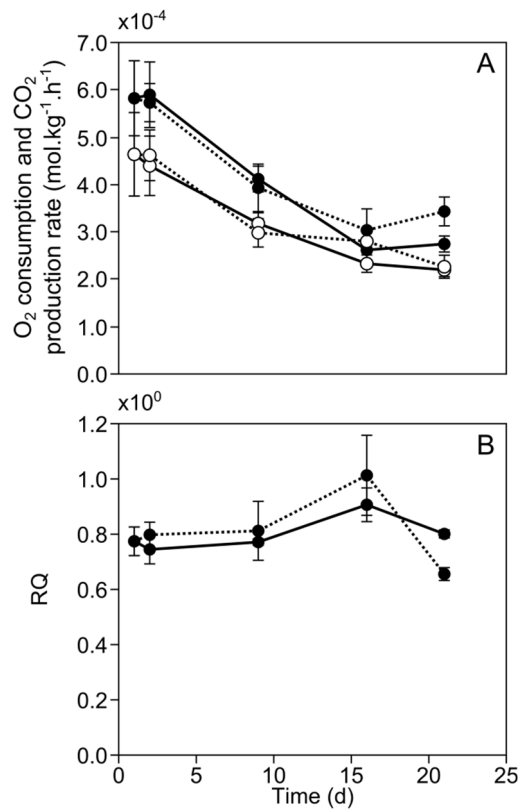


Fig. 3.2 The O₂ consumption (a, ●), CO₂ production (a, ○) and RQ (b) of lamb's lettuce during a storage period at 1 °C (—) and 4 °C (.....). The error bars represent the standard error of the mean (n=6).

3.3.2. Metabolites

Twenty-five metabolites were identified (Fig. 3.4, 3.5 and 3.6). There was a significant effect of grower on the content of all metabolites, except that of beta-alanine (Table 3.4). The variability of the metabolite content between samples from different growers on the same day in storage after harvest, was greater than the technical variability of the QC samples. The fructose and glucose content in samples from six growers are shown in Fig. 3.3. The samples from each grower are marked differently to illustrate the grower effect. The samples from grower 1 are always the ones with the highest fructose and glucose content.

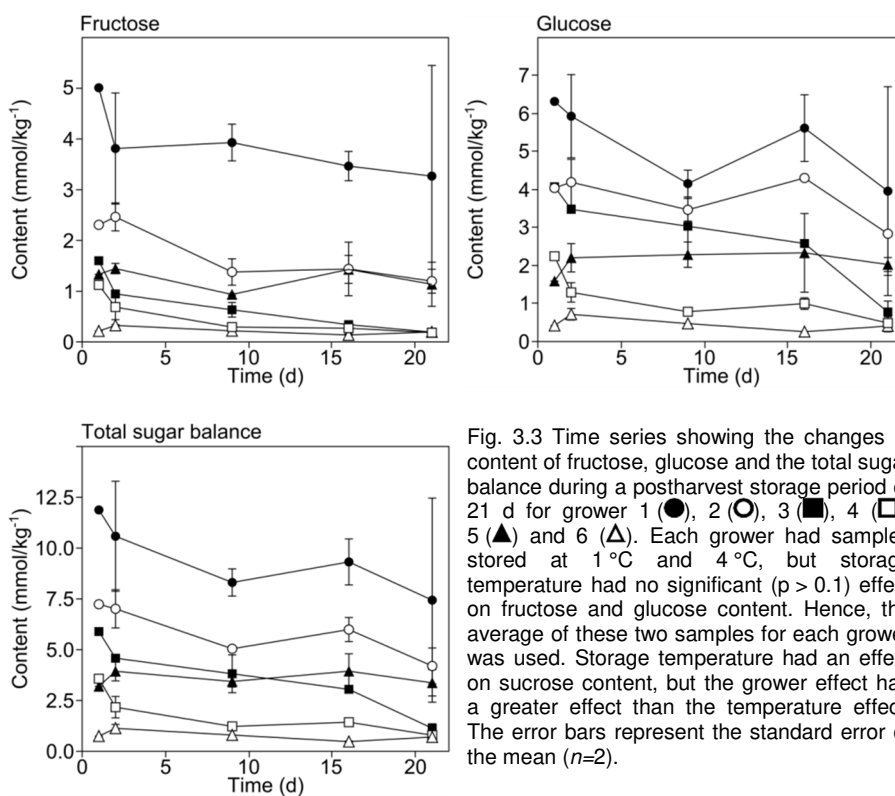


Fig. 3.3 Time series showing the changes in content of fructose, glucose and the total sugar balance during a postharvest storage period of 21 d for grower 1 (●), 2 (○), 3 (■), 4 (□), 5 (▲) and 6 (△). Each grower had samples stored at 1 °C and 4 °C, but storage temperature had no significant ($p > 0.1$) effect on fructose and glucose content. Hence, the average of these two samples for each grower was used. Storage temperature had an effect on sucrose content, but the grower effect had a greater effect than the temperature effect. The error bars represent the standard error of the mean ($n=2$).

Of the sugars and sugar alcohols measured, the content of fructose, glucose, mannitol and sucrose decreased significantly over time, resulting in a decrease of 46.7 %, 43.8 %, 52.1 % and 41.1 %, respectively, after 21 d in storage compared to the first day in storage (Fig. 3.4). The total sugar balance in hexose units decreases over time. Glucose, fructose and sucrose represent over 90 % of the total sugar balance during the entire 21 d storage period. Myo-inositol and ribose content increased significantly resulting in a 31.6 % and 29.1 % increase after 21 d in storage compared to the first day in storage. The glucose-6-phosphate (G6P) content showed no significant influence of storage time. Storage temperature affected only sucrose significantly amongst all measured sugars and sugar alcohols. A higher storage temperature resulted in a content which was 36.2 % smaller at a storage temperature of 4 °C compared to the content at 1 °C after 21 d in storage.

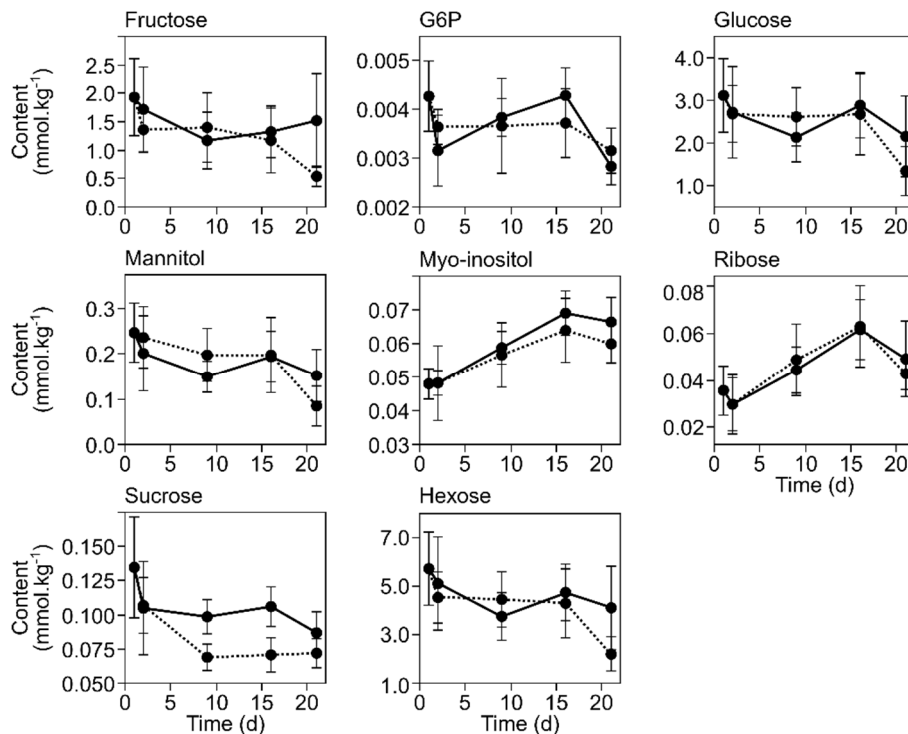


Fig. 3.4 Time series showing the changes in the content of sugars, sugar alcohols and total sugar balance in hexose units during postharvest storage for 21 d at 1 °C (—) and 4 °C (.....). The error bars represent the standard error of the mean ($n=6$).

For all the measured amino acids besides glutamine, norleucine and pyroglutamate (aspartate, beta-alanine, glutamate, glutamine, glycine, isoleucine, L-alanine, leucine, serine, valine) a significant increase in content was observed with increasing storage time (Fig. 3.5). The increase was the most extreme for isoleucine and leucine which both increased 21 and 38 fold over 21 d storage at 1 °C and 4 °C, respectively. Norleucine decreased significantly with 59.6 %, while the glutamine and pyroglutamate content did not change significantly during the 21 d storage period. The content of beta-alanine, glutamate, glutamine, glycine, L-alanine, norleucine and pyroglutamate were not significantly correlated with storage temperature. However, beta-alanine varied significantly with the interaction of storage time and temperature. The content of all other measured amino acids except aspartate (isoleucine, leucine, serine and valine) increased significantly with storage temperature. The aspartate content after 21 d in storage was 21.0 % smaller for samples stored at 4 °C than for samples stored at 1 °C. Also, the interaction between storage time and storage temperature affected the content of isoleucine, leucine, serine and valine significantly. The isoleucine, leucine, serine and valine content after 21 d in storage was respectively 80.1 %, 80.1 %, 54.6 % and 73.4 % higher for a storage temperature of 4 °C than for storage at 1 °C.

The measured metabolites of the tricarboxylic acid (TCA) cycle (citrate, fumarate, malate, succinate), pyruvate and gamma-aminobutyric acid (GABA) had different responses to a storage period (Fig. 3.6). Fumarate, malate, pyruvate and succinate content decreased with 18.1 %, 16.0 %, 31.2 % and 53.2 %, respectively, after 21 d in storage, while the content of GABA increased with 74.7 % over the same period. A negative effect of the storage temperature was significant for fumarate and succinate. This resulted in a decrease of 31.8 % and 23.8 %, respectively, at a storage temperature of 4 °C compared to the content at 1 °C after 21 d in storage.

Table 3.4 P-values for the calculated F-values of the different factors for the analyzed compounds.

Analyte	Time in storage	Storage temperature	Grower	Time in storage x Storage temperature	Time in storage ²
Aspartate	0	0.043	0	0.487	0.813
Beta-alanine	0.664	0.464	0.086	0.003	0.073
Citrate	0.079	0.259	0	0.328	0.365
Fructose	0.001	0.116	0	0.137	0.423
Fumarate	0.015	0.006	0	0.362	0.396
G6P	0.293	0.965	0	0.771	0.302
GABA	0.006	0.199	0.002	0.664	0.035
Glucose	0.027	0.669	0	0.325	0.575
Glutamate	0.003	0.503	0	0.288	0.460
Glutamine	0.765	0.837	0	0.083	0.129
Glycine	0	0.256	0	0.157	0.171
Isoleucine	0	0.000	0.005	0	0.617
L-alanine	0	0.256	0	0.218	0.259
Leucine	0	0.000	0.005	0	0.616
Malate	0.015	0.214	0	0.560	0.110
Mannitol	0.006	0.874	0	0.279	0.857
Myo-inositol	0	0.420	0	0.436	0.186
Norleucine	0.022	0.967	0	0.976	0.765
Pyroglutamate	0.169	0.149	0	0.810	0.802
Pyruvate	0.004	0.275	0	0.331	0.097
Ribose	0	0.980	0	0.718	0.023
Serine	0	0.004	0	0.008	0.660
Succinate	0	0.038	0	0.916	0
Sucrose	0	0.039	0	0.458	0.057
Valine	0	0.004	0	0.006	0.292

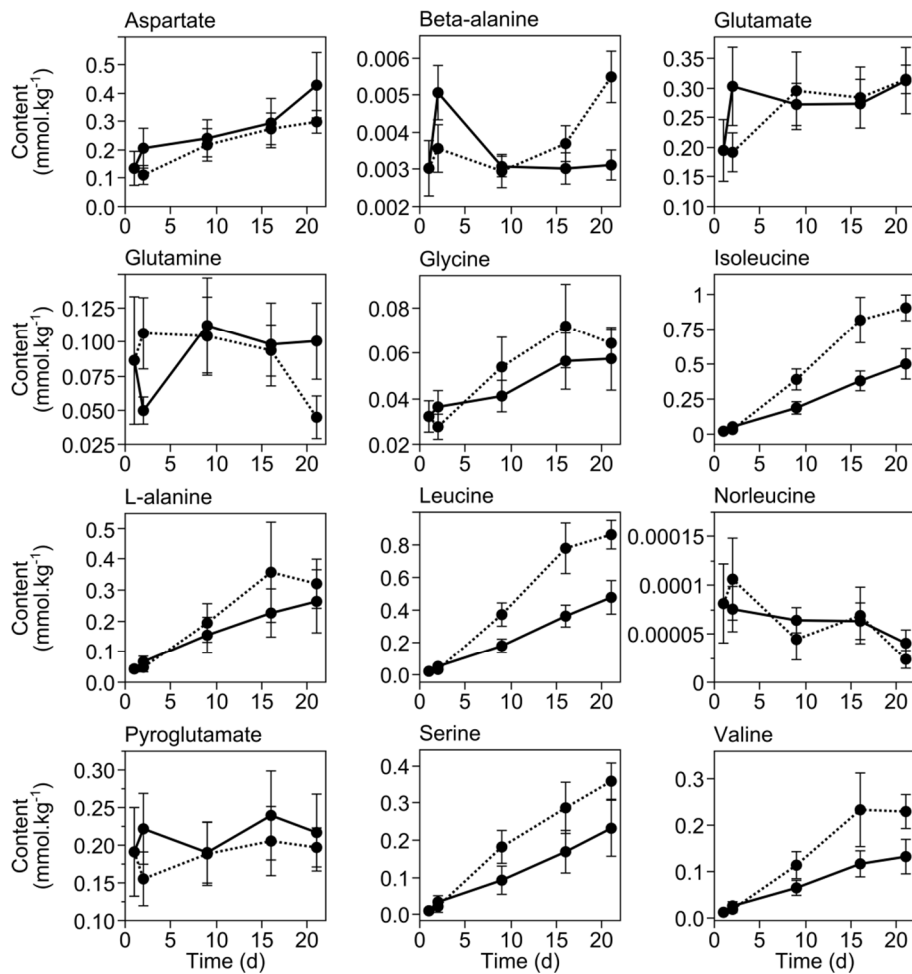


Fig. 3.5 Time series showing the changes in amino acid content during postharvest storage for 21 d at 1 °C (—) and 4 °C (.....). The error bars represent the standard error of the mean ($n=6$).

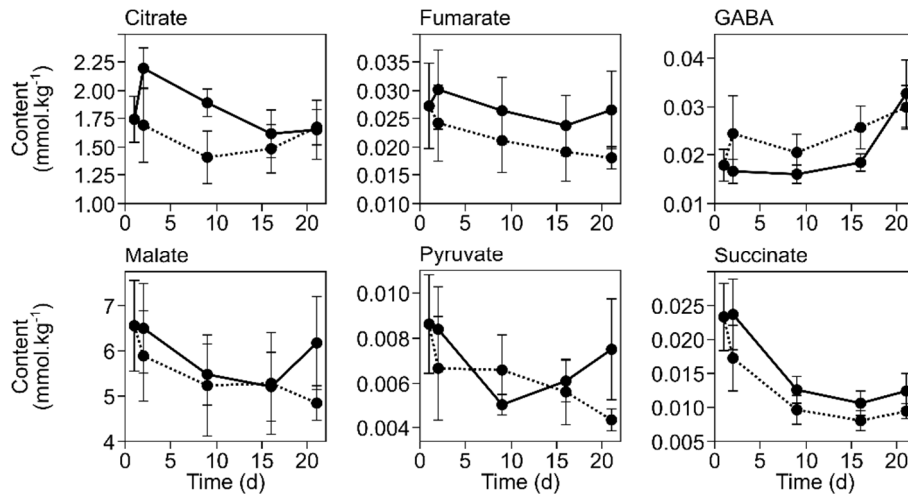


Fig. 3.6 Time series showing the changes in content of pyruvate, GABA and TCA cycle metabolites during postharvest storage of 21 d at 1 °C (—) and 4 °C (.....). The error bars represent the standard error of the mean ($n=6$).

3.4. Discussion

3.4.1. Grower effect

Each batch of plants grown by a different grower has its own specific growing and harvesting conditions which can be grower related (Table 3.1). However, other factors like the local environment and weather are also potential influencing factors. The 'grower' effect has to be seen as a confounded effect of all these different factors together. Hence, the grower itself is not necessary the cause of all this variability. This variability leads to larger standard errors in the graphs of Fig. 3.4, 3.5 and 3.6. Although the 'grower' effect was significant for most of the metabolites and can lead to large differences in sugar content (Fig. 3.3), the respiration rate of the lamb's lettuce plants was not significantly affected by the grower (Fig. 3.2).

3.4.2. Sugars and sugar alcohols

It has been reported that glucose, fructose and sucrose are the main substrates for respiration in lamb's lettuce (Enninghorst and Lippert, 2003). Although the temperature these authors considered was higher, a similar pattern during storage was noticeable. Initially, the amount of sucrose decreased rapidly, while glucose and fructose remained more or less stable. Only after a longer storage period, the amount of glucose and fructose decreased (Fig. 3.4 and 3.7). The conversion of sucrose to glucose and fructose postpones the decrease in glucose and fructose content. The total sugar balance decreased during the storage period of 21 d.

The reason for the increase of ribose content during a starvation period is unknown, although a similar increase has been observed in lamb's lettuce cells and *Arabidopsis thaliana* L. (Mbong et al., 2017b; Thimm et al., 2004). In *A. thaliana*, the increase in ribose content was linked to cell wall and nucleotide degradation (Thimm et al., 2004). The increase in ribose content observed in our data thus may be a general indicator of senescence associated breakdown processes.

In celery, mannitol is converted to fructose-6-phosphate by an enzyme called mannitol dehydrogenase. Mannitol dehydrogenase expression is suppressed when the sugar content is high. This sugar repression allows large amounts of mannitol to be stored as a back-up carbohydrate and osmoprotectant (Stoop et al., 1996). If the same applies to lamb's lettuce, the decrease of mannitol content during storage can be a consequence of the decrease in sugar content, because this leads to an increased conversion of mannitol to fructose-6-phosphate. Other research on lamb's lettuce cells showed an increase in mannitol content during storage (Mbong et al., 2017b). However, this may be due to osmotic stress on these cell cultures by the broth, because it has been reported that osmotic stress has a negative influence on the conversion of mannitol to fructose-6-phosphate (Stoop et al., 1996).

The increase in myo-inositol content has also been documented in lamb's lettuce cells (Mbong et al., 2017b). It has been shown that myo-inositol

accumulates as a response to different environmental stresses (Loewus and Murthy, 2000). As such, it can aid the cells in maintaining their membrane integrity (Lee et al., 2007; Loewus and Murthy, 2000). Also, sugars derived from inositol can be used for ascorbic acid synthesis and as an energy reserve for the respiration metabolism (Kroh et al., 1970; Loewus, 1969, 2006; Loewus et al., 1962). It has been shown that the ascorbic acid content decreases in lamb's lettuce during a storage period at 20 °C, but the relation between an increase in myo-inositol content and the possible use for myo-inositol in ascorbic acid synthesis during storage is unclear from this study (Spinardi and Ferrante, 2012).

3.4.3. Amino acids

During the postharvest storage period there was a general increase in the content of free amino acids noticeable (Fig. 3.5 and 3.7). The amino acid content increased faster at a storage temperature of 4 °C than at 1 °C, which can be explained by a more active metabolism at higher temperatures. Amino acids can be used as an alternative source of energy through autophagy during carbon starvation (Aubert et al., 1996; Brouquisse et al., 1991; Dieuaide-Noubhani et al., 1997; Hildebrandt et al., 2015; Inoue and Moriyasu, 2006; Moriyasu and Ohsumi, 1996). An increase in free amino acid content during a starvation period has been observed in sycamore cells (Journet et al., 1986), Maize root tips (Brouquisse et al., 1991; Dieuaide-Noubhani et al., 1997), rice cells (Chen et al., 1994), *Arabidopsis* cells (Thimm et al., 2004), tobacco cells (Inoue and Moriyasu, 2006) and lamb's lettuce cells (Mbong et al., 2017b). However, the use of amino acids as the main carbon source would have led to a lowered RQ (Fonseca et al., 2002; Gran and Beaudry, 1993; Saglio and Pradet, 1980). The measured RQ values remained stable around 1 which meant that one CO₂ was produced for each O₂ consumed (Fig. 3.2). The RQ value should have decreased considerably during the storage period to assume a shift to amino acids as the main carbon source for respiration, but no significant change was noticeable. The increased amount of free amino acids was most likely due to

proteolysis, but the amino acids did not appear to be the sole dominant substrate for energy production.

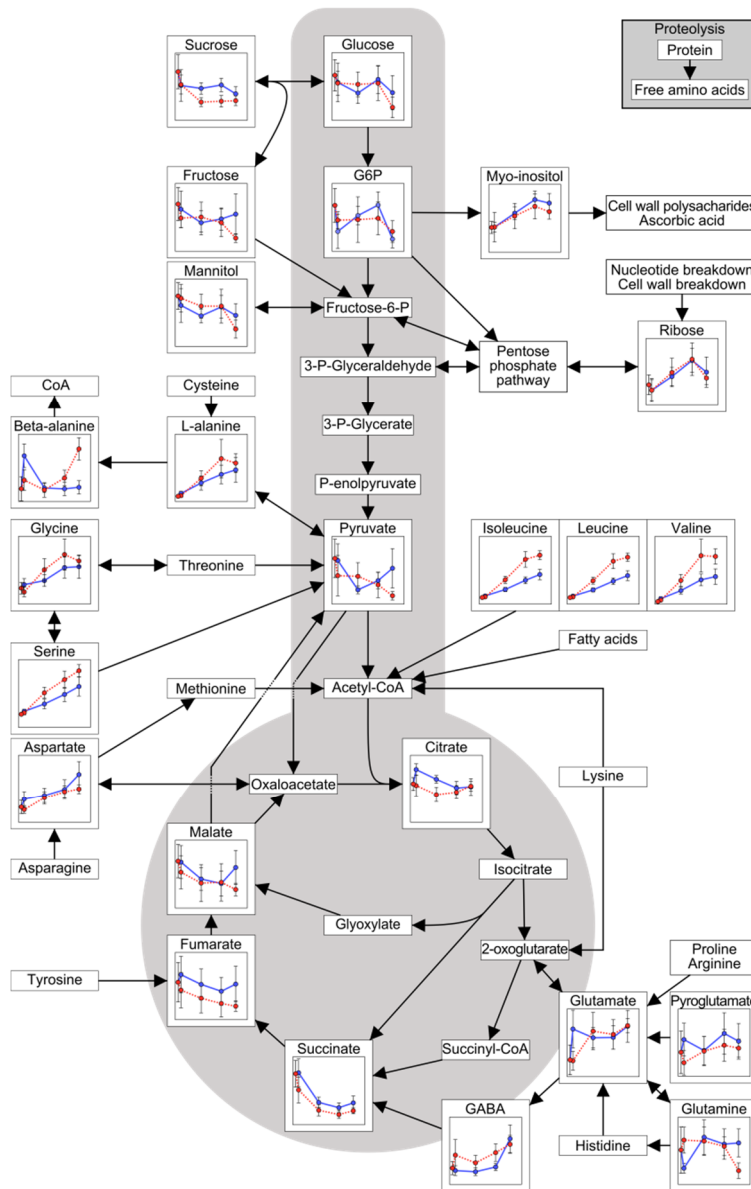


Fig. 3.7 The changes in content during a 21 d storage period at 1 °C (●) and 4 °C (●) are shown in a simplified scheme of the primary metabolism (gray background) and catabolic pathways of other metabolites (white background). The arrows link the relation between metabolites and can contain multiple steps in the actual metabolism. Detailed graphs are located in Fig. 3.4, 3.5 and 3.6 The error bars represent the standard error of the mean ($n=6$).

3.4.4. Pyruvate, GABA and TCA cycle metabolites

Pyruvate is the last metabolite of the glycolysis pathway and many metabolites catabolize to pyruvate which is why it is hard to find a direct link between the decrease in pyruvate content and other compounds (Fig. 3.6 and 3.7). It has been documented that the pyruvate content in onions decreases during a postharvest storage period (Blanchard et al., 1996). On the other hand, Mbong et al. (2017b) reported an increase in pyruvate content in lamb's lettuce cells which could have originated from alanine and malate. However, in our study the total pyruvate content decreased, which means pyruvate was probably consumed in the TCA cycle.

GABA is a non-protein amino acid and is produced from glutamate in a reaction catalyzed by glutamate decarboxylase (Shelp et al., 1999). The increase in GABA content may have different origins (Fig. 3.6 and 3.7). Stress induces glutamate decarboxylase which increases the conversion of glutamate to GABA. Also, a correlation between the increase in GABA and reactive oxygen species or wound stress has been reported (Bown et al., 2006). The function of GABA during postharvest storage is still unclear, but it is possible that GABA has a double function as metabolite and signal molecule (Bouché and Fromm, 2004). Several researchers suggested a role for GABA in controlling the carbon-nitrogen balance, in stress response, regulating pH and as an alternative pathway for utilizing glutamate (Bouché et al., 2003; Bouché and Fromm, 2004; Bown et al., 2006; Shelp et al., 1999).

Metabolites of the TCA cycle had variable responses on the postharvest storage period and the storage temperature only had a significant effect on fumarate and succinate (Fig. 3.6 and 3.7). These redox equivalents produced by the TCA cycle are an important source for oxidative phosphorylation in the mitochondria (Popova and Pinheiro de Carvalho, 1998). In other plants it was observed that during a starvation or dark period the glyoxylate pathway was used in combination with beta-oxidation of fatty acids in peroxisomes or proteolysis of proteins, resulting in a lower RQ (Chen, 2000; Dieuaide-Noubhani et al., 1997; Kunz et al., 2009). This

decrease in RQ can be explained by the fact that when molecules which contain less oxygen per carbon are oxidized, more oxygen has to be consumed. While it was expected that the RQ value would have decreased considerably during the storage period to assume a shift to fatty acids as the main carbon source for respiration, no significant change was noticeable (Fig. 3.2). It is uncertain which carbon source is the main source of energy because no measurements were performed to determine fatty acid content. The decrease in respiration rate during a starvation period has been documented in literature, but the reason for this decrease has been associated with different events. Journet et al. (1986) assumed that during starvation the total number of mitochondria per cell decreases, resulting in a lower respiration rate. They considered the availability of useable carbohydrates to be less important (Journet et al., 1986). Other researchers concluded that the respiration rate is controlled by the sugar supply and the amount of ATP required for metabolic processes on the biosynthetic level (Brouquisse et al., 1991). Research in *Arabidopsis* showed that the expression of many genes associated with the TCA cycle and the electron transport chain in mitochondria was reduced in conditions of low sugar content (Thimm et al., 2004). More recently, a similar decrease in respiration rate has been found in lamb's lettuce cells (Mbong et al., 2017b). This research also showed a higher respiration rate when the cells were not experiencing a sugar starvation period. This indicates that substrate availability is an important factor in the decrease in respiration rate.

3.5. Conclusions

After 21 d of storage, the general sugar content of lamb's lettuce had decreased. The RQ value indicated that carbohydrates remained the main carbon source during storage. However, the increase of free amino acids due to proteolysis indicated that the plants coped with nutrient stress and that amino acids were made available for respiration (Brouquisse et al.,

1991; Chen et al., 1994). The increase in concentration for most of the amino acids depended on the storage temperature in which a higher temperature resulted in a larger increase. However, the storage temperature did not influence the respiration rate. The 21 d in storage led to a significant decrease of the respiration rate, which might have been an indication of a shortage in soluble carbohydrates. In conclusion, after 21 d of storage, carbohydrates were still the main energy source but the lamb's lettuce was preparing to use a mixture of different carbon sources for respiration. As the main purpose of respiration during postharvest storage is to provide energy for maintenance purposes, the energy production decreased and this likely would also affect shelf life potential.

As it has been shown in chapter two, sugar content is detectable by Vis/NIR spectroscopy. Hence, the decrease of sugars during storage might be easily and non-destructively detectable and used for determining and quantifying the time in storage after harvest or even make predictions about the shelf life potential. Therefore, the potential of Vis/NIR spectroscopy as an option for determining the storage time of lamb's lettuce, will be explored in the next chapter.

4. Estimation of storage time of lamb's lettuce based on Vis / NIR spectroscopy

Based on Bert A.J.G. Jacobs, Bert E. Verlinden, Els Bobelyn, An Decombel, Peter Bleyaert, Joris Van Lommel, Isabel Vandeveldel, Wouter Saeys, Bart M. Nicolai, *Estimation of the prior storage period of lamb's lettuce based on visible/near infrared reflectance spectroscopy, Postharvest Biology and Technology, Volume 113, March 2016, Pages 95-105, ISSN 0925-5214*
and Jacobs, B.A.J.G., Verlinden, B.E., Bobelyn, E., Decombel, A., Bleyaert, P., Van Lommel, J., Vandeveldel, I., Saeys, W., Nicolai, B.M., 2015. *Predicting stored period and shelf life potential of Lamb's lettuce using Vis/NIR reflectance spectroscopy. Acta Hort. 1079, 207–213.*

4.1. Introduction

Lamb's lettuce is a popular greenhouse vegetable thanks to its ease of use and ready-to-eat character. It is used both as a leafy salad and as an ingredient in ready to eat salad mixtures (Enninghorst and Lippert, 2003; Ragaert et al., 2004). However, lamb's lettuce presented to the market by the growers is not always freshly harvested. Depending on the season, it can be stored up to three weeks in the cooling facility of the growers. Stored samples are by eye visually indistinguishable from fresh produce, but they have impaired shelf life potential (Rico et al., 2007). This is a crucial problem

as the perceived level of freshness and appearance are two of the most important attributes for ready to eat salad choice (Dinnella et al., 2014; Ferrante et al., 2004). Losses due to batches with limited shelf life lead to significant economic losses in distribution and lower consumption quality (Fao, 1989; Ferrante et al., 2009). During a postharvest storage period sucrose, glucose, fructose and starch are the main substrates of respiration in lamb's lettuce (Enninghorst and Lippert, 2003; Chapter 3). Also, the reduction of chlorophyll content is very slow and depends on the length of storage time (Ferrante and Maggiore, 2007). Carotenoids are stable during the first five days of storage, but decrease after this initial stable period. This in contrast to anthocyanin content which starts to increase after an initial stable period of eight days (Ferrante et al., 2009).

To detect prior storage of lamb's lettuce, a fast and nondestructive measurement set-up is needed which estimates how long a batch of lamb's lettuce has been stored before it is commercialized. Nondestructive measurements using visible / near infrared (Vis/NIR) spectroscopy may provide this nondestructive method. The potential of NIR to characterize and analyze fruit and vegetables has been shown before. Applications include the nondestructive determination of soluble solids content and dry matter of kiwifruit (McGlone et al., 2002); firmness and soluble solids content of pear (Nicolai et al., 2008); soluble solids content of stone fruit (Golic and Walsh, 2006); internal quality and optimal harvest date of apple (Lu et al., 2000; Peirs et al., 2001); bitterness, sweetness and crunchiness of chicory (François et al., 2008); moisture, ascorbic acid and soluble solids content of cabbage (Kramchote et al., 2014), among others. Specifically on leafy greens, NIR spectroscopy has been used to distinguish between differences in production methods of *Lactuca sativa* L. (Brito et al., 2015); determine the nitrogen content in *Lactuca sativa* L. (Mao et al., 2015); determine the chlorophyll content in *Lactuca sativa* L. leaves (Yongli Zhu et al., 2011); predict the nitrate concentration of *Lactuca sativa* L. (Itoh et al., 2015); predict chlorophyll, carotenoid and anthocyanin content of green and red lettuces (Steidle Neto et al., 2017); determine pH, water content and total

phenol content of fresh cut lamb's lettuce (Beghi et al., 2014; Giovenzana et al., 2014), among others.

In the previous chapter, it has been shown that general sugar content decreased during a storage period. Hence, the decrease of sugars during storage might be easily and non-destructively detectable and used for determining and quantifying the time in storage after harvest or even make predictions about the shelf life potential. Therefore, the aim of this study was to investigate the potential of Vis/NIR spectroscopy to estimate how long a batch of lamb's lettuce has been stored before it is presented to the market and to predict its shelf life potential.

4.2. Materials and methods

4.2.1. Plant material and storage conditions

Samples of nine cultivars (Agathe, Audace, Baron, Calarasi, Cirilla, Gala, Pulsar, Trophy, Palace) of lamb's lettuce (*Valerianella locusta* L.) were harvested between September 2012 and November 2014. Batches harvested before 2014 were grown at the experimental station Inagro (Rumbeke-Beitem, Belgium). Batches harvested in 2014 contained more diverse plant material from commercial growers. Different treatments were applied during the postharvest period to induce extra variation. This extra variation was necessary, because the final prediction model had to be able to handle new samples which had different unknown storage conditions. An overview of treatments, cultivars and harvesting periods is given in Table 4.1.

Lamb's lettuce harvested in February 2014 was additionally subjected to a shelf life holding period of 10 d at 8 °C after harvest and storage periods at 1 or 4 °C of 4, 7, 15 and 21 d, respectively.

4.2.2. Quality attributes

The quality of lamb's lettuce harvested in February 2014 was judged by a panel of experts at harvest and after a shelf life holding period. The quality scores ranged from 0 (wilted) to 10 (excellent). At the same days colorimetric measurements were performed using a CM-2600d spectrophotometer (Konica Minolta, Tokyo, Japan) on the adaxial and abaxial sides of the biggest leaf of a rosette. Color was expressed in L*a*b* and L*C*h* color space ((Hunt and Pointer, 2011).

Table 4.1 Harvest periods, cultivars, growers and different treatments of the samples used.

Harvest period	Dataset	Cultivars	Growers	Treatments
September (2012)	Validation (n=191)	Trophy ^a	Experimental station	Different harvesting times (9h, 12h), stored at 1°C
January (2013)	Calibration (n=767)	Agathe ^a , Audace ^a , Calarasi ^b , Cirilla ^b , Trophy ^a , Palace ^a	Experimental station	Different transport temperature (20°C, 4°C), stored at 4°C
March (2013)	External test (n=83)	Baron ^c	Experimental station	Different transport temperature (20°C, 4°C), stored at 4°C
July (2013)	Calibration (n=80)	Audace ^a , Gala ^a , Pulsar ^b , Trophy ^a	Experimental station	Different moistening schedule during storage, stored at 4°C
November (2013)	Calibration (n=139)	Trophy ^a	Experimental station	Moistened during storage, stored at 4°C
February (2014)	Calibration (n=165)	Audace ^a , Calarasi ^b , Trophy ^a	8 Commercial growers	Different wrapping during storage, stored at 1 and 4°C
May (2014)	External test (n=86)	Audace ^a , Pulsar ^b	5 Commercial growers	Different wrapping during storage, stored at 1 and 4°C
November (2014)	Calibration (n=132)	Trophy ^a , Audace ^a	7 Commercial growers	Different wrapping during storage, stored at 1 and 4°C

All cultivars were from the seed companies ^aHM. Clause, ^bRijk Zwaan and ^cBayer.

4.2.3. Vis/NIR transreflectance spectroscopy

From each selected rosette, only the leaf with the largest surface area was used for Vis/NIR transreflectance spectroscopy measurements. Adaxial and abaxial transreflectance spectra (380 - 1690 nm, wavelength increment 2 nm) of 191, 767, 83, 80, 139, 165, 86 and 132 lamb's lettuce leaves harvested in September 2012, January 2013, March 2013, July 2013, November 2013, February 2014, May 2014 and November 2014 respectively were acquired. Vis/NIR transreflectance spectra were acquired using a Zeiss Corona 1.7 (Carl Zeiss, AG, Germany) Silicon (Si) - Indium Gallium Arsenide (InGaAs) diode array with a 0°/45° transreflectance set-up using a fiber optics probe (Nicolai et al., 2007). The full width at half maximum of the Si and InGaAs diode array is 10 nm and 18 nm, respectively. The spectrophotometer was calibrated every 20 minutes. After each calibration, the white reference was measured again and the transreflectance spectrum between 380 and 1690 nm was verified to be between 99% and 101% before proceeding to the actual measurements. If this was not the case the calibration would be performed again. This was done to be sure of a decent calibration. For each measurement, the leaf sample was placed between a polished white PTFE block and the measuring head which had a circular measurement area with a diameter of 2.5 cm. The measurement area includes almost the entire surface area of a lamb's lettuce leaf. Spectra were acquired at least once a week during a period of three to four weeks. At each measurement point during storage new samples from the same batch were used to minimize the effect of sample handling on the quality of the samples.

4.2.4. Prediction model

4.2.4.1. Data matrix

First, the adaxial and abaxial spectra were compared visually and using PCA. The technique used to build prediction models was PLSR (Wold et al., 2001). Preliminary analysis showed a decrease in R^2 , root mean square error of calibration (RMSEC) and cross validation (RMSECV) when only the

adaxial or abaxial spectrum was used compared to concatenated spectra. The R^2 decreased from 0.83 for the concatenated matrix to 0.78 and 0.80 for the adaxial and abaxial spectrum, respectively. Also, the decrease in the RMSEC and RMSECV was 0.5 and 0.1 d for the adaxial side and 0.5 and 0.2 d for the abaxial side. Based on these preliminary results, the independent variables were the concatenated adaxial and abaxial spectra. The dependent variable was storage time after harvest (days). The adaxial and abaxial spectra of the measured lamb's lettuce leaves were placed in succession in the data matrix. The regions in the combined spectra where the noise was too high (380 - 418 nm) were ignored. As the change from a Si to an InGaAs detector resulted in a bump in the spectrum, the range where the detectors change (962 - 992 nm) was also ignored. For possible practical implementations, it would be more interesting to have a cheaper measurement set-up. Preliminary analysis showed a rise in R^2 from 0.81 to 0.86 when the wavelengths above 1100 nm were discarded. Also, a decrease in the RMSEC and RMSECV of respectively 0.5 and 0.7 d was observed with the exclusion of wavelengths above 1100 nm. Therefore, the analyses in this study were limited to the theoretical range of a Si detector (380 - 1100 nm). The lab set-up in this research used an InGaAs detector with wavelengths greater than 950 nm, resulting in a better signal to noise ratio in the 950 - 1100 nm range with higher wavelengths compared to a Si detector. This relative better performance would have to be taken into account if wavelengths in this region were retained in the final prediction model.

From the initial 2843 combined spectra 767 were measured on samples harvested in January 2013. Of all the spectra, 27% originated from the same harvesting period and were grown by the same grower (Table 4.1). To minimize the overrepresentation of this harvesting period, while retaining as much of the variation as possible, a selection of 25% of the 767 spectra was made using the Kennard-Stone algorithm (Kennard and Stone, 1969) using the PLS-Toolbox (Eigenvector Research Inc., Wenatchee WA, USA) in Matlab (MATLAB R2013a, The MathWorks, Inc., Natick, Massachusetts,

United States). Additionally, eight outliers were discarded manually based on Q residuals and Hotelling T^2 statistics.

The 706 spectra acquired in January 2013 (193), July 2013 (79), November 2013 (138), February 2014 (164) and November 2014 (132) were used as calibration data. A cross validation (CV) was applied to evaluate the PLSR model performance during construction. An initial PCA on the combined spectra highlighted that different harvest periods were the cause of the main variation between samples. Hence, each harvest period was used as a separate CV group to assure that the model would be able to cope with unknown new harvest periods. The 190 spectra acquired in September 2012 were used as a validation set for wavelength selection. An external test set was used for validating the accuracy and robustness of the final prediction models. This external test set consisted of 165 spectra acquired in March 2013 (81) and May 2014 (84).

For each PLSR model, an optimal number of LV's was selected based on the RMSEC, RMSECV and the estimated signal to noise ratio (S/N). The latter was calculated using the 'estimatefactors' algorithm in the PLS-Toolbox. This algorithm resamples the data and when the loadings change significantly between resamplings, the factor is probably based on noise and not on signal. An S/N greater than three is considered informative. This way, it is possible to estimate the number of significant factors in multivariate data. (Henry et al., 1999; Sug Park et al., 2000).

4.2.4.2. Wavelength Selection

Different wavelength selection techniques were applied on the spectra to improve the prediction potential and robustness of the PLSR model by removing wavelength variables which are not informative for predicting the dependent variable. Spectra from September 2012 were used as a validation set for wavelength selection to prevent overfitting during wavelength selection. The applied wavelength selection techniques were Variable Importance in Projection (VIP) scores (Chong and Jun, 2005), interval PLS (iPLS) (Nørgaard et al., 2000), Genetic Algorithms PLS

(GA-PLS) (Lucasius et al., 1994) and Monte Carlo Uninformative Variable Elimination PLS (MC-UVE-PLS) (Cai et al., 2008).

iPLS

Interval PLS was performed in automatic mode with an interval size of 2 nm (one variable).

GA-PLS

The GA-PLS parameters used in this study are listed in Table 4.2. Limited convergence in the selection of wavelengths was preferred due to the specific CV of the GA-PLS algorithm in PLS-Toolbox which prohibits a CV for each harvest period. Hence, the maximum convergence was chosen at 40% and 25 replicate runs were performed. The GA-PLS output of the final generations was first analyzed for differences between models with a good and bad RMSECV. Wavelengths related to a higher RMSECV were considered uninformative and were discarded. The remaining wavelengths were analyzed in a different way. The final models of GA-PLS after 50 generations used a different combination of wavelengths. Wavelengths which were retained in more models were considered more important for good predictions. Based on the presence of each wavelength in all of the final models different PLSR models were constructed with different numbers of retained wavelengths. The optimal number of selected wavelengths of the spectra of leaves was based on the RMSECV and RMSEV (root mean square error of validation). The latter was the RMSE of spectra which were harvested in September 2012. The spectra of this harvest period were used as a validation set for wavelength selection. Finally, the performance of the PLSR model based on the GA-PLS wavelength selection based on the presence (GA-PLS) was compared to the PLSR model based on the GA-PLS wavelength selection's best performing selection by the PLS-Toolbox (GA-PLS_{Best})

Table 4.2 GA-PLS parameters.

Setting	Value
Population size	256
Window width	1
Initial terms	30%
Penalty slope	0.1
Max generations	50
% at convergence	40
Mutation rate	0.005
Regression choice	PLS (13 LV's)
Cross validation parameters	Contiguous, 4 splits, 1 iteration
Replicate runs	25

GA-PLS_{10%}

When different repetitions of GA-PLS were evaluated, it was noticeable that there were differences in the RMSECV after 50 generations between different repetitions. This can be explained by the differences in the variables included in the initial population. It is important to retain the information from all the repetitions, but the number of models which retained uninformative wavelengths should be minimized. To cope with this, a second wavelength selection was applied using only the 10% best performing selections for each of the 25 replicate runs (GA-PLS_{10%}). The selection of the optimal number of wavelengths to retain was based on the RMSECV and RMSEV.

MC-UVE-PLS

The selection of the number of wavelength variables to retain was based on the RMSECV and RMSEV of different PLSR models with different numbers of wavelength variables retained. The absolute value of the *RI* ($\text{abs}(RI)$) was the basis on which wavelengths were retained. Wavelength variables with a low $\text{abs}(RI)$ were considered less important for good predictions. The maximum number of LV's in MC-UVE-PLS was set to 13 which is the same number of LV's used by the initial full spectrum model. 1000 Monte Carlo simulations were performed, each of them using 75% of the samples for constructing a calibration model.

Statistical software for wavelength selection

VIP scores and iPLS were performed using the PLS-Toolbox in Matlab. GA-PLS was performed in Matlab and the evaluation of the final wavelength selections after 50 generations were performed in MS Excel (Microsoft Office Professional Plus 2010, Microsoft, Co., Redmond, Washington, United states). MC-UVE-PLS was performed using LibPLS (www.libpls.net) in Matlab. An error occurred in the Matlab script when calculating the RI, so the RI was calculated in MS Excel using the $\bar{\beta}_j$ and σ_j . Further evaluation of the output based on the RI was performed in MS Excel.

Combined wavelength selections

The different wavelength combinations were evaluated based on the RMSECV and RMSEV to identify overfitting. Wavelength combinations which were overfitting on the calibration data were not considered during further evaluation. During further evaluation, a combination of the wavelengths selected by the different wavelength selection techniques might give better results than any selection made by a single technique. Therefore, a combination of the selected wavelengths was made by combining all the selected wavelengths of different techniques or by keeping only the wavelengths on which the different techniques were unambiguous. These wavelength combinations were named C1, C2, C3 and C4 (Table 4.3). Finally, these combinations were compared to the best wavelength selection technique and the combinations which had a similar or better model performance were considered candidates for the final selection of wavelengths. The three best performing wavelength selections were used to construct PLSR models which were tested on robustness using an external test set which contained spectra acquired in March 2013 and May 2014. Two significance tests were performed to test if any of the three models performed significantly better than the rest. The first method compared the absolute values of the residuals of each sample in the external test set between two models (Thomas, 2003). The probability that one model performs better than the other was calculated in Matlab using the 'signtest'

function. The second method was a two-way analysis of variance (ANOVA) on the residuals of the external test set with one random factor and one fixed factor. The random factor was the sample number and the fixed factor was the PLSR model (Cederkvist et al., 2005). The output from these significance tests was used for the selection of the final model.

4.2.4.3. Preprocessing

Initially, the combined spectra were preprocessed using a multiplicative scatter correction (MSC). MSC is a pre-processing step that attempts to account for offset and scaling effects (Geladi et al., 1985). After wavelength selection, a Generalized Least Squares weighting (GLSW) was applied after a full spectrum MSC to further reduce the number of LV's. GLSW is a filter which identifies interfering signals in the spectra and downweights them (Martens et al., 2003; Zorzetti et al., 2011). This is done by comparing samples with a similar Y-value and downweighting wavelength variables which vary among these samples and are a source of variance. This allows the prediction model to obtain a similar performance, while using fewer LV's. A single parameter α defines how large the influence of the filter is on the downweighting of the interfering wavelength variables. A value for α is typically chosen between 1 and 0.0001. A larger value of α means that the filter has less effect.

4.2.5. Predicting shelf life potential

Based on data gathered in February 2014, prediction models were constructed using the PLS-Toolbox (Eigenvector Research Inc., Wenatchee WA, USA). The independent variables were combined Vis/NIR transmittance spectra (380 - 1690 nm, wavelength increment 2 nm) before the start of shelf life. The dependent variables were the data from the colorimetric measurements on the adaxial or abaxial sides of the leaf or the quality scores from the expert panel that were gathered after 10 d of a shelf life holding period at 8°C. A 10-fold cross validation was performed with a

venetian blinds strategy. Due to the small size of the calibration set, no advanced preprocessing and no variable selection were performed to reduce the risk of overfitting. The combined spectra were pre-processed using MSC and mean centering.

4.3. Results and discussion

4.3.1. Adaxial and abaxial spectra

The Vis/NIR spectra of the adaxial and abaxial sides are separated in a PCA score plot (Fig. 4.1A). A distinctive difference between the adaxial and abaxial spectra is noticeable in the visual part of the spectrum (400 to 712 nm), but also in the NIR part of the spectrum (1400 - 1690 nm) where the abaxial signal has a higher intensity than the adaxial (Fig. 4.1B). This difference can be explained by the spatial orientation of the different cell types in leaves which have different properties. Palisade parenchyma cells are located below the upper epidermis and cuticle at the adaxial side of the leaves and contain a large number of chloroplasts per cell. More towards the abaxial side are spongy mesophyll cells which have fewer chloroplasts and between the cells are more intercellular spaces (Mauseth, 2008). When light enters the leaves from the adaxial side, it first encounters densely packed cells which have higher amounts of leaf pigments, resulting in a diffuse reflection with a higher absorbance in spectral regions known for leaf pigment absorption (Vis) and water absorption (1400 - 1500 nm) (Xiaobo et al., 2010).

4.3.2. Evaluation of initial model

The initial full spectrum PLSR model was based on the spectrum of both adaxial and abaxial leaf sides. The combined spectrum was preprocessed with MSC. It is noticeable that the RMSECV increased with the first three LV's and that the RMSEC and RMSECV decreased slowly with each extra

LV. This was due to the influence of different harvest periods which were used as CV groups. Different harvest periods were the main source of external variation and in the initial full spectrum model the CV of extreme harvest periods had problems with correct predictions when using the first three LV's, leading to an increased RMSECV. Also, the spectrum of each sample was influenced by factors which have nothing to do with the dependent variable 'time in storage after harvest'. PLSR has more problems finding a good correlation when the number of wavelengths which are influenced by non-relevant factors increases (Mehmood et al., 2012).

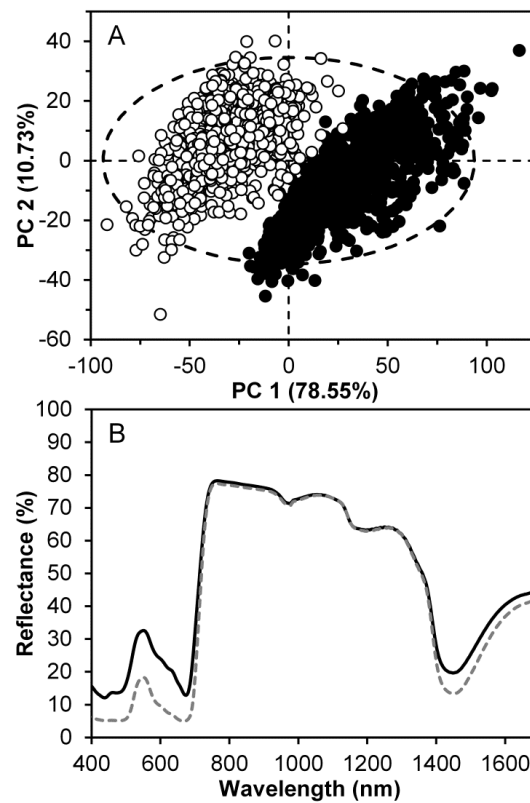


Fig. 4.1 (A) PCA plot of all the mean Vis/NIR transfectance spectra (400 -1690nm) of the abaxial (solid circles) and adaxial (open circles) side of lamb's lettuce leaves. (B) Visualization of the average Vis/NIR transfectance spectra for the abaxial (solid line) and adaxial (dashed line) side of the leaves.

The RMSEC and RMSECV were inconclusive for indicating an optimal value of LV's. There was only a local minimum when eight LV's were used, but the RMSECV gave lower values with increasing LV's and no real minimum was reached (Fig. 4.2A). Therefore, the optimal number of LV's was selected based on the estimated S/N (Fig. 4.2B). An estimated S/N greater than or equal to three is considered good. As the S/N for the 13th LV was still good, the prediction model with 13 LV's was selected. This model had an R^2 of 0.75 and an RMSEC, RMSECV and RMSEV of 3.6, 6.0 and 5.4 d, respectively (Fig. 4.3 and Table 4.3).

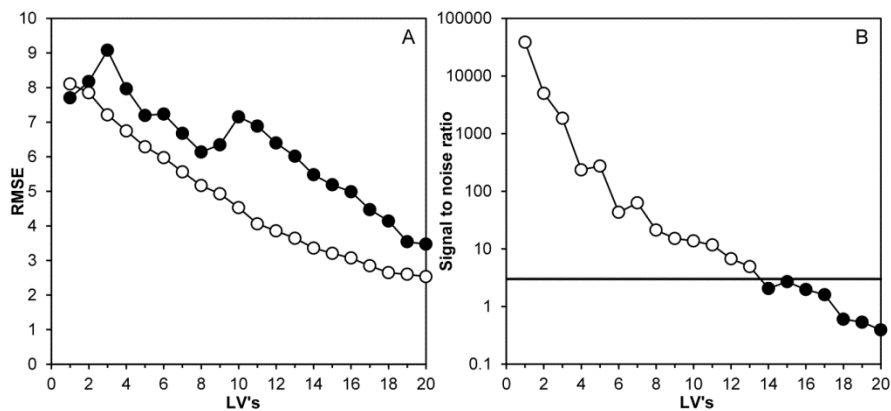


Fig. 4.2 (A) RMSEC (open circles) and RMSECV (solid circles) of the basic PLSR model on concatenated spectrum (420-1100 nm) of adaxial and abaxial leaf sides with limited preprocessing and no wavelength selection. (B) Estimated signal to noise ratios for different LV's. The solid black line is the threshold ($S/N = 3$). Solid and open circles represent good ($S/N \geq 3$) and bad ($S/N < 3$) signal to noise ratios, respectively.

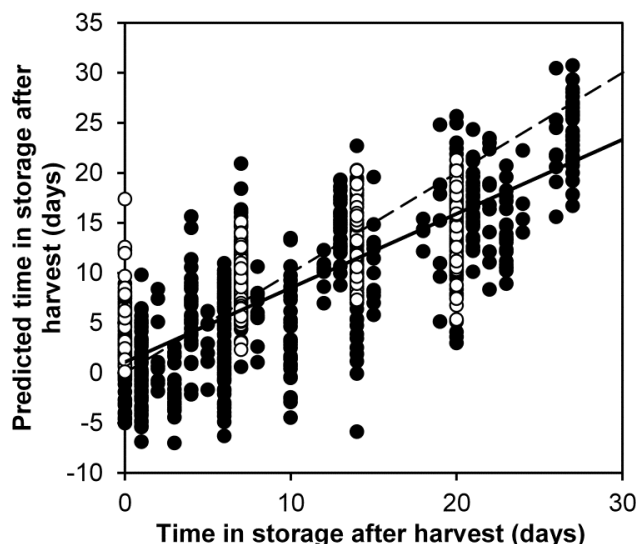


Fig. 4.3 Time in storage after harvest plotted against the predicted time in storage which was predicted by the basic PLSR model on concatenated spectrum (420-1100nm) of adaxial and abaxial leaf sides with limited preprocessing and no wavelength selection. The solid and open circles are samples from the calibration set in cross validation and the validation set, respectively. The dashed and solid lines are the optimal regression line and the regression line of the current model, respectively.

Table 4.3 Performance of PLSR models constructed by using wavelengths selected by different wavelength selection techniques.

Name of combination	Wavelength selection criteria	Number of wavelengths	LV's	R ²	RMSEC (days)	RMSECV (days)	RMSEV (days)
Initial model /		650 (100%)	13	0.75	3.6	6.0	5.4
VIP scores	VIP score	207 (32%)	12	0.75	3.5	4.8	5.6
iPLS	iPLS	40 (6%)	8	0.78	3.4	3.5	5.0
GA-PLS _{Best}	the GA-PLS model with the lowest RMSECV	173 (27%)	10	0.75	3.8	5.5	4.7
GA-PLS	GA-PLS	390 (60%)	13	0.80	3.3	4.5	4.8
GA-PLS _{10%}	GA-PLS _{10%}	98 (15%)	10	0.82	3.1	4.3	4.1
MC-UVE-PLS	MC-UVE-PLS	228 (35%)	14	0.84	3.0	3.7	3.9
C1	Being included by both GA-PLS and MC-UVE-PLS	174 (27%)	13	0.84	3.1	3.5	3.8
C2	Being included by both GA-PLS _{10%} and MC-UVE-PLS	65 (10%)	13	0.82	3.3	3.7	3.9
C3	being included by either GA-PLS or MC-UVE-PLS	444 (68%)	13	0.78	3.5	4.7	4.8
C4	being included by either GA-PLS _{10%} or MC-UVE-PLS	261 (40%)	12	0.81	3.3	4.4	4.2

4.3.3. Wavelength selection

The performance of PLSR models using wavelength variables chosen by different wavelength selection techniques is summarized in Table 4.3. When the different prediction models with a reduced number of wavelength variables were compared with the initial model, it became clear that all the wavelength selection methods improved the RMSECV. The RMSEV calculated on the data from September 2012 was not always similar to the RMSECV, which could indicate overfitting. This was in particular the case for PLSR models based on wavelength variables selected by VIP scores and iPLS. These models gave RMSECV values of 4.8 and 3.5 d, while the corresponding RMSEV's were 5.6 and 5.0 d, respectively. The rather big difference between the RMSECV and RMSEV values suggests that these models were not very robust.

The prediction model based on wavelengths selected by GA-PLS had an RMSECV of 4.5 d and an RMSEV of 4.8 d. The same was true for GA-PLS_{10%} with an RMSECV of 4.3 d and an RMSEV of 4.1 d which implies that both models were quite robust. The model with the lowest RMSECV after GA-PLS (GA-PLS_{best}) was the model which according to GA-PLS should have the best selection of wavelengths. The RMSECV and RMSEV were 5.5 and 4.7 d, respectively. GA-PLS_{best} seems to be robust, but the selected wavelength variables result in a PLSR model with worse prediction performance than GA-PLS and GA-PLS_{10%}.

The performance of the selection based on GA-PLS_{10%} performed better compared to regular GA-PLS. The latter used more LV's (13 compared to 10), had a lower R^2 (0.80 compared to 0.82) and the RMSEC, RMSECV and RMSEV were higher compared to GA-PLS_{10%}, while using more wavelengths (390 compared to 98). Besides the improved performance, wavelength selection was easier based on GA-PLS_{10%} compared to GA-PLS, thanks to the clear minimum in RMSECV and RMSEV which was noticeable in GA-PLS_{10%} and not in GA-PLS (Fig. 4.4A and B).

Of all the applied techniques for wavelength selection MC-UVE-PLS was the most successful, resulting in a PLSR model with the highest R^2 (0.84), the

lowest RMSECV (3.7 d) and the lowest RMSEV (3.9 d) (Table 4.3). Although only 35% of the initial wavelengths were retained for model construction, 14 LV's were used for the predictions. This was the highest number of LV's any of the robust models used.

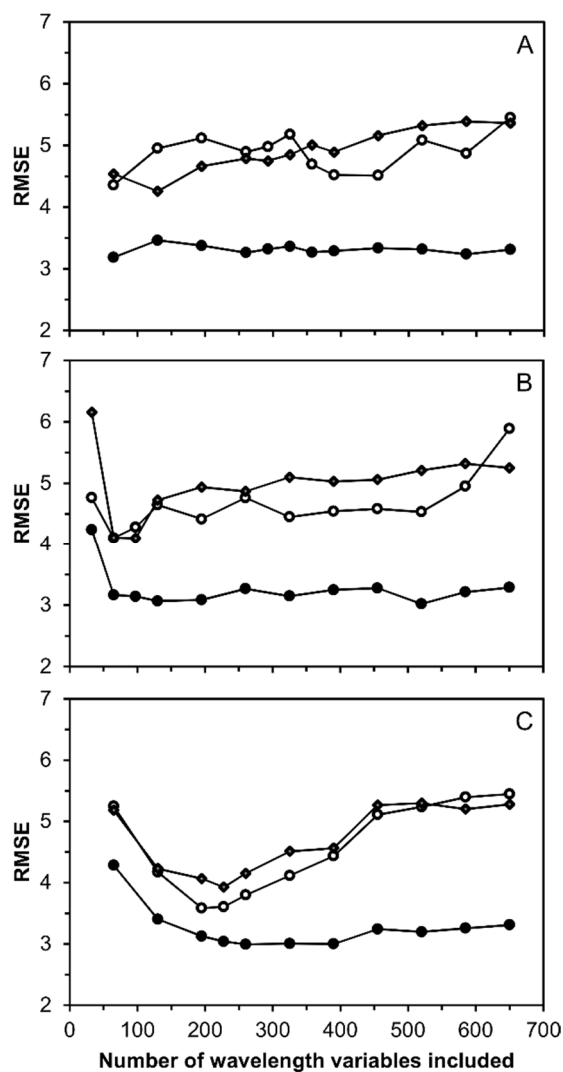


Fig. 4.4 The RMSEC (solid circles), RMSECV (open circles) and RMSEV (diamonds) of PLSR models constructed using different numbers of wavelength variables that were selected from the concatenated adaxial and abaxial spectra ranging from 420 to 1100 nm based on (A) GA-PLS, (B) GA-PLS_{10%}, and (C) MC-UVE-PLS.

4.3.4. Comparison of the selected wavelength variables

The selected wavelength variables based on VIP scores and iPLS are shown in Fig. 4.5. The selection of wavelength variables using GA-PLS, GA-PLS_{10%} and MC-UVE-PLS is shown in Fig. 4.4 and 4.6. Comparing the wavelength variables selected by the different methods revealed that all the techniques included more wavelength variables from the visual part of the spectrum than wavelength variables from the NIR range. The PLSR models constructed using wavelength variables selected by VIP scores and iPLS were not robust. The basis for the lack of robustness of these PLSR models was probably different. Forward iPLS selected 40 (6%) wavelength variables and this selection was probably missing wavelength variables essential for robustness (Fig. 4.5). VIP scores on the other hand, included more wavelength variables, but the resulting PLSR model was not robust. The big difference between the selected wavelength variables based on VIP scores on the one hand and GA-PLS, GA-PLS_{10%} and MC-UVE-PLS on the other hand was the selection of many wavelengths around the red edge (680 - 730 nm) for both leaf sides which seems to have a negative influence on robustness (Fig. 4.5 and 4.6). A property that all robust selections have in common with the selection based on VIP scores in the NIR range was the selection of wavelength variables around 958 nm on the adaxial side of the leaf. NIR wavelength variables which were included by all the robust techniques are 800 nm on both leaf sides and 900 nm on the abaxial side. The inclusion of these wavelengths in the NIR range seems to be crucial for robustness.

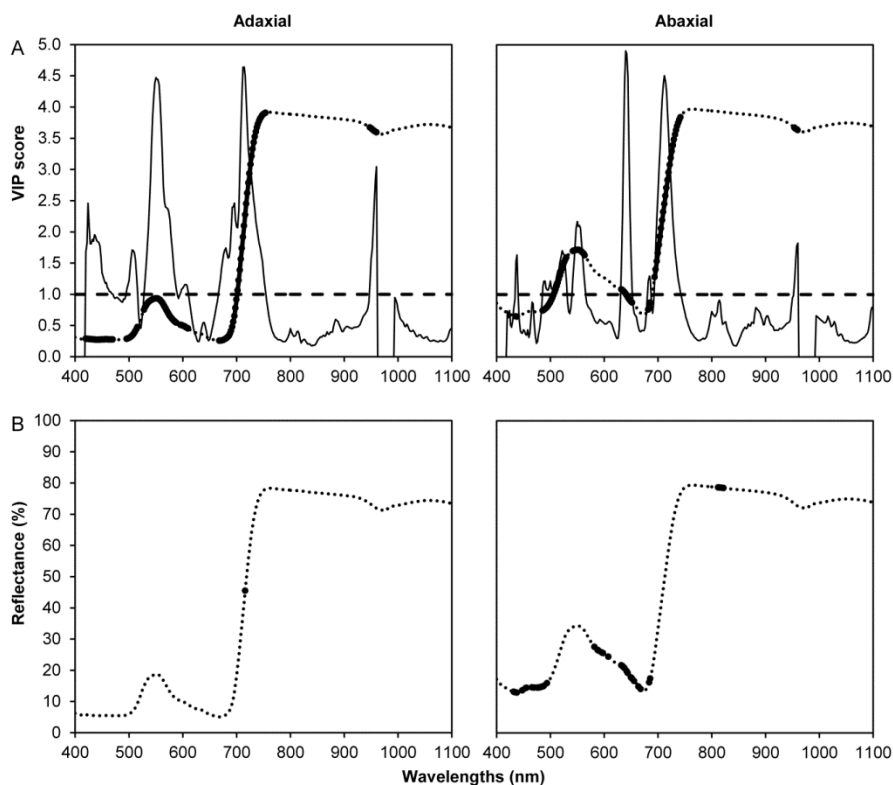


Fig. 4.5 (A) Selected wavelengths with their associated VIP scores for the initial PLSR model, and (B) selected wavelengths by forward iPLS wavelength selection. The dotted line is the mean spectrum of the adaxial and abaxial spectra. The thick solid areas indicate wavelength variables that were selected for constructing the PLSR model. The thin solid line in A is the VIP score for each wavelength and the dashed line is the threshold which discriminates between useful and useless wavelength variables.

4.3.5. Combining wavelength selections

The best performing PLSR models used 98, 228 and 390 wavelengths. It is remarkable that 98 wavelengths selected by GA-PLS_{10%} performed better than the 390 wavelengths selected by GA-PLS, but worse than the 228 wavelengths selected by MC-UVE-PLS. This could be due to the excessive removal of informative wavelengths or the inclusion of interfering non-informative wavelengths. There is a high consistency in the wavelengths which none of these wavelength selection methods selected. Of the initial 650 wavelengths, 32% (206) were discarded by all these techniques (Fig. 4.7).

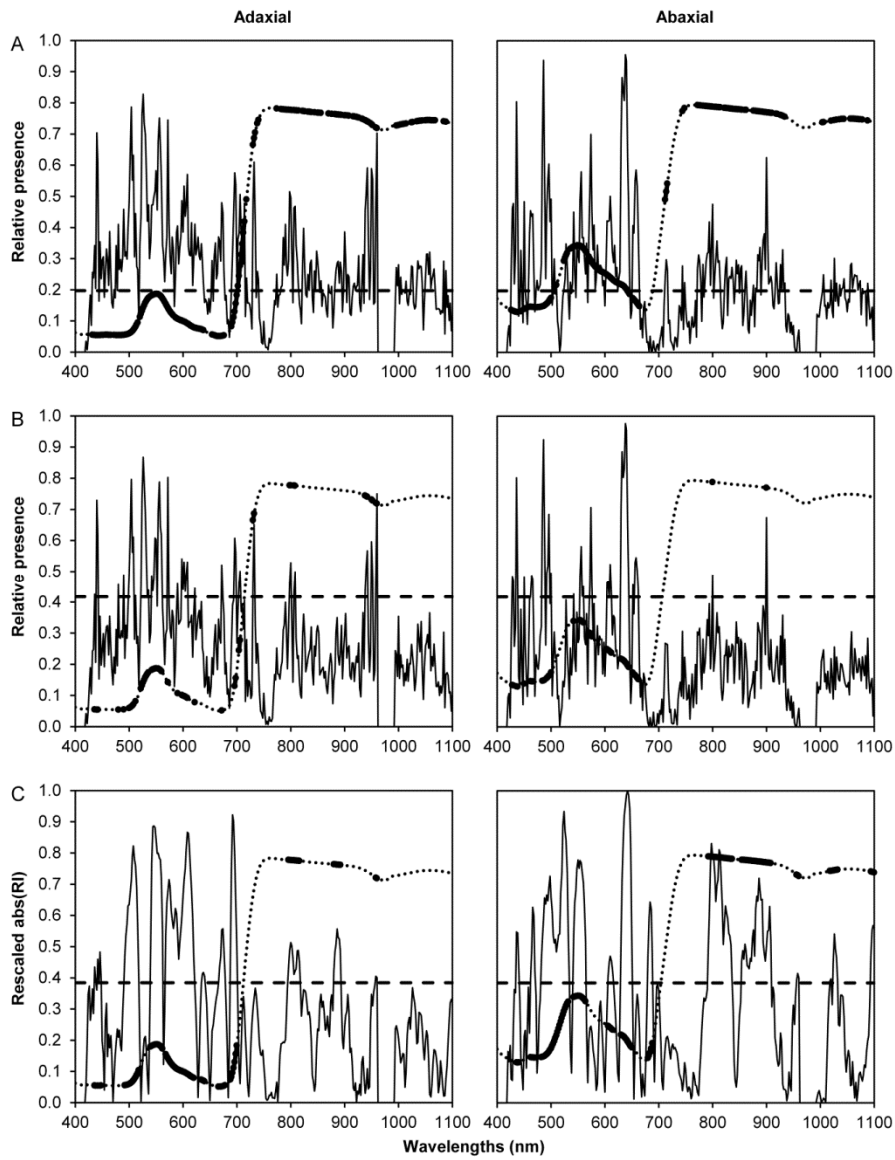


Fig. 4.6 Output and selection of wavelength variables of (A) GA-PLS, (B) GA-PLS_{10%}, and (C) MC-UVE-PLS. The dotted line is the mean spectrum of the adaxial and abaxial spectra. The thick solid areas indicate wavelength variables that were selected for constructing the PLSR model and the dashed line is the threshold which discriminates between useful and useless wavelengths. The thin solid line in A and B is the presence of each wavelength variable in the models constructed by the GA-PLS. The thin solid line in C is the rescaled absolute value of the reliability index ($abs(RI)$).

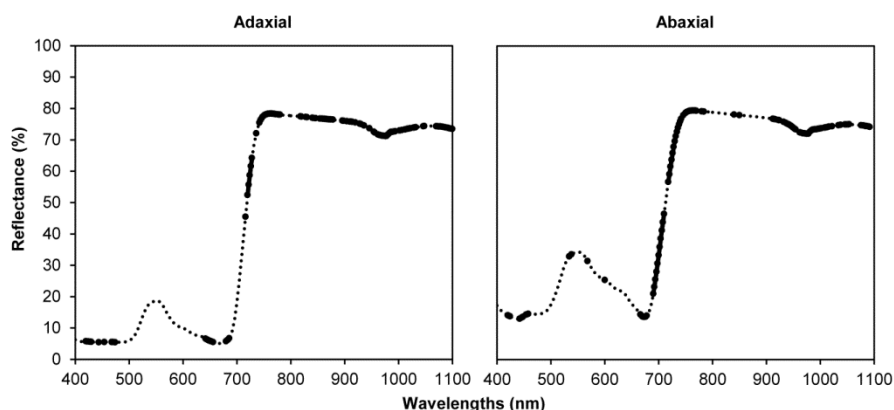


Fig. 4.7 Visual representation of the wavelengths which were excluded by both GA-PLS and GA-PLS_{10%} as well as MC-UVE-PLS from the adaxial and abaxial spectra in the 420 – 1100 nm range. The dotted black line is the mean spectrum. The solid areas are wavelength variables which were always excluded by the wavelength selection techniques.

A combination of the wavelengths selected by these different techniques might give even better results than any selection made by a single technique. Therefore, a combination of the selected wavelengths was made by combining all the selected wavelengths of different techniques or by keeping only the wavelengths on which the different techniques were unambiguous. In Table 4.3, the performance of the different models based on these combinations is presented together with the number of selected wavelengths. C1 and C2 were the only combinations which performed as good as MC-UVE-PLS, but the number of included wavelengths was lower. While the selection based on MC-UVE-PLS used 35% of the initial 650 wavelength variables, combinations C1 and C2 respectively used only 27% and 10%. To reduce the number of LV's, GLSW was applied with a different optimal threshold for each selection (Table 4.4). These final models were tested using an extra external test set which consisted of spectra acquired in March 2013 and May 2014 (Table 4.1). The root mean square error for this extra external test set (RMSEP) was used as an extra indicator for model robustness. All of the selected wavelength sets gave similar results in RMSECV, RMSEV and RMSEP, which indicates that these selections gave

robust PLSR prediction models. A two way ANOVA compared all three models and concluded that C1 was significantly different from C2 ($p=0.031$) based on the residuals of the external test set. MC-UVE-PLS was not significantly different from C1 ($p=0.763$) or C2 ($p=0.161$). A pairwise significance test for evaluating residuals from two models concluded that the probability that C2 performed better than MC-UVE-PLS and C1 was respectively 0.9538 and 0.9995. Based on these results C2 was selected as the final model (Fig. 4.8).

4.3.6. Practical implementation

Measurements have shown that the variance between lamb's lettuce plants in one batch is of the same magnitude as the variance between different batches (Verlinden et al., 2016). As the intention was to estimate the mean time in storage of the whole batch rather than that of individual plants, for example to support a decision to accept either reject a batch or to decrease the quality class of the whole batch, we decided to measure multiple plants of the batch and take the mean value as an improved estimation of the actual time after storage.

Table 4.4 The performance of three models using different numbers of wavelengths tested on data from September 2012 (RMSEV) and data from March 2013 and May 2015 (RMSEP).

Name of combination	Number of wavelengths	GLSW threshold	LV's	R ²	RMSEC (days)	RMSECV (days)	RMSEV (days)	RMSEP (days)
MC-UVE-PLS	228 (35%)	1	5	0.85	3.0	3.5	3.8	3.7
C1	174 (27%)	1.75	8	0.84	3.0	3.5	3.7	3.7
C2	65 (10%)	0.4	7	0.83	3.2	3.6	3.7	3.3

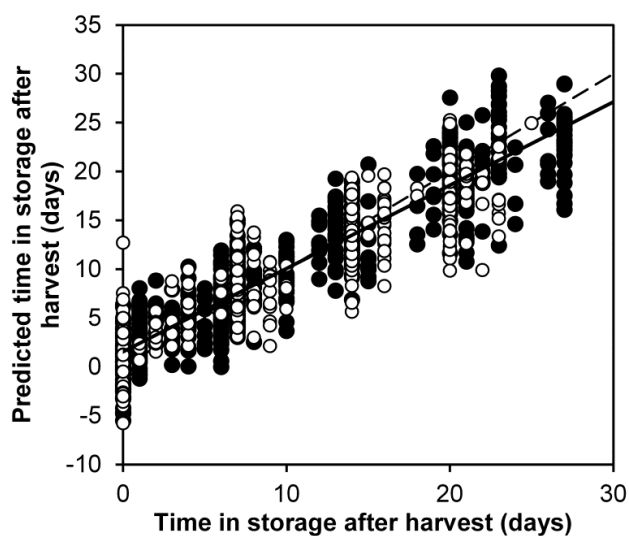


Fig. 4.8 Time in storage after harvest plotted against the time in storage predicted by a PLSR model on the concatenated spectrum (420-1100 nm) of adaxial and abaxial leaf sides with preprocessing (MSC, GLSW) and after wavelength selection using 65 wavelength variables (C2). The solid and open circles are samples from the calibration set in cross validation and external test set, respectively. The dashed line is the optimal regression line and the continuous black line is the regression line for this prediction model.

4.3.7. Physiological interpretation of selected wavelengths

The 65 C2 wavelengths mainly consisted of wavelengths from the visible part of the spectrum and wavelengths in the NIR region just past the red edge. (Fig. 4.9). In green leaves, the wavelengths from the visual part of the spectrum are dominated by the absorption caused by photosynthetic pigments which are mainly chlorophylls having a blue and red absorption peak, and carotenoids absorbing in the blue-green part of the spectrum (Taiz and Zeiger, 2010).

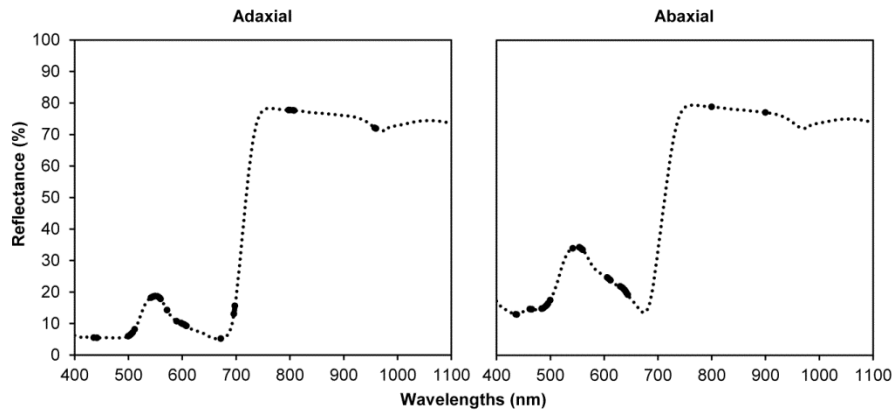


Fig. 4.9 The wavelength variables which were included in selection C2. The dashed gray line is the mean spectrum and the solid areas are wavelength variables selected for constructing the PLSR model.

Certain specific wavelengths which were retained in the final C2 selection were found to be associated with chlorophyll content (Le Maire et al., 2004). The reflectance signals at 542 nm and 556 nm were included in the selection for both the adaxial and abaxial side. These signals have been used to assess the total chlorophyll and chlorophyll b content, respectively (Maccioni et al., 2001). Other wavelength variables which were selected for both leaf sides and appear to be chlorophyll related are 436 nm and 606 - 608 nm. Chlorophyll a has an absorption maximum around 436 nm (Rabinowitch and Govindjee, 1969; Raven et al., 1999; Taiz and Zeiger, 2010) and a small local absorption maximum of chlorophyll b, where the absorption of chlorophyll a is at a local minimum, is around 606 - 608 nm (Raven et al., 1999).

Wavelengths solely associated with carotenoid content are hard to identify in green leaves due to the overlapping absorption with chlorophyll, but the total chlorophyll and carotenoid content can be associated with certain wavelengths (Féret et al., 2011; Merzlyak et al., 1999). The 500 nm wavelength was included in the chosen spectra from both leaf sides and has been associated with the total chlorophyll and carotenoid content (Chappelle and Kim, 1992; Zarco-Tejada et al., 2013).

Chlorophyll and carotenoid content decrease in lamb's lettuce during a post-harvest storage period. Therefore, it is logical that wavelengths associated with these pigments are included in the final selection of 65 wavelength variables (Ferrante et al., 2009; Ferrante and Maggiore, 2007).

In the NIR region of the spectra, only the 800 nm wavelength was included in both adaxial and abaxial spectra. Due to the nature of NIR with broad overlapping peaks, it is hard to identify the origin of the importance of this wavelength (Nicolai et al., 2007; Xiaobo et al., 2010). However, it has been found that a combination of 800 nm with 550 nm can be related to the chlorophyll content of bean leaves. So, the 800 nm wavelength might be a reference wavelength which is essential for determining the height of the chlorophyll peak (Buschmann and Nagel, 1993).

No wavelengths associated with sugar content were found in the final wavelength selection. Sugars were measured (Chapter 3), but the changes in concentration during storage might be too low to be detected by Vis / NIR spectroscopy. This is probably the reason why model performance improved when only wavelengths below 1100 nm were used compared to the use of more wavelengths up to 1690 nm.

For other wavelengths which were identified as important for a correct prediction no obvious relations with leaf pigments, sugars or water content could be found. Therefore, these will not be discussed in detail.

4.3.8. Predicting shelf life potential

Most of the wavelengths included in the prediction models were in the visual part of the spectrum (Fig. 4.7). Therefore, PLSR models for predicting different color parameters after a 10 d shelf life holding period were constructed. The performances of the prediction models are displayed in Table 4.5. None of the parameters gathered during the colorimetric measurements at the end of a shelf life holding period were predictable by the Vis/NIR spectra measured at the start of the shelf life holding period. R^2 values were between 0.02 and 0.13. The RMSEC and RMSECV were high

for all the colorimetric parameters compared to the standard deviation of these parameters. A possible cause could be that the change in color due to the shelf life holding period was too small compared to the changes caused by other effects. A PLSR model based on Vis/NIR spectra for predicting the quality scores after a 10 d shelf life holding period was built. The model had an RMSEC and an RMSECV of 0.85 and 1.37, respectively, with an R^2 of 0.33 while using 16 LV's. This model performed better than any of the models using colorimetric measurements but still lacked accuracy and robustness, having a low R^2 and a high RMSECV. This might be due to the small calibration dataset. Another reason might be that it was too hard to determine the quality of lamb's lettuce resulting in a poor link between the dependent and independent variables. The reason might also be that there was no solid correlation between the Vis/NIR spectrum before and the quality after a shelf life holding period. The reasons why were unclear, and determining shelf life potential using PLSR models for predicting different color parameters and quality scores was shown to be unfruitful.

Table 4.5 An overview of the values from colorimetric measurements and the performance of constructed PLSR models based on the Vis/NIR spectrum for predicting these parameters after a shelf life holding period of 10 d at 8°C.

Dependent variable	Mean	Standard deviation	LV's	R^2	RMSEC	RMSECV
Adaxial color parameters						
a	-9.49	0.49	2	0.03	0.47	0.49
b	26.50	1.23	8	0.11	0.99	1.19
C	28.16	1.22	8	0.10	0.99	1.21
H	109.72	1.03	9	0.13	0.83	0.99
Abaxial color parameters						
a	-9.50	0.48	2	0.02	0.46	0.48
b	26.50	1.22	8	0.11	0.99	1.19
C	28.16	1.21	8	0.09	0.98	1.20
h	109.75	1.03	9	0.12	0.84	0.99

4.4. Conclusions

Vis/NIR transreflectance spectroscopy in combination with PLSR regression was evaluated as a fast and non-destructive method for determination and quantification of a prior storage period for lamb's lettuce. The accuracy and robustness of the predictions improved vastly after wavelength selection with RMSECV, RMSEV and RMSEP values of respectively 3.6, 3.7 and 3.3 d. The number of LV's dropped from 13 to 7, the RMSECV and RMSEV decreased with 2.4 and 1.7 d, respectively, while the R^2 increased from 0.75 to 0.83. The number of used wavelength variables was minimized by combining the output of GA-PLS_{10%} and MC-UVE-PLS, resulting in the selection of 65 essential wavelength variables which made up 10% of the initial 650 wavelength variables. These wavelengths in the Vis/NIR spectrum contained the essential information related to the time in storage after harvest and had a decent signal to noise ratio. It is possible that external factors influence certain wavelength variables, but these influenced wavelength variables can still be corrected by other wavelength variables which are not influenced to prevent an incorrect prediction (Table 4.1). After comparing the selected wavelengths with those reported in literature, it became clear that information on photosynthetic pigment degradation is essential for determining and quantifying a prior storage period of lambs lettuce.

Predicting shelf life potential using PLSR models for predicting different color parameters and quality scores was shown to be unsuccessful. The accuracy and robustness of the predictions were insufficient. The best model had a RMSEC and a RMSECV of 0.85 and 1.37, respectively, with an R^2 of 0.33 while using 16 LV's. The reasons why it was hard to make these prediction were unclear and may be related to the small dataset or the lack of a link between the dependent and independent variables.

Although good prediction results were obtained with Vis/NIR spectroscopy for determining and quantifying a prior storage period, it has been shown in chapter 2 that photosynthetic pigments can also be detected using

chlorophyll fluorescence emission measurements. Hence, this technique might be more suited to estimate the storage duration of lamb's lettuce. Therefore, the use of chlorophyll fluorescence emission signals will be explored in the next chapter as an option for determining the storage time of lamb's lettuce with a higher accuracy.

5. Estimation of storage time of lamb's lettuce based on chlorophyll fluorescence

5.1. Introduction

In the previous chapter, the potential of Vis/NIR spectroscopy for determination and quantification of a prior storage period for lamb's lettuce was evaluated. The wavelengths used by the final prediction model were in the visible part of the spectrum and could be related to photosynthetic pigment degradation. An alternative method to measure this pigment degradation is chlorophyll fluorescence emission. It has already been used on leaves, and direct relations have been made between certain chlorophyll fluorescence emission ratios and chlorophyll, flavonol and anthocyanin content (Agati et al., 2007, 2005; Buschmann, 2007; Cerovic et al., 2002; Sytar et al., 2015; Tempesta et al., 2012; Tremblay et al., 2011). Therefore, the aim of this study was to evaluate the potential of chlorophyll fluorescence emission signals to estimate how long a batch of lamb's lettuce has been stored before it was presented to the market.

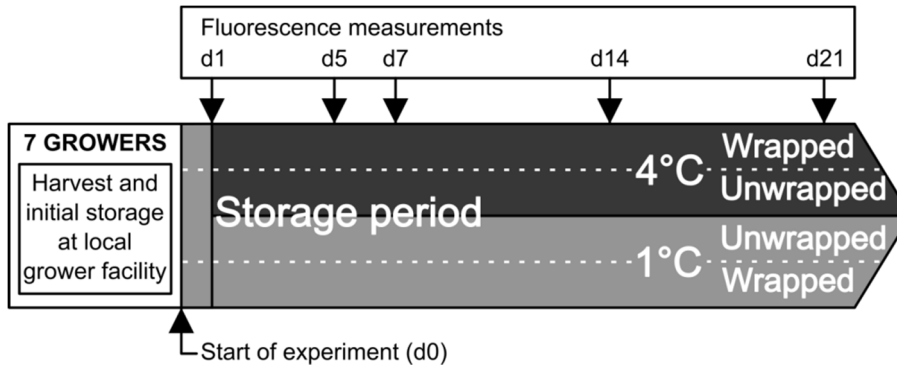


Fig. 5.1 Schematic representation of the experimental setup. The number of days indicates the storage time from the start of the experiment.

5.2. Materials and methods

5.2.1. Plant material and storage conditions

Samples of lamb's lettuce (*Valerianella locusta* L.) grown by seven different commercial producers were harvested in November 2014. The samples were stored directly after harvest at the cooling facility of the producers until the start of the experiment. The maximum storage time at a local facility was five days. Each producer had his own specific growing and harvesting method. An overview of the growing and harvesting conditions for each batch of lettuce is shown in Table 5.1. These samples from different growers were included in the data set to create a realistic image of the variability in products presented to the market.

The storage experiment took place at the experimental station Inagro (Rumbeke-Beitem, Belgium) and started at November 20, 2014. Different producers who store lamb's lettuce have different storage conditions. To mimic this kind of variation half of the samples from each grower were stored at 1 °C and the other half at 4 °C (Fig. 5.1). Half of these samples were wrapped in plastic foil while the other half was left unwrapped. The wrapping is done in practice to prevent drying in the cool room during the storage

Table 5.1 Growing and harvesting conditions for each batch of lamb's lettuce used in the experiment.

Grower	Cultivar*	Sowing density (seeds/m ²)	Growing period (d)	Harvest date	Harvest mechanism	Rinsing date	Storage temp. local facility (°C)	Time at local facility (d)
1	Trophy	444	55	19/11	Manual	20/11	4	1
2	Audace	840	43	15/11	Automated	18/11	3,5	5
3	Trophy	430	55	20/11	Manual	20/11	/	0
4	Audace	800	47	19/11	Automated	19/11	2	1
5	Audace	750	48	19/11	Automated	19/11	2,5	1
6	Trophy	500	51	20/11	Manual	20/11	/	0
7	Audace	800	46	15/11	Automated	19/11	2	5

* All cultivars were from seed company HM. Clause.

period. It is done here to mimic realistic variation in storage conditions. The first night of the experiment, all the crates of lamb's lettuce were stored at 1 °C. Measurements were carried out after 1, 5, 7, 14 and 21 days in storage. At each measurement point during storage, new samples from the same batch were used to minimize the effect of sample handling on the quality of the samples

5.2.2. Chlorophyll fluorescence emission measurements

Chlorophyll fluorescence emission signals were measured using the Multiplex 3 (Force-A, Orsay, France), a portable fluorimetric device. It consists of four excitation Light Emitting Diode (LED) channels, i.e. ultraviolet (UV), blue (B), green (G) and red (R), and three fluorescence detection channels (Silicon photodiodes), i.e., yellow (YF), red (RF) and far-red (FRF) (Chapter 2). Each excitation caused by a certain LED results in three values for fluorescence which leads to 12 output values: YF_{UV}, RF_{UV}, FRF_{UV}, YF_B, RF_B, FRF_B, YF_G, RF_G, FRF_G, YF_R, RF_R and FRF_R. The first part of the name of a variable mentions the fluorescence channel and the subscript mentions the LED excitation channel. The LED's emit light in a pulsating manner and the detection is synchronized. One measured value is an average of 500 measurements. The measurements were taken on site and the stored data was processed later.

Before measuring samples, reference measurements were performed on a reference sample (Force-A, blue standard sheet). The measured values were compared with the reference values to determine if the sensor was still functioning correctly.

Each crate containing samples was measured once in the center to have as little as possible effects of plants which may be affected by the edges of the crates. On the first day of the experiment, each crate was measured three times on three different spots to have more measurements due to the limited amount of samples at our disposal. This way, the first day of the experiment was not underrepresented in the data matrix. At the first day of the experiment, 21 chlorophyll fluorescence emission measurements were performed. During days 5, 7, 14 and 21 of the experiment 112 measurements were performed, 28 on each day. Each measurement was conducted on different samples.

5.2.3. Prediction model with separate temperatures

5.2.3.1. Identifying outliers

First, the chlorophyll fluorescence emission signals were analyzed using Principal Component Analysis (PCA) (Wold et al., 2001). The independent variables were chlorophyll fluorescence emission signals (12) or ratios of these signals (132) combined with specific combinations found in literature (9) (Table 2.3). The variables were preprocessed by autoscaling. Score plots were used to visualize the location of the samples in the model space. Q residuals and Hotelling T^2 statistics were used to identify outliers (MacGregor and Kourti, 1995).

5.2.3.2. Constructing the prediction model

Prediction models were constructed using Partial Least Squares Regression (PLSR) with the PLS-Toolbox (Eigenvector Research Inc., Wenatchee WA, USA) for Matlab (MATLAB R2013a, The MathWorks, Inc., Natick,

Massachusetts, United States) (Wold et al., 2001). The dependent variable was storage time after harvest (d).

The calibration data consisted initially of samples which were measured the first day of the experiment and all samples that were measured later in the storage period at 4 °C. The samples which were stored at 1 °C were used as an external test dataset. After initial testing the selection of samples in the calibration matrix was changed.

The data from samples from both storage temperatures were split in a calibration and test set using the Kennard-Stone algorithm (Kennard and Stone, 1969) available in the PLS-Toolbox (Eigenvector Research Inc., Wenatchee WA, USA) for Matlab. (MATLAB R2013a, The MathWorks, Inc., Natick, Massachusetts, United States). Of all measured samples 66 % were retained for calibration purposes and the remaining 34 % were used as an internal test set. Cross validation (CV) with each measurement day as a separate CV group was applied to evaluate the PLSR model performance as a function of the model complexity.

For each PLSR model an optimal number of LV's was selected based on the RMSEC, RMSECV and the signal to noise ratio (S/N). The latter was calculated using the 'estimatefactors' algorithm in PLS-Toolbox. The algorithm resamples the data and when the loadings change significantly between resamplings, the factor is probably based on noise and not on signal. An S/N greater than three is considered informative. This allows to estimate the number of significant factors in multivariate data (Henry et al., 1999; Sug Park et al., 2000).

5.2.3.3. Monte Carlo Uninformative Variable Elimination PLS

To reduce the number of chlorophyll fluorescence emission ratios in the prediction model, Monte Carlo Uninformative Variable Elimination PLS (MC-UVE-PLS) was applied as a variable selection technique. The selection of the number of variables to retain in our models was based on the RMSECV of different PLSR models with different numbers of variables retained. The absolute value of the RI was the basis on which these

variables were retained. Variables with a low absolute value of the RI were considered less important for decent predictions and were discarded first. The maximum number of LV's in MC-UVE-PLS was set to the number which was selected for the model using all the chlorophyll fluorescence emission ratios. 10000 Monte Carlo simulations were performed, each of them contained 66% of the samples for constructing a calibration model. MC-UVE-PLS was performed using LibPLS (www.libpls.net) in Matlab. An error occurred in the Matlab script when calculating the RI, so the RI was calculated in MS Excel (Microsoft Office Professional Plus 2010, Microsoft, Co., Redmond, Washington, United states) using $\bar{\beta}_j$ and σ_j . Further evaluation of the output based on the RI was also performed in MS Excel.

5.2.3.4. Variable Importance in Projection scores

In the final selection of variables the Variable Importance in Projection (VIP) scores were used to identify interesting variables.

5.2.3.5. Correcting for storage temperature

In March 2015, a similar experiment was carried out in which samples were stored at 1 °C and 4 °C. Gas chromatography - mass spectrometry measurements of these samples revealed an effect of storage temperature on the abundance of metabolites (Chapter 3). Glucose, fructose and sucrose are the largest source of respiratory substrates in lamb's lettuce. Hence, the concentrations of these soluble carbohydrates were combined for each sample and this sum was used as a quality parameter:

$$Q = [\text{glucose}] + [\text{fructose}] + 2 \cdot [\text{sucrose}] \quad \text{Eq. 5.1}$$

where Q is the quality parameter, and $[\text{glucose}]$, $[\text{fructose}]$ and $[\text{sucrose}]$ are the concentrations of glucose, fructose and sucrose, respectively. Sucrose is multiplied by two, because one mole of sucrose is split into one mole of glucose and one mole of fructose, which are used during respiration. The

decline of Q over time was faster for samples stored at higher temperatures (Fig. 5.2). These reactions are enzyme reactions which are typically described by Michaelis-Menten kinetics. One can assume that a substrate limitation is present somewhere during this catabolic process. If the concentration of the limiting substrate is low enough below the Michaelis-Menten constant then the Michaelis-Menten kinetics can be approximated by a first order kinetic model (Michaelis and Menten, 2013):

$$\frac{dQ}{dt} = -k_T Q \quad \text{Eq. 5.2}$$

where k_T is the temperature dependent rate constant. Taking the integral for 1 °C and 4 °C leads to:

$$\int_{Q_0}^{Q_f} \frac{1}{Q} dQ = - \int_0^{t_{4^\circ\text{C}}} k_{4^\circ\text{C}} dt$$

$$\int_{Q_0}^{Q_f} \frac{1}{Q} dQ = - \int_0^{t_{1^\circ\text{C}}} k_{1^\circ\text{C}} dt \quad \text{Eq. 5.3}$$

where Q_0 is the value of Q at the start of the storage period, $k_{1^\circ\text{C}}$ and $k_{4^\circ\text{C}}$ are the rate constants for a storage temperature of 1 °C and 4 °C, respectively, and $t_{1^\circ\text{C}}$ and $t_{4^\circ\text{C}}$ are the time in storage after harvest when the final quality level Q_f has been reached for a storage temperature of 1 °C and 4 °C, respectively. Solving these integrals leads to an equation for each temperature:

$$\ln(Q_f) - \ln(Q_0) = -k_{4^\circ\text{C}} t_{4^\circ\text{C}}$$

$$\ln(Q_f) - \ln(Q_0) = -k_{1^\circ\text{C}} t_{1^\circ\text{C}} \quad \text{Eq. 5.4}$$

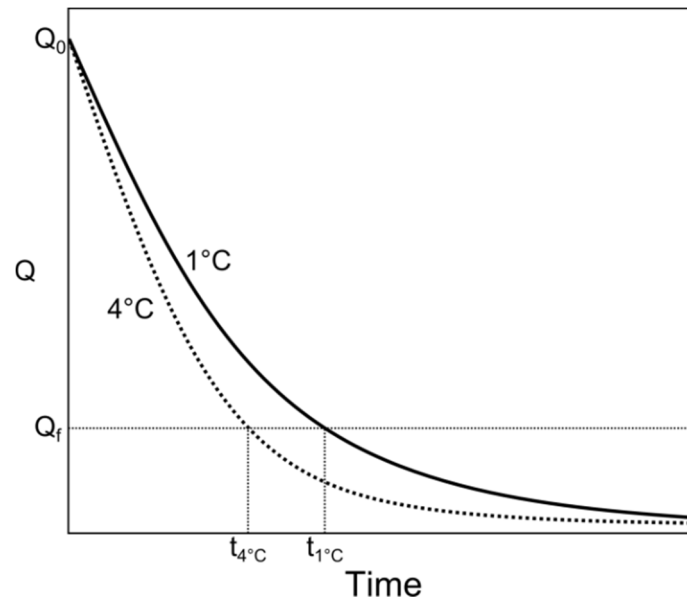


Fig. 5.2 An illustration of the decrease of the quality parameter Q , with increasing storage time at 1 °C (—) and 4 °C (.....). The time in storage after harvest when a sample reaches a final quality level Q_f is longer for samples stored at 1 °C ($t_{1°C}$) than at 4 °C ($t_{4°C}$).

These equations were fitted simultaneously using a linear regression in R (R 3.3.2, R Foundation for Statistical Computing, Vienna, Austria). Thus, it was possible to have the same intercept with the Y axes for both regression lines, because there was no influence of the storage temperature at the start of storage. The angles of these regression lines were equal to the values for the temperature dependent rate constants ($k_{1°C}$ and $k_{4°C}$). Rearranging these equations resulted in:

$$t_{4°C} = \frac{k_{1°C}}{k_{4°C}} t_{1°C} \quad \text{Eq. 5.5}$$

which made it possible to calculate the equivalent postharvest storage period at 4 °C for each postharvest storage period at 1 °C. These time values were used as the new dependent variables for the samples which were stored at 1 °C.

5.3. Results

5.3.1. Chlorophyll fluorescence emission signals

The initial modeling was performed on 12 fluorescence emission signals combined with nine specific combinations found in literature. First, these variables were analyzed using PCA. Next, PLSR was used to make an estimation on a prior storage period.

5.3.1.1. PCA analysis

From the PCA on all the fluorescence signals using two principal components (PC's) no outliers were identified based on Q residuals and Hotelling T^2 statistics (Fig. 5.4A). The score plot revealed no clear difference between wrapped and unwrapped samples, nor samples stored at 1 °C and 4 °C which were the external test set and calibration set, respectively (Fig. 5.3A).

Upon inspection of the samples of the initial measurement day and their corresponding producers, a few things were noteworthy (Fig. 5.3B and 5.4B). First, these samples had a large spread in the Q residuals and Hotelling T^2 statistics, indicating that the producers had a strong influence on the variation of the sample pool which was also noticeable in the score plot. Also, the samples of most producers at the first measurement day were grouped together in the PCA score plot. However, the samples of producer 3 and 6 were spread out over a slightly wider area compared to the others. These were the only producers who harvested their samples at the start of the experiment (Table 5.1). The three samples of producer 1 at the first measurement day are located close to each other in the score plot, so they seem to be very similar. However, the Q residuals of these samples were some of the most extreme of the entire dataset indicating that these samples did not fit well in the model.

5.3.1.2. PLS regression analysis

A PLS regression analysis was carried out with chlorophyll fluorescence emission signals as independent variables and the storage time after harvest as dependent variable. The S/N plot suggested the selection of four LV's, while the RMSECV reached a global minimum at five LV's. To avoid overfitting by including noisy LV's, four LV's were included in the final PLSR model. When the actual storage time was plotted against the predicted storage time, a large spread in the predictions of the samples was noticeable after 15 d in storage (Fig. 5.5A). This can be explained by the lower prediction values for the samples of the internal test set. As a consequence, the model performance was poor with an RMSECV, RMSEP, R^2 in CV (R^2_{CV}) and R^2 in prediction (R^2_{Pred}) of 4.8 d, 6.9 d, 0.60 and 0.28, respectively (Table 5.2).

Table 5.2 PLSR model performance statistics

Data type	Number of variables	LV's	RMSEC (days)	RMSECV (days)	RMSEP (days)	R^2_{Cal}	R^2_{CV}	R^2_{Pred}
Fluorescence signals	12 (100%)	4	3.2	4.8	6.9	0.81	0.60	0.28
Fluorescence Ratios	141 (100%)	4	3.2	4.6	7.0	0.82	0.62	0.24
Fluorescence Ratios	53 (37%)	4	3.1	4.0	6.8	0.83	0.71	0.27

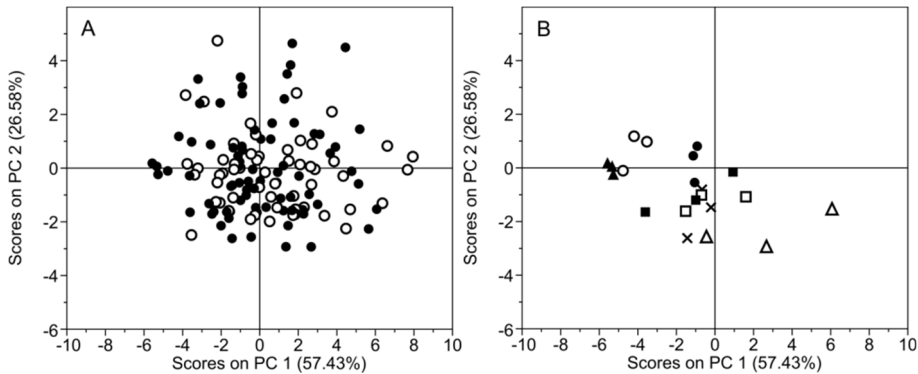


Fig. 5.3 Score plots of the PCA model using two PC's based on solely chlorophyll fluorescence emission signals and no ratios. (A) The symbols represent data of the calibration (●) and external test set (○) data matrix. (B) Only the samples of the first measurement day were included and the symbols indicate which samples were grown by producer 1 (●), 2 (○), 3 (■), 4 (□), 5 (▲), 6 (△) and 7 (×).

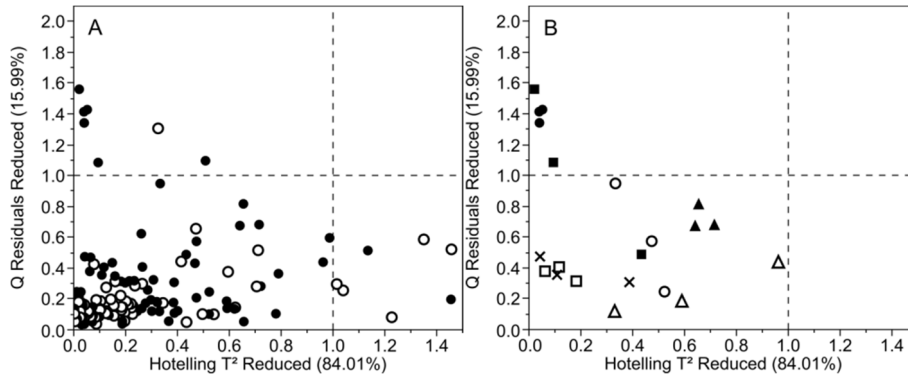


Fig. 5.4 Plots of rescaled Q residuals and rescaled hotelling T^2 statistics of the PCA model using two PC's based on solely chlorophyll fluorescence emission signals and no ratios. The dashed lines represent the 95% confidence limit and were used to rescale the plots. (A) The symbols represent data of the calibration (●) and external test set (○) data matrix. (B) Only the samples of the first measurement day were included and the symbols indicate which samples were grown by producer 1 (●), 2 (○), 3 (■), 4 (□), 5 (▲), 6 (△) and 7 (×).

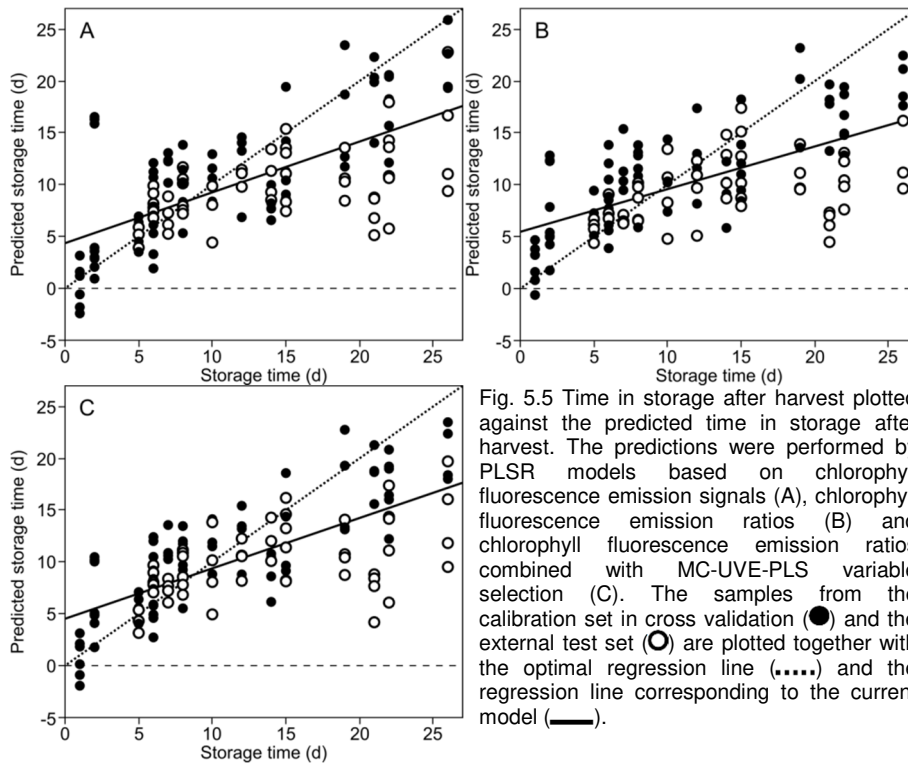


Fig. 5.5 Time in storage after harvest plotted against the predicted time in storage after harvest. The predictions were performed by PLSR models based on chlorophyll fluorescence emission signals (A), chlorophyll fluorescence emission ratios (B) and chlorophyll fluorescence emission ratios combined with MC-UVE-PLS variable selection (C). The samples from the calibration set in cross validation (●) and the external test set (○) are plotted together with the optimal regression line (.....) and the regression line corresponding to the current model (—).

5.3.2. Chlorophyll fluorescence emission ratios

A possible solution to improve the prediction based on fluorescence signals was to use ratios instead of raw signals. Hence, the modeling was performed on 132 fluorescence emission ratios combined with nine specific combinations found in literature. First, these variables were analyzed using PCA. Next, PLSR was used to make an estimation on a prior storage period.

5.3.2.1. PCA analysis

A PCA on the fluorescence ratios using four PC's identified one outlier in the external test set based on Q residuals and Hotelling T^2 statistics (Fig. 5.7A). The score plot revealed no differences between the calibration and external test set which were stored at 4 °C and 1 °C, respectively (Fig. 5.6A), nor were any differences revealed between the wrapped and unwrapped samples.

The data on the initial measurement day show again a large spread in the Q residuals and Hotelling T^2 statistics between producers (Fig. 5.7B). This is also noticeable in the score plot of PC 1 and PC 2 where the range of the sample scores of the first measurement day are almost the same as that of all samples of the whole experiment (Fig. 5.6A and B). The samples of the same producers are still grouped together in the PCA score plot. The samples of producer 3 and 6 are spread out over a slightly wider area compared to the others similar to the PCA model which used only fluorescence emission signals (Fig. 5.3B and 5.6B). The Q residuals for samples from producers 3 and 6 also show big differences (Fig. 5.7B). This variation in Q residuals and Hotelling T^2 statistics for the same producer on the initial measurement day indicates that, although these measurements were performed on the same crate, the fluorescence signals varied between different parts of the crates. The harvest moment for samples from producers 3 and 6 was at the start of the experiment. Hence, it could well be that variation was introduced in these signals by the harvest itself.

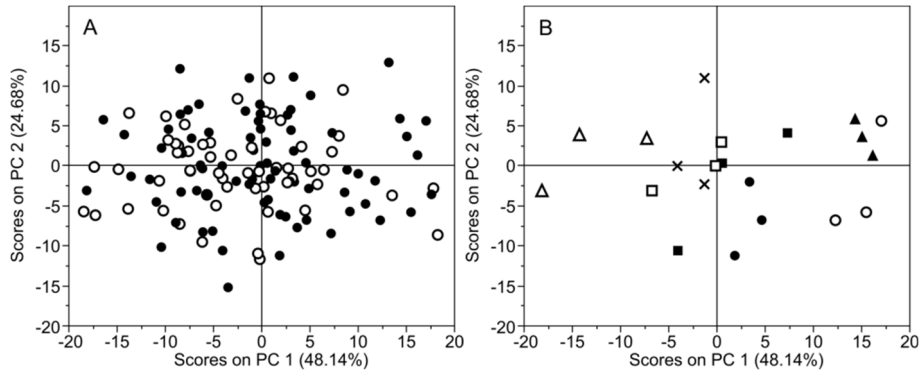


Fig. 5.6 Score plots of the PCA model using two PC's based on chlorophyll fluorescence emission ratios. (A) The symbols contain data of the calibration (●) and external test set (○) data matrix. (B) Only the samples of the first measurement day were included and the symbols indicate which samples were grown by producer 1 (●), 2 (○), 3 (■), 4 (□), 5 (▲), 6 (△) and 7 (×).

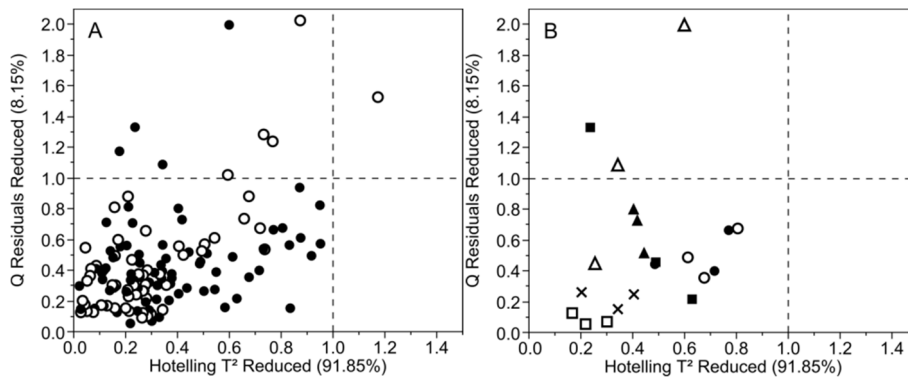


Fig. 5.7 Plots of rescaled Q residuals and rescaled Hotelling T^2 statistics of the PCA model using four PC's based on chlorophyll fluorescence emission ratios. The dashed lines are the 95% confidence limit and were used to rescale the plots. (A) The symbols contain data of the calibration (●) and external test set (○) data matrix. (B) Only the samples of the first measurement day were included and the symbols indicate which samples were grown by producer 1 (●), 2 (○), 3 (■), 4 (□), 5 (▲), 6 (△) and 7 (×).

5.3.2.2. PLS regression analysis

A PLS regression analysis was carried out with the chlorophyll fluorescence emission ratios as independent variables and the storage time after harvest as dependent variable. The S/N plot suggested that a maximum of nine LV's were informative. The RMSECV pointed towards the use of four LV's. Hence, four LV's were used because the chances of overfitting are smaller with less LV's. Compared to the model based on fluorescence emission signals, the model based on the ratios performed slightly better in CV, but worse results were achieved on the internal test set (Table 5.2). In Fig. 5.5B, the actual storage time is plotted against the predicted storage time. A larger spread in the predictions after 15 days in storage can be observed, similar to what was observed for the chlorophyll fluorescence emission signals (Fig. 5.5A). This suggests that the temperature difference in storage between the calibration and external test has a large impact on the fluorescence signals and the underlying physiology as was shown in chapter 3.

5.3.2.3. MC-UVE-PLS

After applying MC-UVE-PLS on the chlorophyll fluorescence emission ratios, the best result in CV was found when 52 (37 %) of the variables were used. The S/N indicated that a maximum of five LV's were informative, but the RMSECV pointed towards the use of four LV's. Hence, four LV's were used because the chances of overfitting are smaller with less LV's. The four LV model had an R^2_{CV} and RMSECV of 0.71 and 4.0 d, respectively (Table 5.2). These values were an improvement compared to both previous models. The prediction results improved, but were still not sufficient for decent predictions with an R^2_{Pred} and RMSEP of 0.27 and 6.8 d. The large spread in the predicted storage times after 15 d was still noticeable after the variable selection was performed (Fig. 5.5C). This indicates that the storage temperature effect could not be filtered out using MC-UVE-PLS.

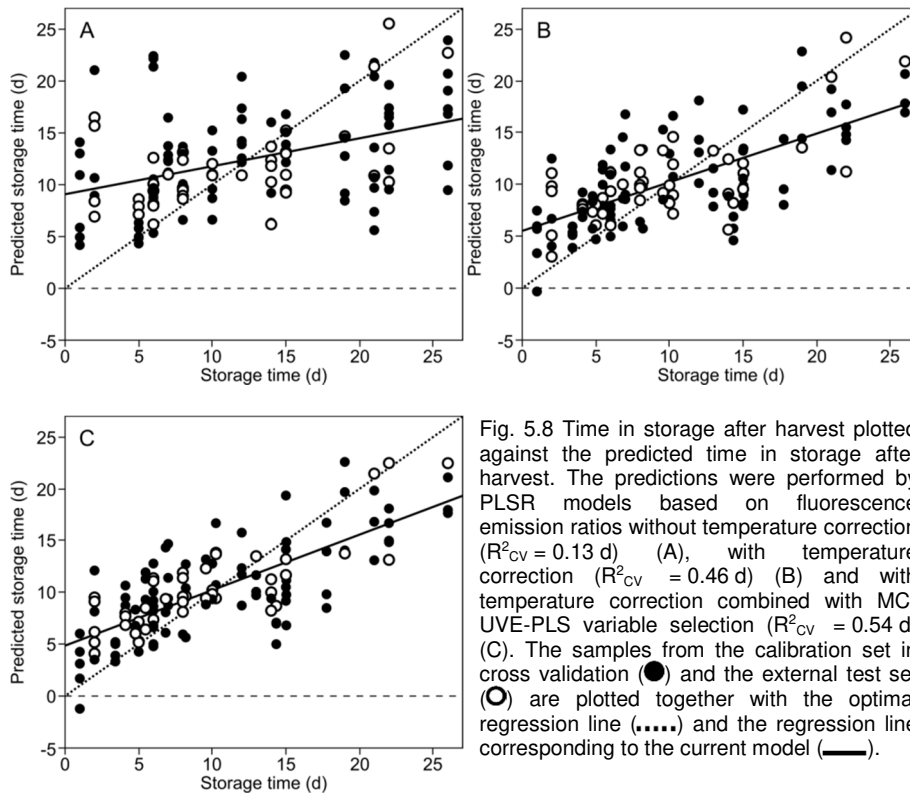
5.3.2.4. Correcting for storage temperature effects

From the previous results, it appeared that the temperature effect during storage on the samples which was visible in the chlorophyll fluorescence emission signals was too large to be filtered out using variable selection. We therefore tried to compensate for these temperature effects using metabolomics data (Chapter 3).

To compare a PLSR model constructed with the actual storage time with a PLSR model with the corrected one, we constructed a PLSR model with the actual time in storage after harvest with a calibration and external test matrix which contained samples stored at both temperatures (Fig. 5.8A). The S/N indicated that a maximum of nine LV's were informative, but the RMSECV had a global minimum at three LV's (Table 5.3). The prediction model which used three LV's gave poor results in CV (RMSECV = 7.5 d, $R^2_{CV} = 0.13$) and in prediction (RMSEP = 5.2 d, $R^2_{pred} = 0.34$). When comparing the PLSR models based on fluorescence emission ratios, it was observed that the new data matrix with samples of both storage temperatures gave better results in prediction, but worse results in CV (Table 5.2 and 5.3). Hence, there was no real progress in combining data of the two temperatures. This indicates that PLSR had problems to fit data stored at both temperatures even though both storage temperatures were included in the calibration data matrix.

Table 5.3 PLSR model performance statistics

Data type	Temperature correction	Number of LV's variables	RMSEC (days)	RMSECV (days)	RMSEP (days)	R^2_{Cal}	R^2_{CV}	R^2_{Pred}	
Fluorescence ratios	No	141(100%)	3	4.9	7.5	5.2	0.59	0.13	0.34
Fluorescence ratios	Yes	141 (100%)	4	3.3	4.9	4.2	0.76	0.46	0.50
Fluorescence ratios	Yes	29 (20%)	3	3.3	4.6	3.5	0.76	0.54	0.67



In an alternative approach, the duration of storage at 1 °C was translated to 4 °C using a conversion factor according to Eq. 5.5. The chlorophyll fluorescence emission ratios were chosen over the raw signals, because they are known to be more stable compared to pure signals (Cerovic et al., 2009). From a similar storage experiment (Chapter 3) we calculated that this conversion factor was equal to 0.68. This indicates that the quality of lamb's lettuce stored at 1 °C decreased 0.68 times slower than lamb's lettuce stored at 4 °C. A new prediction model was subsequently constructed using the converted data (Fig. 5.8B). The S/N indicated that nine LV's were informative, but the RMSECV pointed towards the use of four LV's. This PLSR model which used four LV's gave better results in predicting the postharvest time both in CV (RMSECV = 3.3 d, $R^2_{cv} = 0.46$) and for the external test set (RMSEP = 4.2 d, $R^2_{Pred} = 0.50$) than the PLSR model without the temperature correction (Table 5.3).

After applying MC-UVE-PLS on the temperature corrected data, the best results in CV were achieved when 29 (20%) of the 141 variables were retained (Fig. 5.9, Fig. 5.8C and Table 5.4). The S/N indicated that five LV's were informative, but the RMSECV pointed towards the use of three LV's. The PLSR model using 29 variables performed slightly worse in calibration, but better in CV and prediction with an RMSECV, RMSEP, R^2_{CV} and R^2_{Pred} of 4.6 d, 3.5 d, 0.54 and 0.67, respectively (Table 5.3).

Table 5.4 The 29 variables which were included in the final PLSR model after applying MC-UVE-PLS on the temperature corrected data.

Selected variables				
FLAV	RF _B /YF _{UV}	YF _{UV} /FRF _{UV}	FRF _B /YF _B	RF _B /YF _G
NBIG	FRF _B /YF _{UV}	RF _B /FRF _{UV}	RF _{UV} /RF _B	FRF _{UV} /FRF _G
FERARI	FRF _G /YF _{UV}	YF _{UV} /YF _B	FRF _B /RF _B	RF _B /FRF _G
RF _{UV} /YF _{UV}	FRF _R /YF _{UV}	RF _{UV} /YF _B	FRF _{UV} /FRF _B	FRF _{UV} /FRF _R
FRF _{UV} /YF _{UV}	FRF _{UV} /RF _{UV}	FRF _{UV} /YF _B	RF _B /FRF _B	RF _B /FRF _R
YF _B /YF _{UV}	RF _B /RF _{UV}	RF _B /YF _B	YF _{UV} /YF _G	

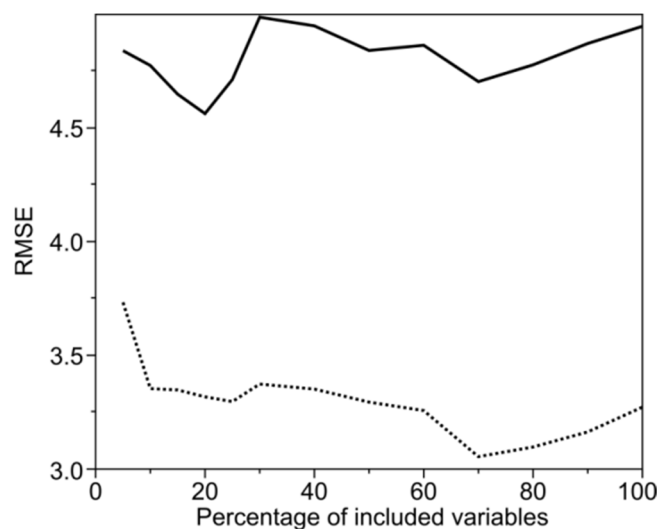


Fig. 5.9 RMSEC (.....) and RMSECV (—) as a function of the number of variables based on MC-UVE-PLS variable selection on the data with temperature correction.

5.4. Discussion

The chlorophyll fluorescence emission ratios combined with MC-UVE-PLS resulted in better PLSR prediction models compared to using the raw fluorescence emission signals. After rescaling of the storage times for the effect of storage temperature, the prediction results improved significantly with the best results when MC-UVE-PLS was applied. From the 29 chlorophyll fluorescence emission ratios which were selected by MC-UVE-PLS after the temperature correction, six were documented in literature, i.e. FLAV, FRF_{UV}/FRF_R , FERARI, YF_{UV}/FRF_{UV} , FRF_{UV}/YF_{UV} , NBI_G (Bilger et al., 2001, 1997; Cartelat et al., 2005; Cerovic et al., 2009, 2008, 2002, 1999; Demotes-Mainard et al., 2008; Ghozlen et al., 2010; Malenovský et al., 2009; Meyer et al., 2006). Both FLAV and FRF_{UV}/FRF_R have been associated with the shielding of leaves by flavonols (Bilger et al., 2001, 1997; Cerovic et al., 2002). This suggests that a significant change in flavonols takes place during the postharvest storage period. Flavonols have a role in photoprotection, specifically as ultraviolet protectants, but they are also known to protect the plant against free radicals (Bogs et al., 2007; Koes et al., 2005). The amount of free radicals increases during a storage time, especially in wounded plants (Ferrante et al., 2009).

FERARI has been shown to be correlated to the anthocyanin content in red grapes (Ghozlen et al., 2010). Hence, it is noteworthy that this variable was included, while the other anthocyanin ratios ($ANTH_{RG}$, $ANTH_{RB}$, FER_{RG}) were not (Table 2.3). However, this could be because these variables contain more or less similar information and the other anthocyanin ratios could be considered as redundant. The anthocyanin content in lamb's lettuce has been reported to increase after a stable period of eight days (Ferrante et al., 2009). It should be noted that FERARI is not a ratio of two fluorescence signals, but a log transformation of the inverse of FRF_R (Table 2.3). The use of chlorophyll fluorescence emission signals without ratios is discouraged unless a constant distance to the samples is maintained

(Cerovic et al., 2009). The latter was the case in our experiments, but one should be cautious when using this variable in future research.

Both YF_{UV}/FRF_{UV} and the inverse FRF_{UV}/YF_{UV} were included in the final selection of variables. YF_{UV}/FRF_{UV} has been linked to multiple stress related situations and the accumulation of specific metabolites and fruit maturation (Cerovic et al., 2008, 1999; Malenovský et al., 2009). For red grapes, the information gathered from this ratio was similar to FERARI (Cerovic et al., 2009).

Chlorophyll fluorescence emission ratios which are influenced by epidermal phenols and chlorophyll were shown to respond to the nitrogen nutrition of the plant (Cartelat et al., 2005; Demotes-Mainard et al., 2008; Meyer et al., 2006). NBI_G is one of these ratios and was included as a variable after MC-UVE-PLS (Table 2.3).

Surprisingly, no ratio solely linked to chlorophyll content (SFR_G , SFR_R) was selected by MC-UVE-PLS, although a decrease in chlorophyll content in lamb's lettuce has been shown during postharvest storage (Ferrante and Maggiore, 2007). In our experiments the decrease in chlorophyll content may have been too small to be detected with fluorescence signals (Ferrante et al., 2009).

For the remaining variables selected by the model no reports on links to specific compounds or stress were found. A first observation was that seven of the 29 selected ratios had YF_{UV} in the denominator. This might indicate that YF_{UV} was a stable signal which was hardly influenced by different surrounding factors, e.g. growing conditions, harvest conditions, cultivar, etc. when there is a correction for storage temperature. Another interesting variable was FRF_{UV}/YF_B which was close to FRF_{UV}/YF_{UV} in the score plot and both of them were on the opposite side of the dependent variable when the first 2 LV's were used (Fig. 5.10). Also, they had the highest VIP scores indicating that these ratios were important for the PLSR model (Fig. 5.11).

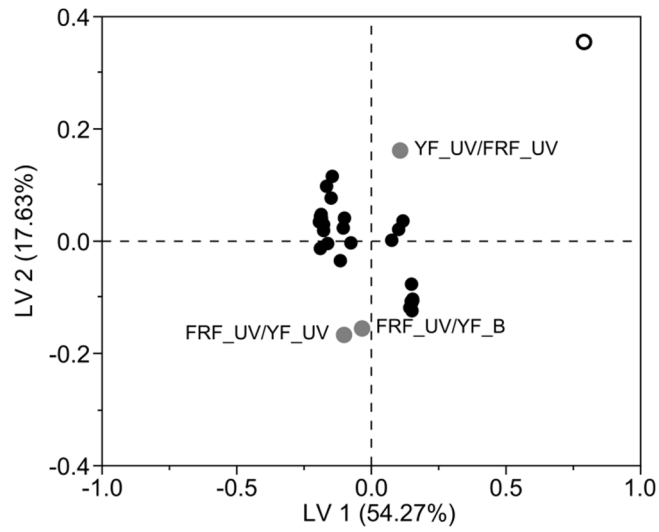


Fig. 5.10 Loadings plot of the PLSR model with temperature correction and variable selection for the first two latent variables. The X (●) and Y variables (○) are shown together with the highlighted X variables (●).

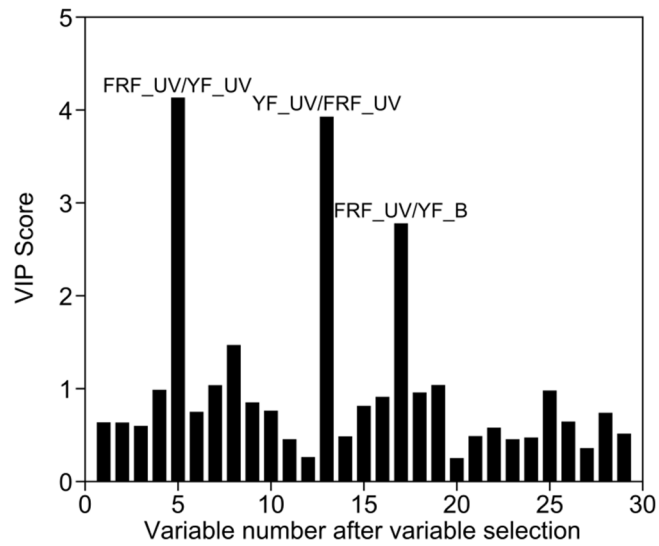


Fig. 5.11 VIP scores of the different variables of the PLSR model with temperature correction and variable selection. The three variables with the highest VIP score have their names displayed.

5.5. Conclusions

Although storage temperature had an effect on the samples in chapter 3, this did not lead to a clear grouping in the PCA scores plot. Also, a large difference between samples of different producers was noticeable on the first day of the experiment. The samples which were harvested on the first day of the experiment grown by the same producer showed a lot of variation in their chlorophyll fluorescence emission signals, indicating that extra variation in these signals might be induced by the stress of harvest itself. The influence of this harvest related stress decreased when lamb's lettuce was stored for a longer time. As it was concluded from the metabolomics study in chapter 3 that the storage temperature has a significant effect on the postharvest aging of lamb's lettuce, the storage times were normalized for this temperature effect. Then, PLSR prediction models were built to predict the normalized storage time from the acquired chlorophyll fluorescence emission signals and ratios calculated from these. MC-UVE-PLS selected 29 variables for inclusion in the PLSR prediction model to obtain a prediction error of 3.5 d and an R^2_{pred} of 0.67. The fact that the storage temperature needs to be known for this PLSR model to work, makes it not usable in practice. A grower who is storing its produce is not likely to share this information. However, this prediction model has led to some insights considering changes in lamb's lettuce during a post-harvest during storage period. Of the 29 selected variables, six were documented in literature. These were related to stress ($\text{FRF}_{\text{UV}}/\text{YF}_{\text{UV}}$, $\text{YF}_{\text{UV}}/\text{FRF}_{\text{UV}}$) and flavonol content (FLAV , $\text{FRF}_{\text{UV}}/\text{FRF}_{\text{R}}$), suggesting that free radicals were produced during storage. $\text{FRF}_{\text{UV}}/\text{YF}_{\text{B}}$ was included in the final selection and had one of the highest VIP scores, but more research is needed to link this ratio to a specific stress condition or metabolite.

6. General conclusions and future perspectives

6.1. General conclusions

Lamb's lettuce presented to the market is not always freshly harvested. It can be stored up to three weeks without any notable visual differences compared to fresh lamb's lettuce plants. However, the stored plants have an impaired shelf life potential which leads to lower consumption quality and losses in distribution. In this dissertation, the main objective was to develop a fast and non-destructive methodology to detect a prior storage period of lamb's lettuce based on non-visual biological information. This was based on the hypothesis that invisible changes during a post-harvest storage period have a physiological base which is detectable by Vis/NIR reflectance spectroscopy or chlorophyll fluorescence emission ratios.

In Chapter 3, the metabolic changes occurring in lamb's lettuce during postharvest storage were studied to get a better view on their effect on the shelf life potential. Leafy vegetables stored in dark environments are incapable of performing photosynthesis. Hence, the carbohydrates synthesized through photosynthesis before harvest result in a limited energy source for respiration during storage. After 21 d of storage, the general sugar content had decreased. The RQ value indicated, though, that carbohydrates were still the main carbon source. However, the increase of free amino acids due to proteolysis indicated that the plants coped with nutrient stress and were preparing to use amino acids for respiration. The increase in concentration for most of the amino acids was sensitive to the storage temperature in which a higher temperature resulted in a larger

increase. However, the storage temperature did not influence the respiration rate. During storage, the respiration rate decreased, which implied a shortage in soluble carbohydrates. Therefore, we can conclude that after 21 d of storage, lamb's lettuce was still using carbohydrates as an energy source and that a mixture of different carbon sources could be used for respiration. Hence, if the storage period was longer, this would lead to a greater change in the energy metabolism. This also implies that the storage of lamb's lettuce has a negative effect on shelf life potential.

In Chapter 4, Vis/NIR spectroscopy in combination with PLS regression was evaluated as a fast and non-destructive method for determination and quantification of a prior storage period for lamb's lettuce. The accuracy and robustness of the predictions improved significantly after selection of 10 % of the initial 650 wavelength variables. The number of latent variables dropped from 13 to 7, the R^2 increased from 0.75 to 0.83, while the RMSECV and RMSEV decreased to 3.6 and 3.7 d, respectively. The results of Chapter 3 suggested that Vis/NIR spectroscopy could be a useful technique, because it could detect the decrease in carbohydrate content during storage. However, the wavelengths included in the PLSR model after variable selection were mostly situated in the visible part of the spectrum and more specifically wavelengths related to photosynthetic pigment degradation rather than sugars. It is possible that the wavelengths related to sugar content were too unstable to make a robust model. Also, in Chapter 3 we found that a lot of variation in soluble carbohydrate content was noticeable when samples were grown by different producers. Finally, it may well be possible that the change in carbohydrate content in lamb's lettuce during storage was simply too small to be detected using NIR spectroscopy on intact leaves.

An attempt was made in Chapter 4 to predict shelf life potential. A prediction of color parameters and quality scores after a shelf life holding period was not feasible. The reasons why the performance of the prediction models was poor were unclear and may be related to the small dataset or the lack of a link between the dependent and independent variables.

In Chapter 5, we investigated the potential of fluorescence spectroscopy to detect postharvest storage changes of lamb's lettuce. A transformation based on the data of Chapter 3 was used to normalize the storage periods for the effect of storage temperature. A lot of variation was observed between the samples from different producers. Also, samples from the same producer had more variation between them when the measurements were performed closer to the moment of harvest. This suggests that extra variation in the fluorescence signals was induced by the stress of harvest itself. Surprisingly, no variable which could be linked solely to chlorophyll content was included in the final selection. This was in contrast with the variables included in the prediction model based on Vis/NIR spectra, where wavelengths related to photosynthetic pigments degradation were used. Comparing the PLSR prediction models of both techniques, the one based on Vis/NIR spectra gave the best performance and seemed to be the more suited option for application in practice. However, the datasets on which both models were constructed were vastly different. Chlorophyll fluorescence measurements were performed on whole crates while Vis/NIR transreflectance measurements were performed on a single leaf of lamb's lettuce. Also, the chlorophyll fluorescence dataset had only one harvest period, while the Vis/NIR calibration dataset contained 5 harvest periods. Hence, a simple one on one comparison was not possible. However, the PLSR prediction models based on chlorophyll fluorescence emission ratios were more sensitive to variations in storage temperature than those based on the Vis/NIR spectra. The prediction model based on Vis/NIR spectra has been implemented in practice with satisfying results. It is currently offered as a service by the Flanders Centre of Postharvest Technology (Heverlee, Belgium).

6.2. Future perspectives

The results presented in this thesis leave several unanswered questions about the changes in lamb's lettuce during storage, the measurement and modelling techniques. Several suggestions for future research are presented in the following paragraphs.

First, the postharvest changes in pigment composition of lamb's lettuce during storage would be interesting to study. In the first place, these would be photosynthetic pigments, i.e., chlorophyll a, chlorophyll b and carotenoids. The prediction model based on Vis/NIR spectroscopy used wavelength variables mainly from the visible part of the spectrum for a robust prediction model. Also, these wavelengths could be linked to photosynthetic pigments. The fact that no chlorophyll fluorescence emission ratios linked to chlorophyll content were selected for the prediction of the postharvest storage period is remarkable. Hence, it would be interesting to investigate the temperature dependency of pigment degradation in lamb's lettuce. Another metabolite worth investigating is ascorbic acid which has already been proposed as a good monitor for quality during storage of leafy vegetables.

Another possibility is to identify a specific metabolite or multiple metabolites that can be considered as biomarkers for shelf life potential. A requirement is that they can be measured fast and nondestructively. Their rate of change or time to cross a certain threshold may also be used as an indicator of shelf-life potential. Even when these metabolites could only be measured destructively, they might be used as a biomarker to, for example, confirm storage duration predictions based on VIS/NIR spectroscopy in case of disputes.

Another topic worth investigating more is the possibility to use fluorescence emission ratios as a fast- and non-destructive measurement technique. The dataset used in this dissertation was small compared to the random variation between the samples measured. It might be possible that inclusion of more samples in the calibration dataset would improve the prediction

performance. Also, if fluorescence emission ratios could be measured on the same samples as Vis/NIR spectra, a one on one comparison could be made to determine the most suited technique.

An interesting research topic would be to use concatenated models. In this method, it would be possible to make an estimate of the storage period based on more than one model. The first model could separate the samples based on the most similar season of growth, which was the biggest source of variation for Vis/NIR spectra. And for each season a separate model which estimates the storage time could be constructed.

Another research topic would be to use a data matrix which contains the Vis/NIR spectrum and fluorescence emission ratios of the same sample or batch of samples. Multi-block PLS can be applied to this combination of data instead of only one of the two. Hence, information from both techniques at the same time can be employed for optimal prediction results. The augmented data matrix would provide an increased complexity. Hence, a correct selection of variables becomes more important. Variable selection techniques can be applied to the concatenated matrix which can lead to an optimal combination of variables from both techniques. If one of both techniques turns out to give redundant information, the variable selection techniques will point this out by not selecting any of the variables in the concatenated matrix.

7. Bibliography

- Abrams, L., Ferris, R.S., 1960. Illustrated Flora of the Pacific States: Vol. IV :Bignonias to Sunflowers, with index to vols. I-IV. Stanford University Press, Stanford.
- Agati, G., Cerovic, Z.G., Pinelli, P., Tattini, M., 2011. Light-induced accumulation of ortho-dihydroxylated flavonoids as non-destructively monitored by chlorophyll fluorescence excitation techniques. *Environ. Exp. Bot.* 73, 3–9.
- Agati, G., Meyer, S., Matteini, P., Cerovic, Z.G., 2007. Assessment of anthocyanins in grape (*Vitis vinifera* L) berries using a noninvasive chlorophyll fluorescence method. *J. Agric. Food Chem.* 55, 1053–1061.
- Agati, G., Pinelli, P., Ebner, S.C., Romani, A., Cartelat, A., Cerovic, Z.G., 2005. Nondestructive evaluation of anthocyanins in olive (*Olea europaea*) fruits by in situ chlorophyll fluorescence spectroscopy. *J. Agric. Food Chem.* 53, 1354–1363.
- Agüero, M.V., Barg, M.V., Yommi, A., Camelo, A., Roura, S.I., 2007. Postharvest Changes in Water Status and Chlorophyll Content of Lettuce (*Lactuca Sativa* L.) and their Relationship with Overall Visual Quality. *J. Food Sci.* 73, S47–S55.
- Agüero, M. V., Ponce, a. G., Moreira, M.R., Roura, S.I., 2011. Lettuce quality loss under conditions that favor the wilting phenomenon. *Postharvest Biol. Technol.* 59, 124–131.
- Ahvenainen, R., 1996. New approaches in improving the shelf life of minimally processed fruit and vegetables. *Food Sci. Technol.* 71, 179–187.
- Andersen, C.M., Bro, R., 2010. Variable selection in regression—a tutorial. *J. Chemom.* 24, 728–737.
- Ansorena, M.R., Agüero, M.V., Goñi, M.G., Roura, S., Ponce, A., Moreira, M. del R., Di Scala, K., 2012. Assessment of lettuce quality during storage at low relative humidity using Global Stability Index methodology. *Food Sci. Technol.* 32, 366–373.
- Aubert, S., Gout, E., Bligny, R., Marty-Mazars, D., Barrieu, F., Alabouvette, J., Marty, F., Douce, R., 1996. Ultrastructural and biochemical characterization of autophagy in higher plant cells subjected to carbon deprivation: Control by the supply of mitochondria with respiratory substrates. *J. Cell Biol.* 133, 1251–1263.
- Baumann, K., 2003. Cross-validation as the objective function for variable-selection techniques. *TrAC - Trends Anal. Chem.* 22, 395–406.
- Beghi, R., Giovenzana, V., Civelli, R., Malegori, C., Buratti, S., Guidetti, R., 2014. Setting-up of a simplified handheld optical device for decay detection in fresh-cut *Valerianella locusta* L. *J. Food Eng.* 127, 10–15.
- Bekele, E.A., Beshir, W.F., Hertog, M.L.A.T.M., Nicolai, B.M., Geeraerd, A.H., 2015. Metabolic profiling reveals ethylene mediated metabolic changes and a coordinated adaptive mechanism of “Jonagold” apple to low oxygen stress. *Physiol. Plant.* 155, 232–247.
- Bengtsson, G.B., Schöner, R., Lombardo, E., Schöner, J., Borge, G.I.A., Bilger, W., 2006. Chlorophyll fluorescence for non-destructive measurement of flavonoids in broccoli. *Postharvest Biol. Technol.* 39, 291–298.
- Bidel, L.P.R., Chomicki, G., Bonini, F., Mondolot, L., Soulé, J., Coumans, M., La Fisca, P., Baissac, Y., Petit, V., Loiseau, A., Cerovic, Z.G., Gould, K.S., Jay-Allemand, C., 2015. Dynamics of flavonol accumulation in leaf tissues under different UV-B regimes in *Centella asiatica* (Apiaceae). *Planta* 242, 545–559.
- Bilger, W., Johnsen, T., Schreiber, U., 2001. UV-excited chlorophyll fluorescence as a tool for

- the assessment of UV-protection by the epidermis of plants. *J. Exp. Bot.* 52, 2007–2014.
- Bilger, W., Veit, M., Schreiber, L., Schreiber, U., 1997. Measurement of leaf epidermal transmittance of UV radiation by chlorophyll fluorescence. *Physiol. Plant.* 101, 754–763.
- Blanchard, M., Castaigne, F., Willemot, C., Makhlof, J., 1996. Modified atmosphere preservation of freshly prepared diced yellow onion. *Postharvest Biol. Technol.* 9, 173–185.
- Bogs, J., Jaffé, F.W., Takos, A.M., Walker, A.R., Robinson, S.P., 2007. The grapevine transcription factor VvMYBPA1 regulates proanthocyanidin synthesis during fruit development. *Plant Physiol.* 143, 1347–61.
- Borek, S., Ratajczak, W., 2002. Sugars as a metabolic regulator of storage protein mobilization in germinating seeds of yellow lupine (*Lupinus luteus* L.). *Acta Physiol. Plant.* 24, 425–434.
- bostonfoodandwhine.com, 2009. What is Mâche? [WWW Document]. URL <http://www.bostonfoodandwhine.com/2009/06/02/what-is-mache/> (accessed 5.23.17).
- Bouché, N., Fromm, H., 2004. GABA in plants: just a metabolite? *Trends Plant Sci.* 9, 110–115.
- Bouché, N., Lacombe, B., Fromm, H., 2003. GABA signaling: a conserved and ubiquitous mechanism. *Trends Cell Biol.* 13, 607–610.
- Bown, A.W., MacGregor, K.B., Shelp, B.J., 2006. Gamma-aminobutyrate: defense against invertebrate pests? *Trends Plant Sci.* 11, 424–427.
- Braidot, E., Petrucci, E., Peresson, C., Patui, S., Bertolini, A., Tubaro, F., Wählby, U., Coan, M., Vianello, A., Zancani, M., 2014. Low-intensity light cycles improve the quality of lamb's lettuce (*Valerianella olitoria* [L.] Pollich) during storage at low temperature. *Postharvest Biol. Technol.* 90, 15–23.
- Brito, A.L.B., Araújo, D.A., Pontes, M.J.C., Pontes, L.F.B.L., 2015. Near infrared reflectance spectrometry classification of lettuce using linear discriminant analysis. *Anal. Methods* 7, 1890–1895.
- Bro, R., Smilde, A.K., Smilde, A.K., Hubert, M., Song, X., Yu, R., Holmberg, M., Lundstrom, I., 2014. Principal component analysis. *Anal. Methods* 6, 2812.
- Brooks, M.D., Niyogi, K.K., 2011. Use of a Pulse-Amplitude Modulated Chlorophyll Fluorometer to Study the Efficiency of Photosynthesis in Arabidopsis Plants. In: Jarvis, P.R. (Ed.), *Chloroplast Research in Arabidopsis*. pp. 299–310.
- Brouquisse, R., James, F., Pradet, A., Raymond, P., 1992. Asparagine metabolism and nitrogen distribution during protein degradation in sugar-starved maize root tips. *Planta* 188, 384–95.
- Brouquisse, R., James, F., Raymond, P., Pradet, a, 1991. Study of glucose starvation in excised maize root tips. *Plant Physiol.* 96, 619–626.
- Bublitz, M.G., Peracchio, L.A., Block, L.G., 2010. Why did I eat that? Perspectives on food decision making and dietary restraint. *J. Consum. Psychol.* 20, 239–258.
- Buschmann, C., 2007. Variability and application of the chlorophyll fluorescence emission ratio red/far-red of leaves. *Photosynth. Res.* 92, 261–271.
- Buschmann, C., Nagel, E., 1993. In vivo spectroscopy and internal optics of leaves as basis for remote sensing of vegetation. *Int. J. Remote Sens.* 14, 711–722.
- Cai, W., Li, Y., Shao, X., 2008. A variable selection method based on uninformative variable elimination for multivariate calibration of near-infrared spectra. *Chemom. Intell. Lab. Syst.* 90, 188–194.
- Candel, M.J.M., 2001. Consumers' convenience orientation towards meal preparation: Conceptualization and measurement. *Appetite* 36, 15–28.
- Cartelat, a., Cerovic, Z.G., Goulas, Y., Meyer, S., Lelarge, C., Prioul, J.L., Barbottin, a., Jeuffroy, M.H., Gate, P., Agati, G., Moya, I., 2005. Optically assessed contents of leaf polyphenolics and chlorophyll as indicators of nitrogen deficiency in wheat (*Triticum aestivum* L.). *F. Crop. Res.* 91, 35–49.
- Cederkvist, H.R., Aastveit, a H., Naes, T., 2005. A comparison of methods for testing differences in predictive ability. *J. Chemom.* 19, 500–509.

- Centner, V., Massart, D.-L., de Noord, O.E., de Jong, S., Vandeginste, B.M., Sterna, C., 1996. Elimination of uninformative variables for multivariate calibration. *Anal. Chem.* 68, 3851–3858.
- Cerovic, Z.G., Ghazlen, N. Ben, Milhade, C., Obert, M., Debuissou, S., Moigne, M. Le, 2015. Nondestructive Diagnostic Test for Nitrogen Nutrition of Grapevine (*Vitis vinifera* L.) Based on Dualex Leaf-Clip Measurements in the Field. *J. Agric. Food Chem.* 63, 3669–3680.
- Cerovic, Z.G., Goutouly, J., Hilbert, G., Destrac-irvine, A., Martinon, V., Moise, N., 2009. Mapping winegrape quality attributes using portable fluorescence-based sensors. In: *Progap INIA*. pp. 301–310.
- Cerovic, Z.G., Moise, N., Agati, G., Latouche, G., Ben Ghazlen, N., Meyer, S., 2008. New portable optical sensors for the assessment of winegrape phenolic maturity based on berry fluorescence. *J. Food Compos. Anal.* 21, 650–654.
- Cerovic, Z.G., Ounis, a., Cartelat, a., Latouche, G., Goulas, Y., Meyer, S., Moya, I., 2002. The use of chlorophyll fluorescence excitation spectra for the non-destructive in situ assessment of UV-absorbing compounds in leaves. *Plant, Cell Environ.* 25, 1663–1676.
- Cerovic, Z.G., Samson, G., Morales, F., Tremblay, N., Moya, I., 1999. Ultraviolet-induced fluorescence for plant monitoring: present state and prospects. *Agronomie* 19, 543–578.
- Ceulemans, I., 2015. Feestelijke groenterayon met veldsla [WWW Document]. URL <http://www.lava.be/documents/fm-prof-dec-2015/feestelijke-groenterayon-met-veldsla.xml?lang=nl> (accessed 5.23.17).
- Ceulemans, I., 2017. LAVA-veilingen: cijfers 2016 [WWW Document]. URL <http://www.lava.be/documents/home/lava-cijfers.xml?lang=nl> (accessed 5.24.17).
- Chappelle, E.W., Kim, M.S., 1992. Ratio analysis of reflectance spectra (RARS) - An algorithm for the remote estimation of the concentrations of chlorophyll a, chlorophyll b, and carotenoids in soybean leaves. *Remote Sens. Environ.* 39, 239–247.
- Chen, M.H., Liu, L.F., Chen, Y.R., Wu, H.K., Yu, S.M., 1994. Expression of alpha-amylases, carbohydrate metabolism, and autophagy in cultured rice cells is coordinately regulated by sugar nutrient. *Plant J.* 6, 625–636.
- Chen, Z.-H., 2000. Are Isocitrate Lyase and Phosphoenolpyruvate Carboxykinase Involved in Gluconeogenesis during Senescence of Barley Leaves and Cucumber Cotyledons? *Plant Cell Physiol.* 41, 960–967.
- Chong, I.-G., Jun, C.-H., 2005. Performance of some variable selection methods when multicollinearity is present. *Chemom. Intell. Lab. Syst.* 78, 103–112.
- Cornish, L.S., 2012. It's good for me: It has added fibre! An exploration of the role of different categories of functional foods in consumer diets. *J. Consum. Behav.* 11, 292–302.
- Cox, D.N., Anderson, A.S., McKellar, S., Reynolds, J., Lean, M.E.J., Mela, D.J., 1998. Take Five, a nutrition education intervention to increase fruit and vegetable intakes: Impact on consumer choice and nutrient intakes. *Br. J. Nutr.* 80, 133–140.
- Creed, P.G., 2001. The potential of foodservice systems for satisfying consumer needs. *Innov. Food Sci. Emerg. Technol.* 2, 219–227.
- Cutler, D.F., Botha, T., Stevenson, D.W., 2008. *Plant Anatomy: an applied approach*. Wiley-Blackwell.
- Dalton, S.S., Linke, R.A., Simko, M.D., 1986. Worksite food choices: An investigation of intended and actual selections. *J. Nutr. Educ.* 18, 182–187.
- Demotes-Mainard, S., Boumaza, R., Meyer, S., Cerovic, Z.G., 2008. Indicators of nitrogen status for ornamental woody plants based on optical measurements of leaf epidermal polyphenol and chlorophyll contents. *Sci. Hortic. (Amsterdam)*. 115, 377–385.
- Dhanoa, M.S., Lister, S.J., Sanderson, R., Barnes, R.J., 1994. The link between Multiplicative Scatter Correction (MSC) and Standard Normal Variate (SNV) transformations of NIR spectra. *J. Near Infrared Spectrosc* 2, 43–47.
- Dieuaide-Noubhani, M., Canioni, P., Raymond, P., 1997. Sugar-Starvation-Induced Changes of Carbon Metabolism in Excised Maize Root Tips. *Plant Physiol.* 115, 1505–1513.

- Dinnella, C., Torri, L., Caporale, G., Monteleone, E., 2014. An exploratory study of sensory attributes and consumer traits underlying liking for and perceptions of freshness for ready to eat mixed salad leaves in Italy. *Food Res. Int.* 59, 108–116.
- Encyclopaedia Britannica, 2018. Electromagnetic spectrum [WWW Document]. *Encycl. Br.* URL <https://www.britannica.com/science/electromagnetic-radiation/The-electromagnetic-spectrum#ref273240> (accessed 7.17.18).
- Enninghorst, A., Lippert, F., 2003. Postharvest Changes in Carbohydrate Content of Lamb's Lettuce. In: *International Conference on Quality in Chains. Acta Horticulturae*, pp. 553–558.
- FAO/WHO, 2003. Diet, nutrition and the prevention of chronic diseases. World Health Organ. *Tech. Rep. Ser.* 916, i–viii, 1-149, backcover.
- Fao, 1989. Prevention of post-harvest food losses fruits, vegetables and root crops a training manual, 17/2. ed, FAO code: 17 AGRIS: J11. FAO, Rome.
- Féret, J.-B., François, C., Gitelson, A., Asner, G.P., Barry, K.M., Panigada, C., Richardson, A.D., Jacquemoud, S., 2011. Optimizing spectral indices and chemometric analysis of leaf chemical properties using radiative transfer modeling. *Remote Sens. Environ.* 115, 2742–2750.
- Ferrante, A., Incrocci, L., Maggini, R., Serra, G., Tognoni, F., 2004. Colour changes of fresh-cut leafy vegetables during storage. *J. Food, Agric. Environ.* 2, 40–44.
- Ferrante, A., Maggiore, T., 2007. Chlorophyll a fluorescence measurements to evaluate storage time and temperature of Valeriana leafy vegetables. *Postharvest Biol. Technol.* 45, 73–80.
- Ferrante, A., Martinetti, L., Maggiore, T., 2009. Biochemical changes in cut vs. intact lamb's lettuce (*Valerianella olitoria*) leaves during storage. *Int. J. Food Sci. Technol.* 44, 1050–1056.
- Fonseca, S.C., Oliveira, F.A., Brecht, J.K., 2002. Modelling respiration rate of fresh fruits and vegetables for modified atmosphere packages: a review. *J. Food Eng.* 52, 99–119.
- François, I.M., Wins, H., Buysens, S., Godts, C., Van Pee, E., Nicolai, B., De Proft, M., 2008. Predicting sensory attributes of different chicory hybrids using physico-chemical measurements and visible/near infrared spectroscopy. *Postharvest Biol. Technol.* 49, 366–373.
- Garrett, R.H., Grisham, C.M., 2005. *Biochemistry*. Thomson Brooks/Cole.
- Geladi, P., MacDougall, D., Martens, H., 1985. Linearization and scatter-correction for NIR reflectance spectra of meat. *Appl. Spectrosc.* 39, 491–500.
- Ghozlen, B.N., Moise, N., Latouche, G., Martinon, V., Mercier, L., Besançon, E., Cerovic, Z.G., 2010. Assessment of Grapevine Maturity Using a New Portable Sensor: Non-Destructive Quantification of Anthocyanins. *J. Int. des Sci. la Vigne du Vin* 1–8.
- Giovenzana, V., Beghi, R., Buratti, S., Civelli, R., Guidetti, R., 2014. Monitoring of fresh-cut *Valerianella locusta* Laterr. shelf life by electronic nose and VIS–NIR spectroscopy. *Talanta* 120, 368–375.
- Glanz, K., Basil, M., Maibach, E., Goldberg, J., Snyder, D., 1998. Why Americans eat what they do: Taste, nutrition, cost, convenience, and weight control concerns as influences on food consumption. *J. Am. Diet. Assoc.* 98, 1118–1126.
- Golic, M., Walsh, K.B., 2006. Robustness of calibration models based on near infrared spectroscopy for the in-line grading of stonefruit for total soluble solids content. *Anal. Chim. Acta* 555, 286–291.
- Gran, C.D., Beaudry, R.M., 1993. Determination of the low oxygen limit for several commercial apple cultivars by respiratory quotient breakpoint. *Postharvest Biol. Technol.* 3, 259–267.
- Hagen, S.F., Solhaug, K.A., Bengtsson, G.B., Borge, G.I.A., Bilger, W., 2006. Chlorophyll fluorescence as a tool for non-destructive estimation of anthocyanins and total flavonoids in apples. *Postharvest Biol. Technol.* 41, 156–163.
- Henriques, F.S., 2009. Leaf chlorophyll fluorescence: Background and fundamentals for plant biologists. *Bot. Rev.* 75, 249–270.

- Henry, R.C., Park, E.S., Spiegelman, C.H., 1999. Comparing a new algorithm with the classic methods for estimating the number of factors. *Chemom. Intell. Lab. Syst.* 48, 91–97.
- Heyes, D.J., Neil Hunter, C., 2009. Biosynthesis of Chlorophyll and Barteriochlorophyll. In: *Tetrapyrroles*. Springer New York, New York, NY, pp. 235–249.
- Hildebrandt, T.M., Nunes Nesi, A., Araújo, W.L., Braun, H.-P., 2015. Amino Acid Catabolism in Plants. *Mol. Plant* 8, 1563–79.
- Ho, Q.T., Verboven, P., Verlinden, B.E., Schenk, A., Nicolaï, B.M., 2013. Controlled atmosphere storage may lead to local ATP deficiency in apple. *Postharvest Biol. Technol.* 78, 103–112.
- Höskuldsson, A., 2001. Variable and subset selection in PLS regression. *Chemom. Intell. Lab. Syst.* 55, 23–38.
- Hunt, R.W.G., Pointer, M.R., 2011. *Measuring Colour*. John Wiley & Sons, Ltd, Chichester, UK.
- Inoue, Y., Moriyasu, Y., 2006. Autophagy is not a main contributor to the degradation of phospholipids in tobacco cells cultured under sucrose starvation conditions. *Plant Cell Physiol.* 47, 471–480.
- Itoh, H., Nomura, K., Shiraishi, N., Uno, Y., Kuroki, S., Ayata, K., 2015. Continuous Measurement of Nitrate Concentration in Whole Lettuce Plant by Visible-near-infrared Spectroscopy. *Environ. Control Biol.* 53, 205–215.
- Journet, E.P., Bigny, R., Douce, R., 1986. Biochemical changes during sucrose deprivation in higher plant cells. *J. Biol. Chem.* 261, 3193–3199.
- Kader, A.A., 2002. *Postharvest technology of horticultural crops*. University of California, Agriculture and Natural Resources.
- Kader, A.A., 2013. *Postharvest Technology of Horticultural Crops -An Overview from Farm to Fork*. *J. Appl. Sci. Technol.* (Special Issue No.1) 1–8.
- Kennard, R.W., Stone, L.A., 1969. Computer Aided Design of Experiments. *Technometrics* 11, 137–148.
- Klieber, A., Porter, K., Collins, G., 2002. Harvesting at different times of day does not influence the postharvest life of Chinese cabbage. *Sci. Hortic. (Amsterdam)*. 96, 1–9.
- Koes, R., Verweij, W., Quattrocchio, F., 2005. Flavonoids: a colorful model for the regulation and evolution of biochemical pathways. *Trends Plant Sci.* 10, 236–242.
- Kolb, C.A., Kopecký, J., Riederer, M., Pfündel, E.E., 2003. UV screening by phenolics in berries of grapevine (*Vitis vinifera*). *Funct. Plant Biol.* 30, 1177–1186.
- Kramchote, S., Nakano, K., Kanlayanarat, S., Ohashi, S., Takizawa, K., Bai, G., 2014. Rapid determination of cabbage quality using visible and near-infrared spectroscopy. *LWT - Food Sci. Technol.* 59, 695–700.
- Krause, G.H., Weis, E., 1991. Chlorophyll Fluorescence and Photosynthesis: The Basics. *Annu. Rev. Plant Physiol. Plant Mol. Biol.*
- Kroh, M., Miki-Hirosige, H., Rosen, W., Loewus, F., 1970. Inositol Metabolism in Plants. *Plant Physiol.* 45, 86–91.
- Kumpulainen, T., Sandell, M., Junell, P., Hopia, A., 2016. The effect of freshness in a foodservice context. *J. Culin. Sci. Technol.* 14, 153–165.
- Kunz, H.H., Scharnewski, M., Feussner, K., Feussner, I., Flugge, U.I., Fulda, M., Gierth, M., 2009. The ABC transporter PXA1 and peroxisomal beta-oxidation are vital for metabolism in mature leaves of Arabidopsis during extended darkness. *Plant Cell* 21, 2733–2749.
- Latouche, G., Bellow, S., Poutaraud, A., Meyer, S., Cerovic, Z.G., 2013. Influence of constitutive phenolic compounds on the response of grapevine (*Vitis vinifera* L.) leaves to infection by *Plasmopara viticola*. *Planta* 237, 351–361.
- Le Maire, G., François, C., Dufrène, E., 2004. Towards universal broad leaf chlorophyll indices using PROSPECT simulated database and hyperspectral reflectance measurements. *Remote Sens. Environ.* 89, 1–28.
- Lee, D., 2007. *Nature's Palette: The Science of Plant Color*. The university of Chicago press, Chicago and London.

- Lee, E.-J., Matsumura, Y., Soga, K., Hoson, T., Koizumi, N., 2007. Glycosyl Hydrolases of Cell Wall are Induced by Sugar Starvation in Arabidopsis. *Plant Cell Physiol.* 48, 405–413.
- Lennernäs, M., Fjellström, C., Becker, W., Giachetti, I., Schmitt, A., Remaut de Winter, A., Kearney, M., 1997. Influences on food choice perceived to be important by nationally-representative samples of adults in the European Union. *Eur. J. Clin. Nutr.* 51 Suppl 2, S8-15.
- Lin, W., Jolliffe, P., 2000. Chlorophyll Fluorescence Of Long english Cucumber Affected By Storage Conditions. *Acta Hortic.* 449–456.
- Loewus, F., 1969. Metabolism of inositol in higher plants. *Ann N Y Acad Sci* 165, 577–598.
- Loewus, F. a, Murthy, P.P.N., 2000. myo-Inositol metabolism in plants. *Plant Sci.* 150, 1–19.
- Loewus, F.A., 2006. Inositol and Plant Cell Wall Polysaccharide Biogenesis. In: Intergovernmental Panel on Climate Change (Ed.), *Biology of Inositols and Phosphoinositides*. Springer US, Cambridge, pp. 21–45.
- Loewus, F.A., Kelly, S., Neufeld, E.F., 1962. METABOLISM OF MYO-INOSITOL IN PLANTS: CONVERSION TO PECTIN, HEMICELLULOSE, D-XYLOSE, AND SUGAR ACIDS. *Proc. Natl. Acad. Sci. U. S. A.* 48, 421–5.
- Lu, Q., Lu, C., Zhang, J., Kuang, T., 2002. Photosynthesis and chlorophyllafluorescence during flag leaf senescence of field-grown wheat plants. *J. Plant Physiol.* 159, 1173–1178.
- Lu, R., Guyer, D.E., Beaudry, R.M., 2000. Determination of firmness and sugar content of apples using near-infrared diffuse reflectance. *J. Texture Stud.* 31, 615–630.
- Lucasius, C.B., Beckers, M.L.M., Kateman, G., 1994. Genetic algorithms in wavelength selection: a comparative study. *Anal. Chim. Acta* 286, 135–153.
- Maccioni, A., Agati, G., Mazzinghi, P., 2001. New vegetation indices for remote measurement of chlorophylls based on leaf directional reflectance spectra. *J. Photochem. Photobiol. B Biol.* 61, 52–61.
- MacGregor, J.F., Kourti, T., 1995. Statistical process control of multivariate processes. *Control Eng. Pract.* 3, 403–414.
- Malenovský, Z., Mishra, K.B., Zemek, F., Rascher, U., Nedbal, L., 2009. Scientific and technical challenges in remote sensing of plant canopy reflectance and fluorescence. *J. Exp. Bot.* 60, 2987–3004.
- Mao, H., Gao, H., Zhang, X., Kumi, F., 2015. Nondestructive measurement of total nitrogen in lettuce by integrating spectroscopy and computer vision. *Sci. Hortic. (Amsterdam)*. 184, 1–7.
- Martens, H., Høy, M., Wise, B.M., Bro, R., Brockhoff, P.B., 2003. Pre-whitening of data by covariance-weighted pre-processing. *J. Chemom.* 17, 153–165.
- Martens, H., Naes, T., 1989. *Multivariate calibration*. Wiley.
- Mauseth, J.D., 2008. *Botany. An introduction to plant biology*, 4th ed, Jones and Bartlett Titles in Biological Science. Jones & Bartlett Learning.
- Maxwell, K., Johnson, G.N., 2000. Chlorophyll fluorescence--a practical guide. *J. Exp. Bot.* 51, 659–668.
- Mbong, V.B.M., Ampofo-Asiama, J., Hertog, M., Geeraerd, A.H., Nicolai, B.M., 2017a. Metabolic profiling reveals a coordinated response of isolated lamb's (Valerianella locusta, L.) lettuce cells to sugar starvation and low oxygen stress. *Postharvest Biol. Technol.* 126, 23–33.
- Mbong, V.B.M., Ampofo-Asiama, J., Hertog, M.L.A.T.M., Geeraerd, A.H., Nicolai, B.M., 2017b. The effect of temperature on the metabolic response of lamb's lettuce (Valerianella locusta, (L), Laterr.) cells to sugar starvation. *Postharvest Biol. Technol.* 125, 1–12.
- McGlone, V.A., Jordan, R.B., Seelye, R., Martinsen, P.J., 2002. Comparing density and NIR methods for measurement of Kiwifruit dry matter and soluble solids content. *Postharvest Biol. Technol.* 26, 191–198.
- Mehmood, T., Liland, K.H., Snipen, L., Sæbø, S., 2012. A review of variable selection methods in Partial Least Squares Regression. *Chemom. Intell. Lab. Syst.* 118, 62–69.
- Merzlyak, M.N., Gitelson, A.A., Chivkunova, O.B., Rakitin, V.Y., 1999. Non-destructive optical

- detection of pigment changes during leaf senescence and fruit ripening. *Physiol. Plant.* 106, 135–141.
- Merzlyak, M.N., Melo, T.B., Naqvi, K.R., 2008. Effect of anthocyanins, carotenoids, and flavonols on chlorophyll fluorescence excitation spectra in apple fruit: signature analysis, assessment, modelling, and relevance to photoprotection. *J. Exp. Bot.* 59, 349–359.
- Meyer, S., Cerovic, Z.G., Goulas, Y., Montpied, P., Demotes-Mainard, S., Bidet, L.P.R., Moya, I., Dreyer, E., 2006. Relationships between optically assessed polyphenols and chlorophyll contents, and leaf mass per area ratio in woody plants: A signature of the carbon-nitrogen balance within leaves? *Plant, Cell Environ.* 29, 1338–1348.
- Michaelis, L., Menten, M.M.L., 2013. The kinetics of invertin action: Translated by T.R.C. Boyde Submitted 4 February 1913. *FEBS Lett.* 587, 2712–2720.
- Moriyasu, Y., Ohsumi, Y., 1996. Autophagy in Tobacco Suspension-Cultured Cells in Response to Sucrose Starvation. *Plant Physiol.* 111, 1233–1241.
- Morkunas, I., Borek, S., Formela, M., Ratajczak, L., 2012. Plant Responses to Sugar Starvation. In: Chang, C.-F. (Ed.), *Carbohydrates - Comprehensive Studies on Glycobiology and Glycotechnology*. InTech, pp. 409–438.
- Müller, V., Albert, A., Barbro Winkler, J., Lankes, C., Noga, G., Hunsche, M., 2013. Ecologically relevant UV-B dose combined with high PAR intensity distinctly affect plant growth and accumulation of secondary metabolites in leaves of *Centella asiatica* L. Urban. *J. Photochem. Photobiol. B Biol.* 127, 161–169.
- Naes, T., Isaksson, T., Fearn, T., Davies, T., 2002. A User-friendly Guide to Multivariate Calibration and Classification. *NIR Publ.* 46, 7–289.
- Neumark-Sztainer, D., Story, M., Perry, C., Casey, M.A., 1999. Factors influencing food choices of adolescents: Findings from focus- group discussions with adolescents. *J. Am. Diet. Assoc.* 99, 929–937.
- Nicolai, B.M., Beullens, K., Bobelyn, E., Peirs, A., Saeys, W., Theron, K.I., Lammertyn, J., 2007. Nondestructive measurement of fruit and vegetable quality by means of NIR spectroscopy: A review. *Postharvest Biol. Technol.* 46, 99–118.
- Nicolaï, B.M., Defraeye, T., De Ketelaere, B., Herremans, E., Hertog, M.L.A.T.M., Saeys, W., Torricelli, A., Vandendriessche, T., Verboven, P., 2014. Nondestructive Measurement of Fruit and Vegetable Quality. *Annu. Rev. Food Sci. Technol.* 5, 285–312.
- Nicolai, B.M., Verlinden, B.E., Desmet, M., Saevels, S., Saeys, W., Theron, K., Cubeddu, R., Pifferi, A., Torricelli, A., 2008. Time-resolved and continuous wave NIR reflectance spectroscopy to predict soluble solids content and firmness of pear. *Postharvest Biol. Technol.* 47, 68–74.
- Nørgaard, L., Saudland, a., Wagner, J., Nielsen, J.P., Munck, L., Engelsen, S.B., 2000. Interval partial least-squares regression (iPLS): A comparative chemometric study with an example from near-infrared spectroscopy. *Appl. Spectrosc.* 54, 413–419.
- Oms-Oliu, G., Hertog, M.L.A.T.M., Van de Poel, B., Ampofo-Asiama, J., Geeraerd, A.H., Nicolai, B.M., 2011. Metabolic characterization of tomato fruit during preharvest development, ripening, and postharvest shelf-life. *Postharvest Biol. Technol.* 62, 7–16.
- Peirs, A., Lammertyn, J., Ooms, K., Nicolai, B.M., 2001. Prediction of the optimal picking date of different apple cultivars by means of VIS/NIR-spectroscopy. *Postharvest Biol. Technol.* 21, 189–199.
- Pfündel, E.E., Ben Ghazlen, N., Meyer, S., Cerovic, Z.G., 2007. Investigating UV screening in leaves by two different types of portable UV fluorimeters reveals in vivo screening by anthocyanins and carotenoids. *Photosynth. Res.* 93, 205–221.
- Popova, T.N., Pinheiro de Carvalho, M.Â., 1998. Citrate and isocitrate in plant metabolism. *Biochim. Biophys. Acta - Bioenerg.* 1364, 307–325.
- Rabinowitch, E., Govindjee, 1969. *Photosynthesis*. John Wiley & Sons, Inc.
- Ragaert, P., Verbeke, W., Devlieghere, F., Debevere, J., 2004. Consumer perception and choice of minimally processed vegetables and packaged fruits. *Food Qual. Prefer.* 15, 259–270.
- Raven, P.H., Ray, E.F., Eichhorn, S.E., 1999. *Biology of Plants*, 6th ed, Biology of Plants. W.H.

- Freeman and Company/Worth Publishers, New York.
- Reich, G., 2005. Near-infrared spectroscopy and imaging: Basic principles and pharmaceutical applications. *Adv. Drug Deliv. Rev.* 57, 1109–1143.
- Rico, D., Martín-Diana, A.B., Barat, J.M., Barry-Ryan, C., 2007. Extending and measuring the quality of fresh-cut fruit and vegetables: a review. *Trends Food Sci. Technol.* 18, 373–386.
- Rinnan, Å., Berg, F. van den, Engelsen, S.B., 2009. Review of the most common pre-processing techniques for near-infrared spectra. *TrAC - Trends Anal. Chem.* 28, 1201–1222.
- Rodgers, S., 2007. Deriving Strategic Advantages from Extended Shelf-Life Foods in the Hospitality Sector. *J. Culin. Sci. Technol.* 5, 111–129.
- Roessner, U., Wagner, C., Kopka, J., Trethewey, R.N., Willmitzer, L., 2000. Simultaneous analysis of metabolites in potato tuber by gas chromatography-mass spectrometry. *Plant J.* 23, 131–142.
- Roger, J.-M., Chauchard, F., Bellon-Maurel, V., 2003. EPO-PLS external parameter orthogonalisation of PLS application to temperature-independent measurement of sugar content of intact fruits. *Chemom. Intell. Lab. Syst.* 66, 191–204.
- Rose, T.L., Bonneau, L., Der, C., Marty-Mazars, D., Marty, F., 2006. Starvation-induced expression of autophagy-related genes in *Arabidopsis*. *Biol. Cell* 98, 53–67.
- Saeyns, W., 2014. *Chemometrics (B-KUL-G0B70A)*.
- Saglio, P.H., Pradet, A., 1980. Soluble Sugars, Respiration, and Energy Charge during Aging of Excised Maize Root Tips. *Plant Physiol* 66, 516–519.
- Schofield, R.A., DeEll, J.R., Murr, D.P., Jenni, S., 2005. Determining the storage potential of iceberg lettuce with chlorophyll fluorescence. *Postharvest Biol. Technol.* 38, 43–56.
- Shelp, B.J., Bown, A.W., McLean, M.D., 1999. Metabolism and functions of gamma-aminobutyric acid. *Trends Plant Sci.* 4, 446–452.
- Spinardi, A., Ferrante, A., 2012. Effect of storage temperature on quality changes of minimally processed baby lettuce. *J. Food, Agric. Environ.* 10, 38–42.
- Steidle Neto, A.J., Moura, L. de O., Lopes, D. de C., Carlos, L. de A., Martins, L.M., Ferraz, L. de C.L., 2017. Non-destructive prediction of pigment content in lettuce based on visible-NIR spectroscopy. *J. Sci. Food Agric.* 97, 2015–2022.
- Stoop, J., Williamson, J., Masonpharr, D., 1996. Mannitol metabolism in plants: a method for coping with stress. *Trends Plant Sci.* 1, 139–144.
- Strasser, R.J., Srivastava, A., 1995. Polyphasic Chlorophyll a Fluorescence Transient in Plants and Cyanobacteria. *Photochem. Photobiol.* 61, 32–42.
- Sug Park, E., Henry, R.C., Spiegelman, C.H., 2000. Estimating the number of factors to include in a high-dimensional multivariate bilinear model. *Commun. Stat. - Simul. Comput.*
- Sytar, O., Bruckova, K., Hunkova, E., Zivcak, M., Konate, K., Brestic, M., 2015. The application of multiplex fluorimetric sensor for the analysis of flavonoids content in the medicinal herbs family Asteraceae, Lamiaceae, Rosaceae. *Biol. Res.* 48, 5.
- Sytar, O., Kosyan, A., Taran, N., Smetanska, I., 2014. Anthocyanin's as marker for selection of buckwheat plants with high rutin content. *Gesunde Pflanz.* 66, 165–169.
- Taiz, L., Zeiger, E., 2010. *Plant Physiology*, 5th ed. Sinauer Associates.
- Tassi, F., Maestri, E., Restivo, F.M., Marmioli, N., 1966. R N A Synthesis in Isolated Chloroplasts Effects of Actinomycin D and Mitomycin C on the Synthesis of Chlorophyll 83, 174–176.
- Tempesta, M., Tremblay, N., Vigneault, P., Bouroubi, Y., 2012. Remote Sensing of Nitrogen and Water Status on Boston Lettuce Transplants in a Greenhouse Environment Peat blocks for transplants • Less transplant shock • Better rooting • Better yield • How to go organic? In: MacKenzie, J., Savard, M. (Eds.), *Proceedings of the Canadian Organic Science Conference and Science Cluster Strategic Meetings*. Winnipeg, Manitoba, p. 87.
- The Angiosperm Phylogeny Group, 2009. An update of the Angiosperm Phylogeny Group Classification for the orders and families of floweringplants: APG III. *Bot. J. Linn. Soc.*

- 161, 105–121.
- Thimm, O., Bläsing, O., Gibon, Y., Nagel, A., Meyer, S., Krüger, P., Selbig, J., Müller, L.A., Rhee, S.Y., Stitt, M., 2004. MAPMAN: A user-driven tool to display genomics data sets onto diagrams of metabolic pathways and other biological processes. *Plant J.* 37, 914–939.
- Thomas, E. V., 2003. Non-parametric statistical methods for multivariate calibration model selection and comparison. *J. Chemom.* 17, 653–659.
- Tipler, P.A. (Paul A., Mosca, G., 2008. *Physics for scientists and engineers: with modern physics.*
- Tremblay, N., Wang, Z., Cerovic, Z.G., 2011. Sensing crop nitrogen status with fluorescence indicators. A review. *Agron. Sustain. Dev.* 32, 451–464.
- Varoquaux, P., Mazollier, J., Albagnac, G., 1996. The influence of raw material characteristics on the storage life of fresh-cut butterhead lettuce. *Postharvest Biol. Technol.* 9, 127–139.
- Verlegh, P.W.J., Candel, M.J.J.M., 1999. The consumption of convenience foods: reference groups and eating situations. *Food Qual. Prefer.* 10, 457–464.
- Verlinden, B.E., Jacobs, B.A.J.G., Decombel, A., Bleyaert, P., Van Lommel, J., Vandevelde, I., 2016. Verbetering van de houdbaarheid van veldsla en kropsla - Eindverslag IWT-project 100885. Heverlee.
- Viña, S.Z., Chaves, A.R., 2003. Texture changes in fresh cut celery during refrigerated storage. *J. Sci. Food Agric.* 83, 1308–1314.
- Visser, A.J.W.G., Rolinski, O.J., 2017. *Basic Photophysics.*
- Ward, A., 1911. *Encyclopedia of foods and beverages*, 1st ed. Baker & Taylor, New York.
- Weng, X.Y., Xu, H.X., Jiang, D.A., 2005. Characteristics of gas exchange, chlorophyll fluorescence and expression of key enzymes in photosynthesis during leaf senescence in rice plants. *J. Integr. Plant Biol.* 47, 560–566.
- Wise, B.M., Gallagher, N.B., Bro, R., Shaver, J., Windig, W., Koch, R.S., 2006. *PLS Toolbox 4.0, Eigenvector Research Incorporated: Wenatchee, WA, USA. Eigenvector Research, Inc., Wenatchee, WA.*
- Wold, S., Antti, H., Lindgren, F., Öhman, J., 1998. Orthogonal signal correction of near-infrared spectra. *Chemom. Intell. Lab. Syst.* 44, 175–185.
- Wold, S., Sjöström, M., Eriksson, L., 2001. PLS-regression: A basic tool of chemometrics. *Chemom. Intell. Lab. Syst.* 58, 109–130.
- Wright, S., 1921. Correlation and Causation. *J. Agric. Res.* 20, 557–585.
- Xiaobo, Z., Jiewen, Z., Povey, M.J.W., Holmes, M., Hanpin, M., 2010. Variables selection methods in near-infrared spectroscopy. *Anal. Chim. Acta* 667, 14–32.
- Yamauchi, N., 2015. Postharvest Chlorophyll Degradation and Oxidative Stress. In: *Abiotic Stress Biology in Horticultural Plants.* Springer Japan, Tokyo, pp. 101–113.
- Yongli Zhu, Hanping Mao, Pingping Li, Yanyou Wu, 2011. Measurement of lettuce leaf chlorophyll content by means of VIS-NIR spectroscopy. In: *2011 International Conference on Remote Sensing, Environment and Transportation Engineering.* IEEE, pp. 2250–2253.
- Zarco-Tejada, P.J., Guillén-Climent, M.L., Hernández-Clemente, R., Catalina, A., González, M.R., Martín, P., 2013. Estimating leaf carotenoid content in vineyards using high resolution hyperspectral imagery acquired from an unmanned aerial vehicle (UAV). *Agric. For. Meteorol.* 171–172, 281–294.
- Zivcak, M., Brückova, K., Sytar, O., Brestic, M., Olsovska, K., Allakhverdiev, S.I., 2017. Lettuce flavonoids screening and phenotyping by chlorophyll fluorescence excitation ratio. *Planta* 245, 1215–1229.
- Zorzetti, B.M., Shaver, J.M., Harynuk, J.J., 2011. Estimation of the age of a weathered mixture of volatile organic compounds. *Anal. Chim. Acta* 694, 31–7.

8. List of publications

8.1. Articles in internationally reviewed journals

Jacobs, B.A.J.G., Verlinden, B.E., Bobelyn, E., Decombel, A., Bleyaert, P., Van Lommel, J., Vandevelde, I., Saeys, W., Nicolai, B.M., 2016. Estimation of the prior storage period of lamb's lettuce based on visible/near infrared reflectance spectroscopy. *Postharvest Biol. Technol.* 113, 95–105.

8.2. Conference proceedings

Jacobs, B.A.J.G., Verlinden, B.E., Bobelyn, E., Decombel, A., Bleyaert, P., Saeys, W., Nicolai, B.M., 2015. Determining stored period of lamb's lettuce using VIS/NIR reflectance spectroscopy. *Acta Hortic.* 1091, 187–194.

Jacobs, B.A.J.G., Verlinden, B.E., Bobelyn, E., Decombel, A., Bleyaert, P., Van Lommel, J., Vandevelde, I., Saeys, W., Nicolai, B.M., 2015. Predicting stored period and shelf life potential of Lamb's lettuce using Vis/NIR reflectance spectroscopy. *Acta Hortic.* 1079, 207–213.

Jacobs, B.A.J.G., Verlinden, B.E., Bobelyn, E., Decombel, A., Bleyaert, P., Van Lommel, J., Vandevelde, I., Saeys, W., Nicolai, B.M., 2017. Determining lamb's lettuce postharvest age based on visible/near-infrared reflectance spectroscopy. *Acta Hortic.* 9–16.

8.3. Science popularisation

Decombel, A., Jacobs, B., Bleyaert, P., Verlinden, B., 2013. Kwaliteitsvolle veldsla grotendeels afhankelijk van bewaarmethode. *Proeftuinnieuws* 11.

- Jacobs, B., De Roeck, A., Verlinden, B., Decombel, A., Bleyaert, P., Van Lommel, J., Vandeveld, I., 2015. Snelle bepaling van de frisheid van veldsla, Van laboratoriummeting naar praktisch bruikbaar toestel. Proeftuinnieuws 6.
- Jacobs, B., Decombel, A., Bleyaert, P., Van Lommel, J., Leenknecht, I., Verlinden, B., 2013. Verbetering houdbaarheid veldsla en kropsla. Flandria Spec. 1, 42–43.
- Jacobs, B., Verlinden, B., 2014. Minder kroppen per bak verbetert houdbaarheid. Proeftuinnieuws 6, 26–27.
- Van Lommel, J., Jacobs, B., Verlinden, B., 2013. Houdbaarheid rassen kropsla verschilt. Proeftuinnieuws 11.
- Van Lommel, J., Vandeveld, I., Decombel, A., Bleyaert, P., Jacobs, B., Verlinden, B., 2015. Houdbaarheid van kropsla en veldsla verbeteren. Manag. en Tech. 21.
- Van Lommel, J., Vandeveld, I., Decombel, A., Bleyaert, P., Verlinden, B., De Roeck, A., Jacobs, B., 2015. Houdbaarheid kropsla - voorzichtigheid en snel inkoelen van groot belang. Proeftuinnieuws 6, 18.
- Verlinden, B., De Roeck, A., Jacobs, B., Decombel, A., Bleyaert, P., Van Lommel, J., Vandeveld, I., 2015. Snelle meting van frisheid van veldsla. Proeftuinnieuws 6, 20–21.
- Verlinden, B., Jacobs, B., 2014. Snelle bepaling van frisheid van veldsla zonder schade toe te brengen aan het gewas. Proeftuinnieuws 6, 24–25.